

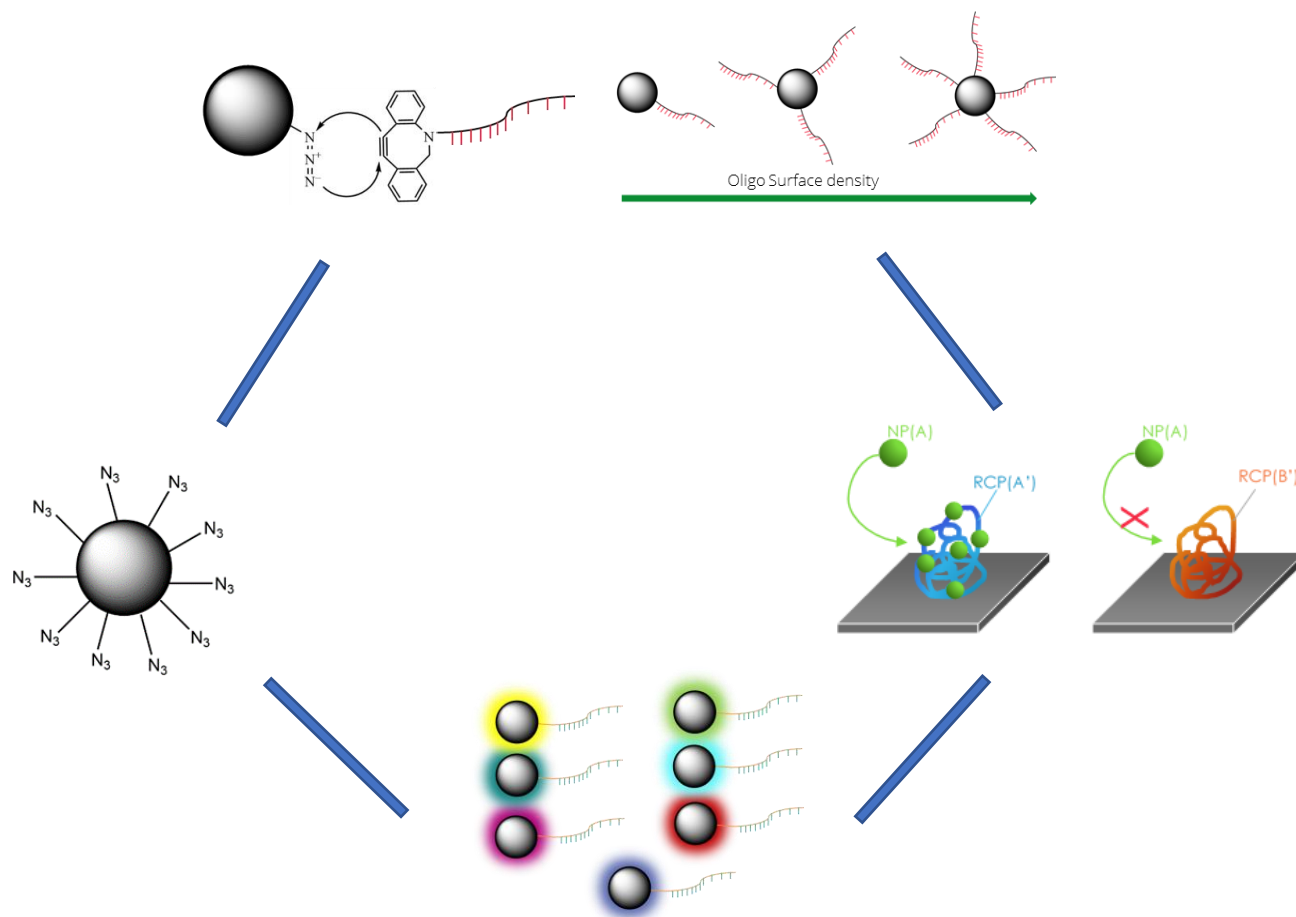
Functionalization and Evaluation of Nanoparticle Probes for the Development of a 14 Plex Diagnostic assay

Author: Samuel Narmack, Samuel@Aplex.bio Snarmack@kth.se

Supervisors: Umear Naseem, Ruben Soares, Mats Nilsson

Examiner: James Gardner

Aplex Bio, Scilifelab, KTH



Abstract

This work was a collaboration between Apex Bio AB and Scilifelab with the aim of developing a molecular assay capable of detecting and discriminating between 14 different pathogenic targets. There are 4 chapters with focus on different goals. In chapter one a method of evaluating nanoparticle emissions was developed. The first approach of evaluating nanoparticle emissions was to utilize click chemistry to bind nanoparticles to macroscale structures of amplified DNA targets. The second evaluated approach was the formation of aggregated complexes of nanoparticles and amplified DNA targets. The second chapter of the thesis used azide functionalized nanoparticles supplied by Apex Bio AB to utilize azide groups as crosslinkers and use them to functionalize the nanoparticles with DBCO oligos. A hybridization-based method was then developed to quantify relative oligo densities on the nanoparticles, enabling reproducible oligo functionalization of nanoparticles, producing nanoparticle probes. The final task of chapter 2 was evaluating the binding efficiency and specificity of the developed nanoparticle probes. The third chapter of the thesis evaluated amplification of synthetic ssDNA sequences corresponding to genetic markers of 14 pathogenic targets using RCA. The goal was to confirm specificity of chosen padlock probes and corresponding synthetic targets for each pathogen. Specific amplification of each target was a prerequisite to enable detecting and discriminating between the 14 pathogenic targets. In chapter 4 the goal was to develop a cost-effective method of oligo functionalization for nanoparticles. This chapter evaluated two main approaches of using DBCO-NHS-ester reagents to perform DBCO modification of amine-oligos. The realization of this work would develop an assay that has the potential to impact the field of diagnostics on a global scale. When fully developed, the molecular assay can be modified to detect any RNA/DNA targets which enables numerous applications, making the assay a competitive diagnostic tool which can be implemented in existing microscopy systems.

Abbreviations

NP Nanoparticles

RCP Rolling circle amplification product

DBCO Dibenzocyclooctyne

SEM Scanning electron microscopy

TEM Transmission electron microscopy

PLP padlock probe

Table of Contents

1. Development of a method for evaluating nanoparticle emissions by formation of clusters.....	7
1.1 Introduction	7
1.1.1 Nanoparticles supplied by Apex Bio.....	7
1.1.2 Functionalization.....	7
1.1.3 Click chemistry	8
1.1.4 Dispersion stability of colloidal nanoparticles	9
1.1.5 Stabilizing ligands, azide functionalization and coating types.....	9
1.1.6 Azide functionalization.....	10
1.1.7 Rolling Circle Amplification – RCA.....	11
1.1.8 Nucleic acid hybridization	12
1.1.9 Addition of DBCO groups to RCPs.....	12
1.1.10 Nanoparticle to RCP binding using click chemistry.....	12
1.1.11 Confirming the presence of DBCO groups on RCPs using Cy5-azide	13
1.1.12 Amplified targets for evaluation of nanoparticle binding	13
1.2 Materials and methods	14
1.2.1 Materials	14
1.2.2 Methods.....	15
1.3 Results and discussion	20
1.3.1 Size characterization using SEM.....	20
1.3.2 Size characterization using TEM	20
1.3.3 Size analysis conclusion	21
1.3.4 Quantification of NP azide density using Cy5-DBCO.....	21
1.3.5 Coating deterioration.....	23
1.3.6 Evaluation of stabilizing ligands	23
1.3.7 Confirmation of DBCO groups on labelled RCPs using CY5-azide.....	25
1.3.8 Nanoparticle to RCP binding using coating 1,2,3.....	26
1.3.9 Denaturation of hybridized detection oligo in polar solvents	27
1.3.10 Nanoparticle to RCP binding using coating 2,3 with modified solvent conditions.....	28
1.3.11 Evaluation of nanoparticle emission using aggregation method	29
1.4 Conclusions	31
2. Oligo functionalization of nanoparticles for efficient probing.....	32
2.1 Introduction	32

2.1.1 Oligo functionalization	32
2.1.3 Nucleic acid hybridization of functionalized nanoparticles to RCPs	33
2.2 Materials and methods	34
2.2.1 Materials	34
2.2.2 Methods	35
2.3 Results and discussion	39
2.3.1 Developing method of oligo density quantification	39
2.3.2 Evaluation of nanoparticle to RCP hybridization efficiency	40
2.3.3 Hybridization specificity	45
2.4 Conclusions	48
3. Development of 14 plex pathogen panel	49
3.1 Pathogen targets for development of 14 plex panel	49
3.2 Synthetic targets	50
3.3 Padlock probes	51
3.4 Padlock probe specificity	52
3.5 Materials and methods	53
3.5.1 Materials	53
3.5.2 Methods	54
3.6 Results and discussion	57
3.6.1 Imaging of amplified and labelled targets: SARS-COV-2, NL63, 229E	57
3.6.2 Imaging of amplified and labelled targets: OC43, HKU1, Inf.H3N2	58
3.6.3 Imaging of amplified and labelled targets: Influenza H1N1, Influenza Victoria, Yamagata	59
3.6.4 Imaging of amplified and labelled targets: OC43, HKU1, Inf.H3N2	60
3.6.5 Imaging of amplified and labelled targets: Saureus, Paeroginosa	61
3.6.6 Data analysis of padlock probe specificity	62
3.7 Conclusions: padlock probe specificity	65
4. Oligo modification for cost effective nanoparticle functionalization	66
4.1 Introduction	66
4.1.1 Oligo modification by formation of covalent bonds	66
4.1.2 Concentration measurement of oligos and DBCO-NHS-ester in solution	67
4.1.3 Goal of experiments	67
4.2 Materials and methods	68
4.2.1 Materials	68

4.2.2 Methods.....	68
4.3 Results and discussion	71
4.3.1 Yield estimation of oligo modification with oligo excess.....	71
4.4 Conclusions	78
Bibliography	79

1. Development of a method for evaluating nanoparticle emissions by formation of clusters

1.1 Introduction

The aim of this chapter is to develop a method to evaluate the fluorescent emission of clusters of NPs rather than measurement of bulk fluorescence or single particles measurement. The reason for measuring NP clusters is to mimic the signal that is expected when a number of NPs bind to a biomolecule in the form of an amplified DNA sequence. For the development of the method, Apex Bio supplied a reference nanoparticle (NP) batch with internal fluorescence that can be measured in the corresponding Cy3 channel of the epifluorescent microscope used for this project. The first step of the project characterizes the size of the supplied NPs using SEM and TEM to ensure inter-batch reproducibility of the developed method. To enable representative measurement of the NP emissions the NP clusters must be of similar size as the biomolecule targets, close to 1 μm in size. The size of the clusters is important to accurately evaluate the NP emission as the number of NPs in the cluster will directly correlate to the measured intensity. The second step of developing the method utilizes functionalization of the surface of NPs with azide groups to enable conjugation to amplified biomolecules using click chemistry. Azide groups are non-polar and will decrease the stability of the nanoparticle dispersion in polar solvents, favoring attractive hydrophobic interactions. The hydrophobic interaction arises from the non-polar azide groups on the surface of the particles interacting with polar water molecules in the solvent. The decrease in NP dispersion stability arising from the non-polar azide groups on the NP surface will hinder the NP to RCP binding using click chemistry conjugation. In the case of an unstable NP dispersion the NPs in solution will be comprised of a speciation of aggregates with varying size which limits the surface area of the NPs able to react and bind to their biomolecule target. To enable NP to RCP binding by utilizing click chemistry the NPs must be stabilized for the use in buffer conditions suitable for the amplification and hybridization of DNA sequences. To increase the NP dispersion stability, several ligands were screened with the aim of improving dispersion stability of functionalized NPs. The NP to RCP binding was evaluated by developing coatings comprised of azide functional groups and stabilizing ligands.

1.1.1 Nanoparticles supplied by Apex Bio

For the experiments performed in chapter 1 of the thesis, Apex Bio supplied a batch of NPs with internal fluorescence that can be measured in the corresponding Cy3 channel to facilitate the development of quantification methods based on measurement of fluorescence intensity from clusters of NPs. The surface of the particles is comprised of silica which can be used to covalently bind functional molecules by utilizing the hydrolysis and condensation of siloxane bonds to covalently bind ligands to the surface of the particles.

1.1.2 Functionalization

Functionalization of the silica surface utilizes the condensation reaction of hydrolysed siloxane bonds to covalently bind ligands to the surface of the NPs. The reaction is catalyzed by increasing the pH using ammonium hydroxide causing the silanol groups on the surface of the NPs to deprotonate while simultaneously hydrolysing the Si-O bonds of the ligand, further favouring the condensation reaction resulting in the formation of siloxane bonds. The functionalization of the surface of silica NPs changes the surface charge of the particles decreasing the electrostatic repulsion, simultaneously binding the nonpolar azide group which will reduce stability in polar solvents. This reaction was used to covalently

bind all ligands evaluated in this chapter 1. The schematics of the ligand functionalization are illustrated in figure 1.[6][9]

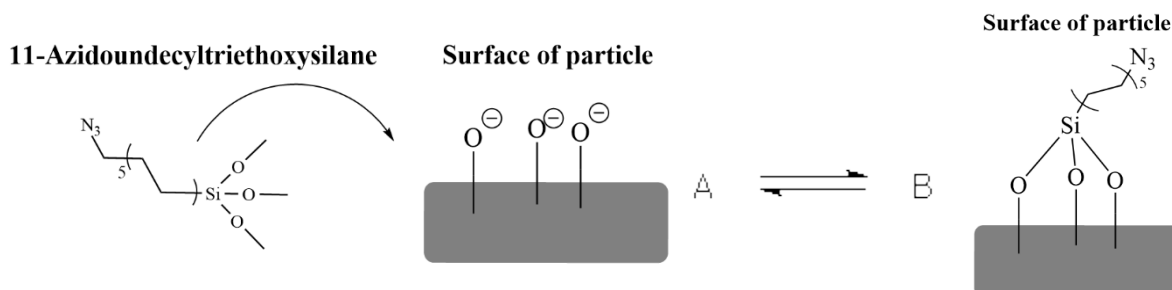


Figure 1: Schematic overview of functionalization of the silica surface on nanoparticles

1.1.3 Click chemistry

Click reactions have the function of forming a covalent link between two molecules using the cycloaddition of an azide group with an alkyne group forming a stable triazole compound. The cycloaddition of alkynes with azides have relatively high activation energy and require a catalyst or high temperature using non-cyclic alkyne reagents. Using dibenzocyclooctyne as the alkyne in the click reaction significantly reduces the activation energy compared to non-cyclic alkynes. The reduction in energy of the cycloaddition is caused by the ring strain induced in cyclic hydrocarbons containing linear SP-hybridized carbon bonds. The linear nature of triple bonded carbons causes significant ring strain in cyclic hydrocarbons with less than 10 carbon atoms in the ring. The enthalpy of a reaction

is determined by the net energy resulting from breaking and making bonds while the activation energy is determined by the energy difference between the initial state of the molecule and the transition state which the reactants will assume before converting into the product. The energy of the ring strain will increase the energy of the alkyne complex effectively decreasing the energy gap between the dibenzocyclooctyne (DBCO) molecule and its transition state. This allows the molecule to react at room temperature without any catalyst present which is why DBCO is an efficient crosslinker commonly used for biomolecule conjugation. In this work, we will investigate how the click reaction can be used to bind NPs to biomolecule targets containing DBCO groups. [8] The reaction is illustrated in figure 2.

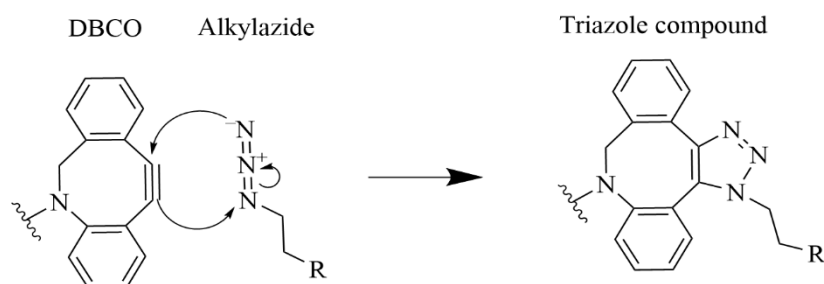


Figure 2: Schematic of the reaction mechanism of copper-free click reaction, DBCO molecule reacts with azide group forming a stable triazole compound.

1.1.4 Dispersion stability of colloidal nanoparticles

Stability of nanoparticle dispersions is determined by several factors. One of the main factors is the intermolecular interaction between the surfaces of nanoparticles. The silica surface of the NPs has negatively charged silanol groups on the surface due to deprotonation causing electrostatic repulsion between particles. This repulsion is preventing the motion of the particles to cause aggregation allowing them to form stable suspensions in water and ethanol. The interaction between the surface of the NPs is described by the DLVO-theory. [5]

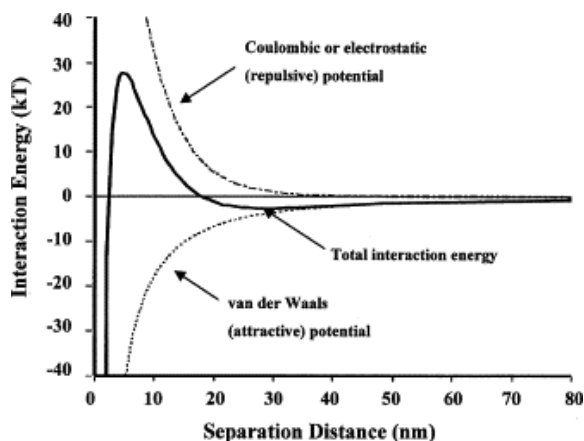


Figure 3: DLVO-graph, positive values represent repulsion and negative values represent attraction. DLVO energy is based on the sum of electrostatic and VDW forces.

The total interaction energy between nanoparticles can either be repulsive or attractive depending on the distance between them. The interactive forces between the particles are comprised of repulsive electrostatic forces and attractive van der Waals (VDW) forces. The theory assumes that the electrostatic and the VDW forces are independent of each other which makes them superimposed meaning they can be added to each other for any distance between the particles down to 5nm. The electrostatic repulsion creates an energy barrier separating the particles, the electrostatic repulsion is highly affected by salt concentration. In the presence of high salt concentrations positively charged ions will form a layer around the negatively charged surface of the particles screening the charges on the NP surface resulting in the reduction of electrostatic repulsion while the VDW interaction are not susceptible to shielding. The presence of salt will thus lower the energy barrier enough for the kinetic energy of colliding particles to overcome the repulsive barrier causing an unstable suspension.[5]

1.1.5 Stabilizing ligands, azide functionalization and coating types

To enable NP to RCP binding the dispersion formed by the NPs must be stable in buffer conditions suitable for DNA hybridization, the NPs are stabilized by modification of their surface and functionalized with azide groups to facilitate binding to biomolecules by utilizing click chemistry. In this chapter, steric stabilization of NP dispersions was evaluated. Three coating types comprised of two stabilizing ligands displayed in figure 4 and 11-azidoundecyltriethoxysilane displayed in figure 5 were evaluated for the surface modification with the aim of stabilizing the nanoparticles for use in buffer conditions, enabling click chemistry conjugation.

Ligand one was mPEG5k-silane which is a polyethylene glycol with a molar weight of 5000. The ligand has three siloxane bonds which can hydrolyse and covalently bind to the silica surface of the NPs. This introduces steric hindrance which increases the separation distance between individual particles by

introducing steric repulsion caused by overlapping electron clouds of the polyethylene glycol chains. The introduced repulsion increases the minimum separation distance between individual NPs reducing the magnitude of attractive VDW forces. The second ligand chosen for this project was Silane-PEG5k-azide. The purpose of this ligand was to functionalize the nanoparticle with azide groups and simultaneously introduce steric hindrance. The evaluated ligands are illustrated in figure 6. [10]

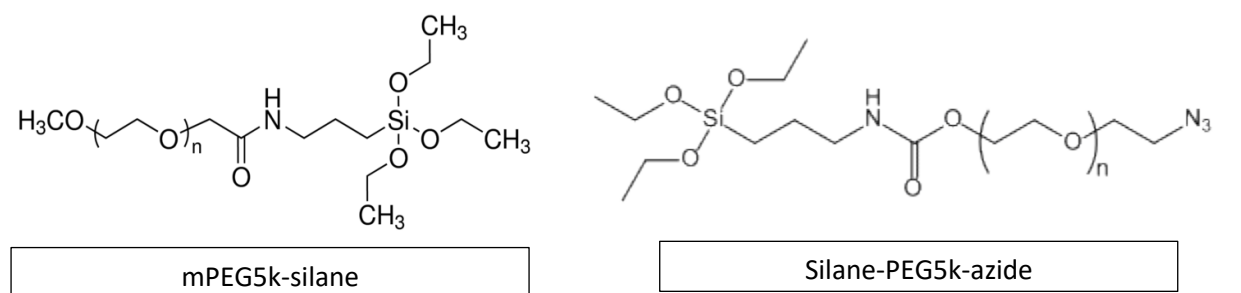


Figure 4: Ligands mPEG5k-silane and silane-PEG5k-azide evaluated during this chapter

In this chapter three types of coating were evaluated. Coating one uses a combination of PEG ligands for stabilization and azide functionalization. Coating 2 uses on the silane-PEG5k-azide for stabilization and azide functionalization. Coating 3 uses mPEG5k-silane for stabilization and 11-undecyltriethoxysilane for azide functionalization. The coating types were evaluated based on stability and azide density. The ligand types of coatings 1-3 are listed in table 1.

Coating type	Ligand 1	Ligand 2
Coating 1	silane-PEG5k-azide	mPEG5k-silane (DMSO)
Coating 2	silane-PEG5k-azide	-
Coating 3	mPEG5k-silane (DMSO)	11-undecyltriethoxysilane

Table 1: Ligands mPEG5k-silane and silane-PEG5k-azide evaluated during this chapter.

1.1.6 Azide functionalization

The purpose of functionalizing the silica surface of the NPs with azide groups is the use of them as crosslinkers for direct RCP binding. Direct RCP binding utilizes DBCO oligos hybridized to RCPs to facilitate the binding mechanism using the click reaction between the azide groups on the particles and the DBCO molecules attached to the RCPs by hybridization. In this work 11-azidoundecyltriethoxysilane is used to functionalize the surface by formation of covalent bonds utilizing the condensation reaction between silanol groups on the surface of the particles and the siloxane bonds of the ligand. The reaction is illustrated in figure 5.

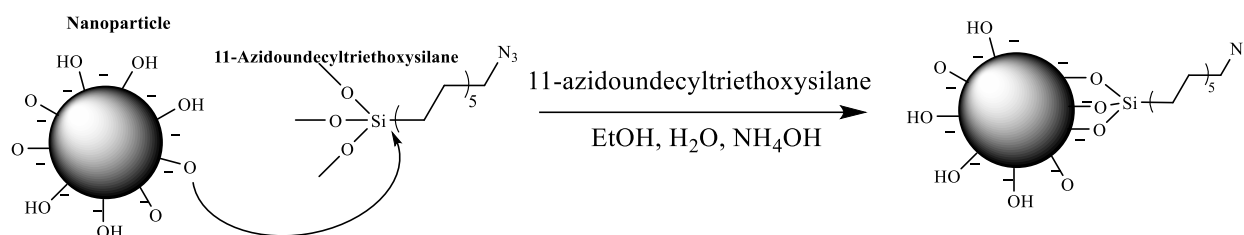


Figure 5: Schematic overview of the azide functionalization of the silica surface on the nanoparticles. The reaction is catalysed by ammonium hydroxide resulting in formation of siloxane bonds between the ligand and the surface of the particles.

1.1.7 Rolling Circle Amplification – RCA

Rolling circle amplification is an enzymatic isothermal amplification method used for amplifying short nucleotide sequences of RNA/DNA. RCA utilizes Phi-29 polymerases that requires a circular template created from the target nucleotide sequence and a padlock-probe (PLP). The first step of creating the circular template is hybridization of the padlock-probe to the target nucleotide sequence, the PLP is a linear oligonucleotide sequence. The ends of the PLPs consist of 20 base pairs(bp) complementary sequences connected by 40-50 bp non-complementary linker sequence [1]. Upon hybridization with the target a circular template is created leaving a nick at the ends of the target nucleotide sequence. The nick is then sealed using DNA/RNA ligase by creating a phosphodiester bond completing the circular template. RCA has high specificity which relies on the specific hybridization of the PLP to the target at both ends of the nucleotide sequence and DNA/RNA ligase which discriminates against mismatches by preventing ligation of the circular template, un-ligated templates will not be amplified as Phi-29 requires circular targets to enable the amplification. Once the circular templates are created, the amplification step is carried out by Phi-29 polymerase resulting in continuous linear amplification of the circular template. The amplification step produces a long single stranded DNA (ssDNA) or RNA (ssRNA) consisting of the repeating sequence of the circular template folding into a macroscale structure. The produced macroscale structure is particularly useful for bio-detection because the repeating nucleotide sequence allows for a high number of detection probes to be bound to each amplified target resulting in high intensity signal and high signal to noise ratio [2]. An overview of RCA is illustrated in figure 6.

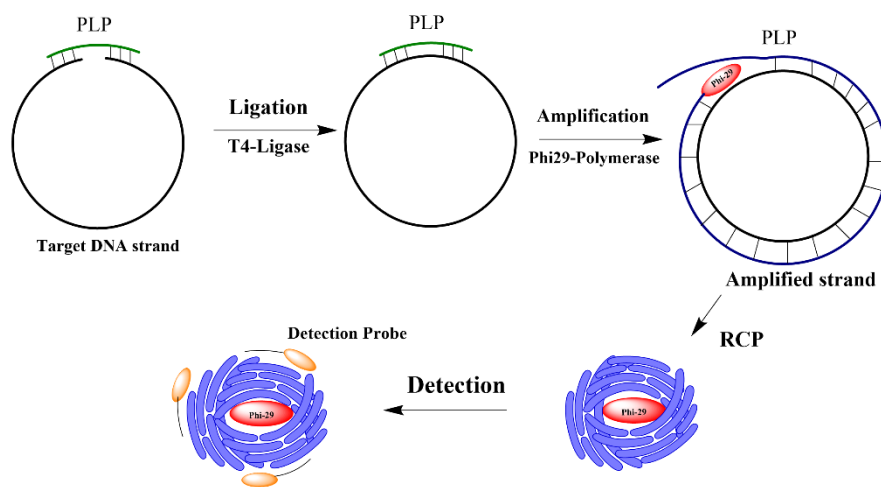
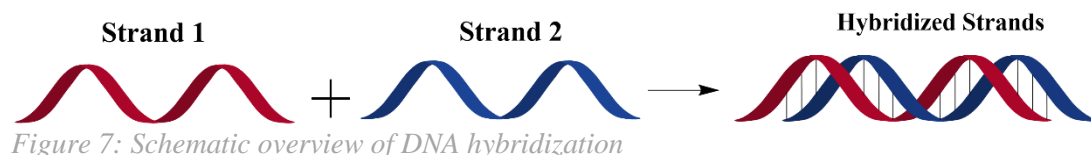


Figure 6: Schematic overview of Rolling Circle amplification.

1.1.8 Nucleic acid hybridization

Nucleic acid hybridization is the process of joining two complementary single stranded DNA (ssDNA) to form double stranded DNA (dsDNA) by annealing complementary nucleotide bases. The dsDNA is facilitated by the formation of hydrogen bonds between complementary nucleotide bases. One important criterion for hybridization to be possible is melting of the nucleic acid strand to be hybridized. The melting temperature T_m reflects the temperature at which equilibrium between breaking and formation of the hydrogen bonds between complementary bases takes place [3]. The schematic of DNA hybridization is illustrated in figure 7.



There are several factors influencing the melting temperature T_m that must be taken into consideration. The concentration of oligonucleotides in the hybridization solution influences T_m by up to ± 10 degrees. T_m is also influenced by the specific nucleotide base sequence which affects the enthalpy of the hydrogen bond formation. A significant factor to consider is salt concentration in the hybridization solution, changing the salt concentration from 30mM to 1M can change the T_m temperature as much as ± 20 degrees. The final factor to consider is the presence of solvents in the hybridization solution, formamide is commonly used in hybridization procedure. The presence of formamide favours denaturation of DNA and bonds to single strands effectively lowering T_m [4].

1.1.9 Addition of DBCO groups to RCPs

To enable click chemistry conjugation of NPs to RCPs, DBCO modified oligos were hybridized to RCP. With the DBCO groups bound to RCP by hybridization the azide groups on the NPs can covalently bind to the RCPs. The binding of DBCO groups to RCPs requires buffer conditions enabling hybridization in all subsequent steps of the NP to RCP binding procedure. A change in solvent conditions can cause the hybridized oligo to denature from the RCP and result in a loss of DBCO groups.

1.1.10 Nanoparticle to RCP binding using click chemistry

This chapter evaluates the binding of nanoparticles to RCPs using click conjugation. The RCPs are labeled with a fluorescent detection oligo and incubated with azide functionalized NPs to facilitate binding by covalent bonding to the DBCO oligo hybridized to the RCP. This method of conjugation is not specific, only the hybridization of the DBCO oligo can facilitate specific binding as the hybridization of the oligo to the RCP can only occur with complementary nucleotide sequences. The Schematic of the reaction is illustrated in figure 8.

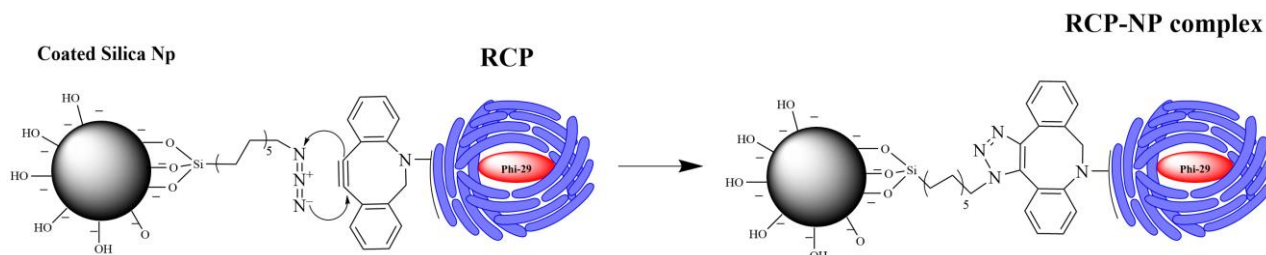


Figure 8: Schematic overview of nanoparticle to RCP binding using click conjugation

1.1.11 Confirming the presence of DBCO groups on RCPs using Cy5-azide

To enable conjugation of NPs to RCPs using click chemistry DBCO oligos must be hybridized to the RCPs to facilitate the click reaction with the azide groups on the surface of the NPs. The following method of confirming the hybridization of the DBCO oligos was evaluated during this chapter. Sulfo-Cy5-azide was incubated with DBCO oligo to fluorescently label the DBCO oligo with Cy5 to enable the detection of the oligo. Following the fluorescent labeling, the DBCO oligo was hybridized to RCPs co-labeled with Cy3-detection oligo. The aim of the designed method was to confirm the binding of the DBCO oligo to the RCPs and evaluate the click chemistry conjugation by utilizing sulfo-Cy5-azide. The schematics of the reaction are illustrated in figure 9. In the case of successful conjugation and labeling of RCPs, colocalized intensities of Cy5 and Cy3 can be measured and compared. If no signal of Cy5 can be detected there are two factors that need to be evaluated. The first factor is the conjugation step of the fluorescent labeling, if it is unsuccessful no Cy5 signal will be detected. The second factor is the hybridization step of the fluorescently labeled oligo, if unsuccessful no Cy5 signal will be detected.

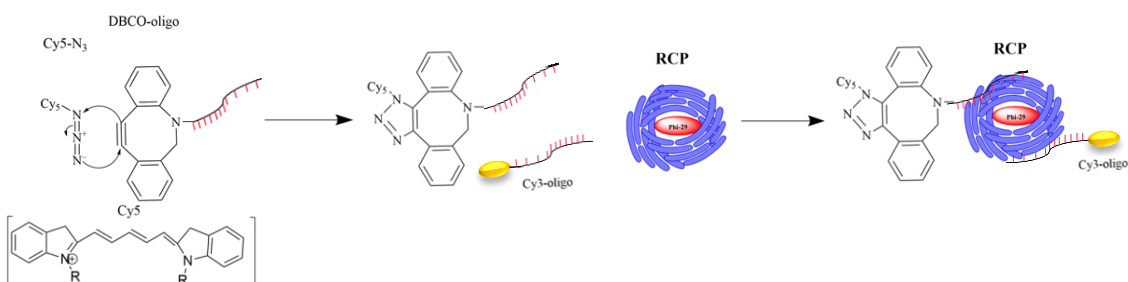


Figure 9: Schematic of Cy5-azide binding to RCPs labelled with DBCO oligo for the evaluation of the conjugation method and the presence of DBCO oligo on RCPs.

1.1.12 Amplified targets for evaluation of nanoparticle binding

In order to evaluate the NP to RCP binding synthetic targets were amplified using a standard RCA protocol listed in methods (1.2.1.4). The synthetic ssDNA used in this chapter was chosen from the genome of HIV virus. The synthetic target and PLP are listed in methods (1.2.1.1). Amplified synthetic targets are called RCPs and are stored in solution, all experiments with RCPs performed in chapter 1-4 used RCP amplified using the described RCA protocol.

1.2 Materials and methods

1.2.1 Materials

1.2.1.1 Amplified targets

The following synthetic target and padlock probe was used for the amplification using RCA. The synthetic target was a nucleic acid sequence specific to the genome of HIV. The padlock probe and synthetic target are listed in table 2. The synthetic targets were ordered from IDT.

Type	Nucleic acid sequence
Synthetic target	CTCTCTCTCTCTATACTATATGTTTTAGTTTATATTGTTCTTTCCCCCTGGCCTTAACCGAATTTTTCCCATTTA TCTAATTCTCCCCGCT
Padlock probe	AAGGCCAGGGGGAAAG AGTAGCCGTGACTATCGACT TCGCTCTATTTAGTGGAGCC TTAAATGGGAAAAAATTCGGTT

Table 2: Synthetic target and padlock probe sequences used for RCP synthesis in chapter 1

1.2.1.2 Oligos

The following oligos were used for the detection of RCPs and NP to RCP binding using DBCO oligo to bind the DBCO group to RCPs facilitating click conjugation. The detection oligos used in chapter 1 are listed in table 3. The detection oligos used in this chapter were ordered from IDT.

Type	Nucleic acid sequence
Cy3 Detection Oligo	5'Cy3-AGTAGCCGTGACTATCGACT
AF750 Detection Oligo	5'AF750-AGTAGCCGTGACTATCGACT
DBCO Detection oligo	5'DBCO-TTTTTTTTTTTTTCGCTCTATTTAGTGGAGCC

Table 3: List of detection oligos used for the labelling of RCPs in chapter 1.

1.2.1.3 Table of chemicals

All chemicals used in chapter 1 are listed in table 4.

Chemical	CAS	Ordered from
Hybridization buffer 1x	-	Prepared by Scilife
Ammonium hydroxide, 28%	62948-80-5	Sigmaaldrich
Silane-PEG5k-azide	-	Nanocs
mPEG5k-silane	-	Sigmaaldrich
11-azidoundecyltriethoxysilane	663171-33-3	Sigmaaldrich
Phi29 polymerase	-	supplied by Scilife
Tth (Dansk) ligase	-	supplied by Scilife
Ethanol (absolute)	64-17-5	Sigmaaldrich
Sulfo-Cy5-azide	-	Lumiprobe
Sulfo-Cy5-DBCO	-	Lumiprobe
BSA	-	Supplied by Scilife
dNTPs	-	Supplied by Scilife
Amplification buffer	-	Supplied by Scilife
Phi29 buffer	-	Supplied by Scilife

Table 4: list of chemicals used during chapter 1

1.2.2 Methods

1.2.2.1 Rolling circle amplification, preparation of RCP solution

1. Ligation, Ligation solution was prepared by adding 31,8 μL of MilliQ water followed by 12 μL of amplification buffer [10x], 12 μL of Padlock probe [1nM], 1,2 μL BSA and 3 μL of Tth ligase enzyme (5U/ μL). Solution was mixed by pipette. 1 μL of synthetic target [10nM] was added to 5 PCR tubes followed by 9 μL MilliQ water. 10 μL of the prepared ligation solution was added to each PCR tube followed by 30 minutes incubation at 60°C using a Biorad S-1000 thermal cycler.

2. Amplification, RCA mix was prepared by adding 25,2 μL of MilliQ water follow by 18 μL of Phi-29 buffer [10x], 9 μL of dNTPs, 0,6 μL of BSA and 7,2 μL of Phi-29 polymerase [10U/ μL]. The RCA mix was mixed by pipette. After the ligation step 10 μL of RCA mix was added to each sample followed by 2-hour incubation at 37°C. After the 2-hour incubation the samples are incubated at 85°C for 15 minutes.

<i>1.Ligation</i>	Stock Concentration	Final Concentration	In each tube [μL]	Ligation mix [μL]
Synthetic target (S03923)	10 nM	1 nM	10	0
Padlock probe (S03877)	1 nM	100 pM	2	12
BSA	20 $\mu\text{g}/\mu\text{l}$	0.2 $\mu\text{g}/\mu\text{l}$	0,2	1,2
Ampl Buffer	10 \times	1 \times	2	12
Tth (Gdansk)	5 U/ μl	0.125 U/ μL	0,5	3
H2O mQ	-		5,3	31,8
		Mix to add	10	60
		Total with mix	20	Total Mix
Reaction time	30 min. 60°C			
<i>2.RCA (in solution)</i>	Stock conc	Final Concentration	In each tube [μL]	RCA mix
dNTP's	2.5 mM	125uM	1,5	9
phi 29 buffer	10x	1 x	3	18
BSA	20 $\mu\text{g}/\mu\text{l}$	0.2 $\mu\text{g}/\mu\text{l}$	0,1	0,6
phi 29 polymerase	10 U/ μL	400mU/ μL	1,2	7,2
H2O mQ			4,2	25,2
		Mix to add	10	60
		Total with mix	30	Total Mix
Reaction Time	37 °C 2 h,	85°C 15 min.		

Table 5: Rolling circle amplification protocol used for the amplification experiment evaluating padlock probe specificity. Step 1 is the reaction conditions for the ligation step creating the circular target. Step 2 is the amplification step which amplifies the ligated circular target. Step 3 is the labelling procedure used for the labelling and detection of the RCPs.

1.2.1.5 Imaging – fluorescent microscopy

All fluorescent microscopy imaging was performed using a standard epifluorescent microscope (Zeiss Axio Imager.Z2) with an external LED light source (Lumencor SPECTRA X light engine). The microscope setup used a light engine with filter paddles (395/25, 438/29, 470/24, 555/28, 635/22, 730/50). Images were obtained with a sCMOS camera (2048 x 2048, 16bit, ORCA-Flash4.0LT Plus, Hamamatsu) using objectives 20x (0.8 NA, air, 420650-9901) and 5x (0.16NA, air, 420630-9900). The setup used filtercubes for wavelength separation including quad band Chroma 89402 (DAPI, Cy3, Cy5) and quad band Chroma 89403 (Atto425, TexasRed, AlexaFluor750). All samples were mounted on an automatic multi-slide stage (PILine, M-686K011).

1.2.1.6 Imaging – SEM

All SEM images were acquired using [1:100] dilution of the nanoparticle stock in pure ethanol followed by deposition of the diluted nanoparticle stock to a silicon wafer by pipetting and drying 4-5 μ L. After the deposition, the sample was covered with a gold layer by gas phase deposition to ensure that the conductivity of the NPs is high enough to prevent charge accumulation & subsequently prevent artefacts in the images. Details about the SEM used for acquiring the images are not currently known.

1.2.1.7 Imaging – TEM

All TEM images were acquired using [1:100] dilution of the nanoparticle stock in pure ethanol followed by deposition of 1-2 μ L of the diluted nanoparticle stock to Formvar-carbon coated copper grid (200 mesh formvar-carbon, Ted Pella, USA). The samples were then dried in ambient condition and imaged using a Hitachi HT-7700 high resolution microscope operated at 100kV.

1.2.1.8 Azide quantification using Cy5-DBCO

1. Sample preparation and incubation, Nanoparticle stock was sonicated for 30 seconds prior to pipetting. 30 μ L of nanoparticle solution was pipetted to a screwcap tube (1.5 mL) followed by 69 μ L MilliQ water and 1 μ L of Sulfo-Cy5-DBCO. The solution in the screwcap tube was then vortexed for 10 seconds at max setting. The sample was then incubated at 37°C for 1 hour with 1000RPM mix. The sample was incubated using an Eppendorf comfort (5355) thermomixer. The reaction conditions are listed in table 6.

2. Washing, upon completed incubation the sample was centrifuged for 15 minutes at 21350 CRF followed by the removal of supernatant. The sample was then redispersed in 1ml of absolute ethanol. The washing procedure was repeated 3x times and the sample was redispersed in 30 μ L of absolute ethanol.

Cy5-DBCO click	Concentration	Volume to add	Final concentration
Azide functionalized nanoparticle stock	-	30 μ L	-
Sulfo-Cy5-DBCO	0.5mM	1 μ L	5 μ M
Water (MilliQ)	-	69 μ L	-
Total volume	100 μ L		
Incubation after chambers filled	37°C 1h		
2. Washing	Centrifugation 3x	15min at 21350 CRF	Redispersion in 30 μ L

Table 6: Reaction protocol for the quantification of azide density using Cy5-DBCO.

3. **Preparation of imaging slide**, two hybridization chamber (Grace Bio-labs, Secure-seal hybridization chamber 8-9mm Diameter x 0,8mm depth) were attached to a coverglass (Menzel-Gläser 24 x 50 mm #1,5).

4. **Filling of hybridization chambers**, The desired nanoparticle solution was diluted [2:100] in MilliQ water, 50 μL of the diluted solution was pipetted to the hybridization chambers. The circular holes of the hybridization chambers were covered with circular plastic covers (3M VHB). The prepared cover glass with the attached and filled hybridization chambers was placed on a superfrost slide with the hybridization chambers oriented towards the glass.

5. **Imaging**, After the slide preparation the samples were imaged using the microscope setup described under methods in section 1 of the thesis. The images were acquired with the 5x (0.16NA, air, 420630-9900) objective. The imaging parameters used 50 μm total Z-height with 2,5 μm slice thickness.

1.2.1.9 Ligand functionalization of nanoparticles

1. **Sample preparation and incubation**, Nanoparticle stock was sonicated for 30 seconds prior to pipetting. Ethanol, MilliQ water and ammonium hydroxide was pipetted to a screwcap tube (1,5 mL). 100 μL of nanoparticle stock was pipetted to the screwcap tube following by pipetting of the ligands (11-undecyltriethoxysilane, mPEG5k, silane-PEG5k-azide). The sample was vortexed for 10 seconds on max setting. The sample was then incubated at 37°C over night with 1000RPM mix. The sample was incubated using an Eppendorf comfort (5355) thermomixer. The reaction conditions of coatings 1-3 are listed in table 7,8,9.

2. **Washing**, upon completed incubation the sample was centrifuged for 15 minutes at 21350 CRF followed by the removal of supernatant. The sample was then redispersed in 1ml of absolute ethanol. The washing procedure was repeated 3x times and the sample was redispersed in 30 μL of absolute ethanol.

Coating 1	Concentration	Volume to add	Final concentration
Nanoparticle stock	-	100 μL	-
Ammonium hydroxide	2,8 vol%	20 μL	5 μM
silane-PEG5k-azide	10mM	10 μL	0,16mM
mPEG5k (DMSO)	20mM	45 μL	1,5mM
Water (MilliQ)	-	425 μL	-
Total volume	600 μL		
Incubation after chambers filled	37°C O.N 1000RPM		
2. Washing	Centrifugation	15min at 21350	Redisperion in 30 μL
	3x	CRF	

Table 7: Protocol conditions used for functionalization of nanoparticles, coating 1.

Coating 2	Concentration	Volume to add	Final concentration
Nanoparticle stock	-	100 µL	-
Ammonium hydroxide	2,8 vol%	20 µL	0,093 vol%
silane-PEG5k-azide	10mM	10 µL	0,16mM
Water (MilliQ)	-	425 µL	-
Total volume	600 µL		
Incubation after chambers filled	37°C O.N 1000RPM		
2. Washing	Centrifugation 3x	15min at 21350 CRF	Redisperion in 30µL

Table 8: Protocol conditions used for functionalization of nanoparticles, coating 2.

Coating 3	Concentration	Volume to add	Final concentration
Nanoparticle stock	-	100 µL	-
Ammonium hydroxide	2,8 vol%	20 µL	0,093 vol%
11-Azidoundecyltriethoxysilane	256,3	2,5 µL	0,16mM
mPEG5k-silane (DMSO)	20mM	10 µL	0,33mM
Ethanol absolute		243	
Water (MilliQ)	-	225 µL	-
Total volume	600,5 µL		
Incubation after chambers filled	37°C O.N 1000RPM		
2. Washing	Centrifugation 3x	15min at 21350 CRF	Redisperion in 30µL

Table 9: Protocol conditions used for functionalization of nanoparticles following coating 3.

1.2.1.10 Protocol for RCP labelling

Hybridization buffer used in following protocol had the composition listed in table 10.

Hybridization buffer (in MilliQ water)	
Component	Concentration
Tris-HCL	20mM
EDTA	20mM
NaCL	200mM
Tween-20	0,2 vol%

Table 10: Composition of Hybridization buffer used in following protocols

1. preparation of labelling solution, 90 μL of hybridization buffer 2x was pipetted to a Eppendorf tube (1,5 mL) followed by 88,2 μL of MilliQ water and 1,8 μL of detection oligo [1 μM], mixed by pipette. If the labelling solution contains multiple oligos, 1.8 μL of each oligo was used and the volume subtracted from the MilliQ water resulting in a total volume of 180 μL .

3. Labeling solution	Stock Conc.	Final Conc.	Volume
Detection oligo	1 μM	5 nM	1,8 μL
Hybridization buffer	2x	1x	90 μL
H2O mQ			88,2 μL
			180 μL
			Total Mix
Reaction Time	> 75°C 2 min, 55°C 15 min		

Table 11: Protocol conditions for the labelling procedure of RCPs

2. Sample preparation and incubation, 10 μL of RCP solution was pipetted to a PCR tube (200 μL) followed by 10 μL of labelling solution. The sample was incubated for 75°C for 2 minutes followed by 55°C for 15 minutes. The incubation was performed using a Bio-Rad S-1000 thermal cycler.

3. Imaging, After incubation, 10 μL of each sample was pipetted to a superfrost-plus slide (25x75x2mm) and covered with a coverglass. The samples were imaged using following the imaging protocol described under methods.

1.2.1.11 Click protocol of NPS to mobile RCPs

1. Preparation of labelling solution, following the above labelling protocol 86,4 μL MilliQ water is pipetted to an Eppendorf tube (1,5 mL) followed by 90 μL Hybridization buffer 2x. 1,8 μL of AF750-detection oligo is pipetted to the tube followed by 1,8 μL of DBCO-oligo. The solution is mixed by pipette.

2. labelling of RCPs, labelled following “Protocol for RCP labelling”

3. NP-RCP click reaction, 10 μL of DBCO and AF750 labelled RCP solution was pipetted to a PCR tube (200 μL) followed by 10 μL of [2:100] nanoparticle solution diluted in MilliQ water. Sample was incubated at 37°C for 1 hour using a Bio-Rad S-1000 thermal cycler.

4. Imaging, samples were imaged following ‘labelling protocol –Imaging’

1.3 Results and discussion

1.3.1 Size characterization using SEM

The size of the nanoparticles supplied by Apex Bio was characterized using SEM. The mean size of the particles was calculated by manual measurement of individual particles using ‘Image J’ software with a population size of 40 particles. Overlapping particles and aggregates were excluded in the analysis to increase the accuracy of the size measurement. The measured mean size and distribution can be seen in figure 10. The standard deviation of the supplied nanoparticles was measured to 5 % with the size population ranging from 75-95 nm. The results of the size characterization using SEM concludes that the nanoparticles supplied by Apex Bio are highly monodisperse.

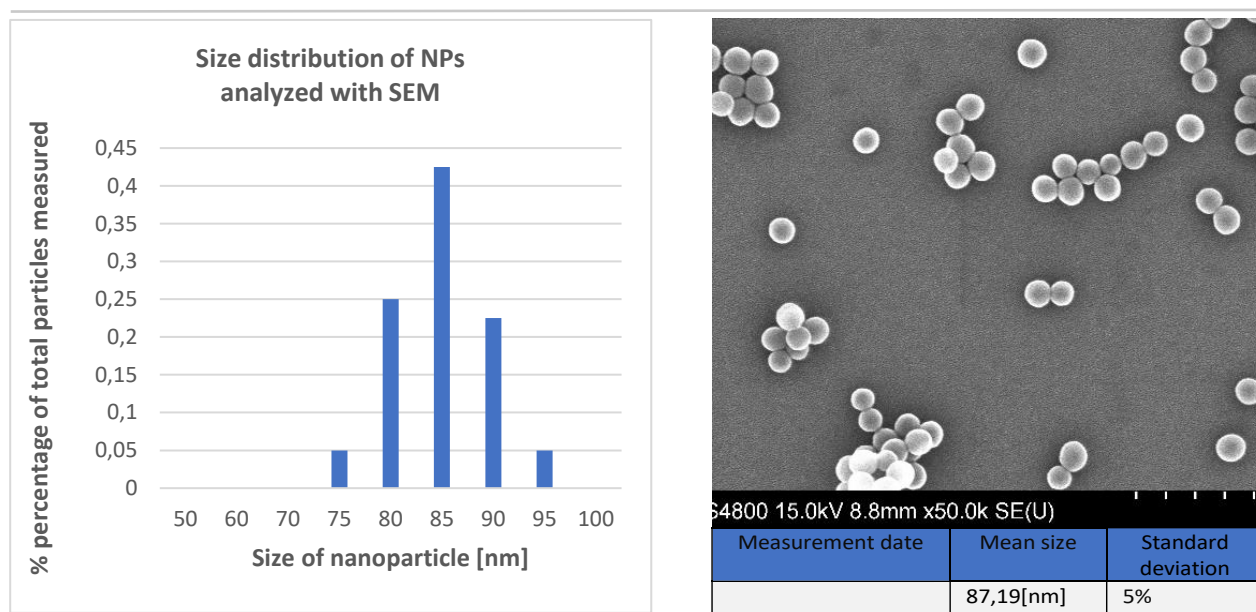


Figure 10: Calculated mean size and distribution of from images obtained by SEM using 15kV and 50x magnification. The mean size and distributions were calculated with manual measurement of particles using Image J software

1.3.2 Size characterization using TEM

To complement the size characterization using SEM the supplied nanoparticles were characterized using TEM. The obtained TEM images were analysed with the same method of manual measurement using ‘Image J’ software and a population size of 40 particles. Overlapping particles and aggregates were excluded in the analysis in the analysis to increase the accuracy of the size measurement. The calculated mean size of the particles and the size distribution can be seen in figure 11. The calculated mean size of the particles was 95,36 [nm] with a standard deviation of 4% which is slightly larger compared to the SEM measurement. The low standard deviation indicates that the nanoparticles supplied by ‘Apex Bio’ are highly monodisperse.

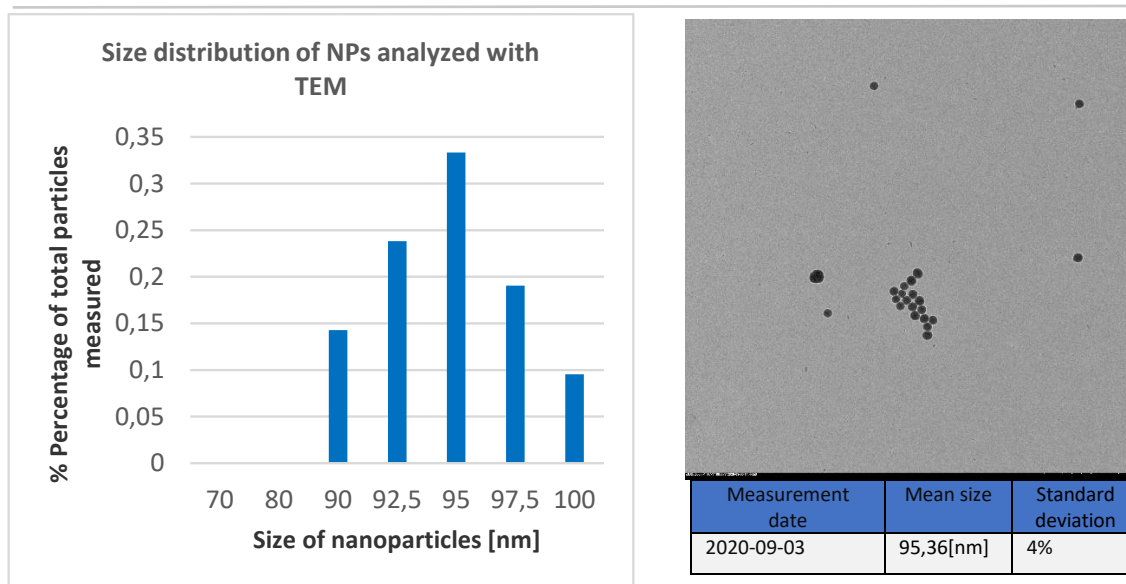


Figure 11: Calculated mean size and distribution of from images obtained by SEM using 100kV and 6k magnification. The mean size and distributions were calculated with manual measurement of particles using Image J software

1.3.3 Size analysis conclusion

SEM and TEM analysis yielded precise size distribution measurements with SEM yielding 5 % standard deviation and TEM yielding 4% standard deviation. There are several factors that can account for the difference in the calculated mean size. For the SEM analysis the particles were covered with a gold layer that might have an impact on the size of the particles displayed in the obtained images. The second factor is the time difference of the performed imaging as the particle stock was used to the extent of depletion between the two imaging occasions. The reason this can have an impact on the imaged & calculated size is that larger particles sediment to the bottom of the NP stock container faster than the smaller particles. The impact of this should not be significant as the particle stock is vortexed before aliquots for experiments are made. The final factor that could have had an impact on the measured size is the sampling process for the SEM and TEM measurement. The pipetting of the NP stock removes 1-2 μl of the stock which is a small percentage of the total stock volume. This introduces the risk of the sampling being inhomogeneous and not depicting the size distribution accurately, additionally the deposition of the sample to prior to imaging can cause a variation of size distribution depending on which part of the sample was imaged. Having this in mind the mean size of the particles in the range of 87-95 nm is acceptable for the purpose of using them for the development of the emission evaluation method considering the low standard deviation of the particle size.

1.3.4 Quantification of NP azide density using Cy5-DBCO

In order to quantify the azide density on the surface of the particles the click reaction was utilized to bind a labelling agent to the azide groups on the surface of the functionalized NPs. DBCO functionalized Cy5 was incubated with the azide functionalized NPs, after the incubation step free Cy5-DBCO was removed by centrifugation and removal of supernatant followed by bulk imaging to measure the intensity ratio of Cy5 fluorescence and NP fluorescence imaged in the Cy3 channel. The purpose of measuring the intensity ratio instead of absolute intensities of Cy5 was to calculate a relative azide density without knowing the exact concentration of NPs in the solution. For this project no reliable method of estimating

the NP concentration was available and a concentration loss of NPs will occur after every washing step, for this reason it was not feasible to use a single measurement of stock concentration combined with absolute intensities of Cy5 fluorescence to measure the relative azide density. The reaction is illustrated in figure 12.

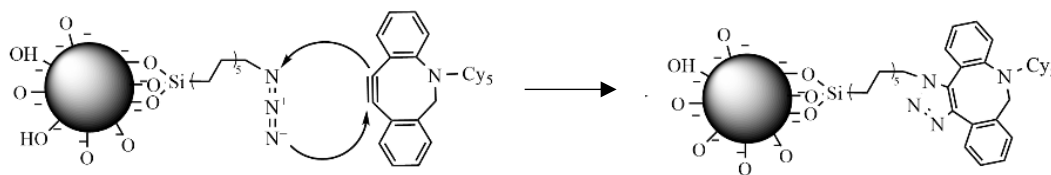


Figure 12: Schematic overview of the click reaction binding Cy5-DBCO to the azide groups on the surface on NPs.

First step of developing the azide quantification method using Cy5-DBCO was finding the optimal incubation time for the click reaction. The azide functionalized NP batch was diluted [30:100] in water with 5 μ M concentration of Cy5-Sulfo-DBCO incubated at 37C and 1000RPM. Every two hours an aliquot of the reaction was removed and washed by centrifugation. After the washing step all aliquots were diluted and imaged following the imaging protocol described in methods, the resulting Cy5/Cy3 ratio are displayed in figure 13. The 2 hour incubation aliquot yielded the highest Cy5/Cy3 ratio, meaning that longer incubation reduced this value. The likely cause for the decrease in Cy5/Cy3 ratio with time is the hydrolysis of siloxane bonds in the presence of water. The reaction kinetics of the click reaction is significantly faster than of the hydrolysis of siloxane bonds, the optimal incubation time for the CY5-DBCO control was determined to be within the span of 0-2 hour, 1 hour incubation time was used for future quantification experiments. To further optimize the quantification method a repeat of the experiment should be performed using a time span of 0-2 hours incubation with measurements occurring every 30 minutes. There is a risk of using suboptimal incubation time in the case of 1 hour incubation yielding lower Cy5/Cy3 ratio compared to 2 hours incubation. The Cy5/Cy3 ratios of the reaction are plotted in figure 13.

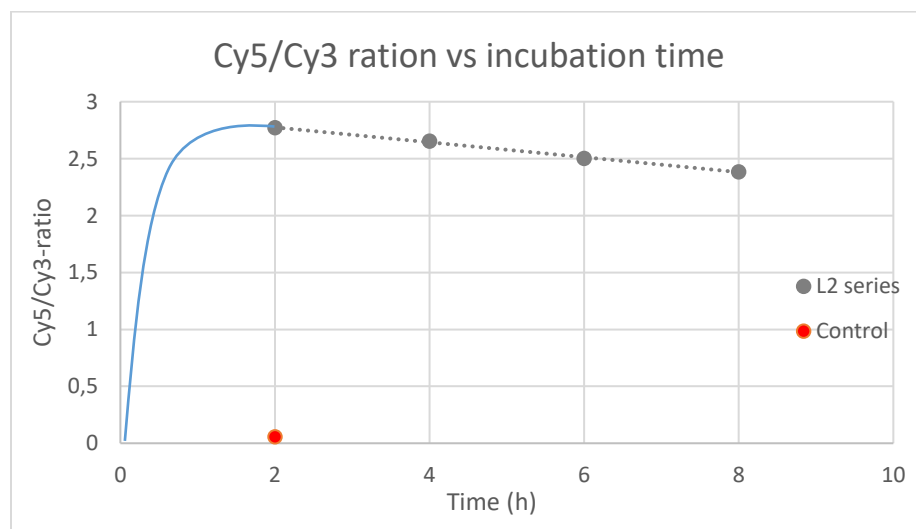


Figure 13: Cy5/cy3 ratio measurements of azide functionalized nanoparticles conjugated to Cy5 fluorophores. The Cy5/Cy3 ratio is plotted against the incubation time of the Cy5 conjugation reaction

and is measure by imaging the sample in hybridization chambers using the 5x objective and 100ms exposure time for both channels. The sample was imaged using z-stacks, total height 50 μ m with 2.5 μ m slice thickness.

1.3.5 Coating deterioration

The hydrolysis of siloxane bonds presents an issue for b storage of functionalized nanoparticles and incubation time of reactions. To determine which solvent would be feasible for storage of functionalized nanoparticles a batch of nanoparticles was functionalized with azidosilane and separate aliquots of the same functionalized NP batch were stored in different solvents. The Cy5-DBCO control was performed on both batches at day 1, 7 and 19. The results of the experiment indicate that the batch stored in water shows significant hydrolysis of the siloxane bonds while the aliquot stored in ethanol shows a slight increase in Cy5/Cy3 ratio. This increase of the fluorophore intensity ratio can be explained by bleaching of the internal fluorescence (Cy3) of the NP batch which indicates that the intensity decrease of the aliquot stored in water is greater than presented in the results. With the conclusion of this experiment all NP batches were stored in ethanol with the vials stored in dark boxes in the fridge to avoid bleaching. The hydrolysis of the stabilizing bonds was an important factor to consider, the kinetics of the hydrolysis mechanism are highly temperature and PH dependent. When using functionalized NPs to label RCPs the incubation time will have a correlation with the stability of the NP dispersion as the PH of buffers used in DNA application are slightly basic and will increase the rate of hydrolysis. The measured Cy5/Cy3 ratios are plotted in figure 14.

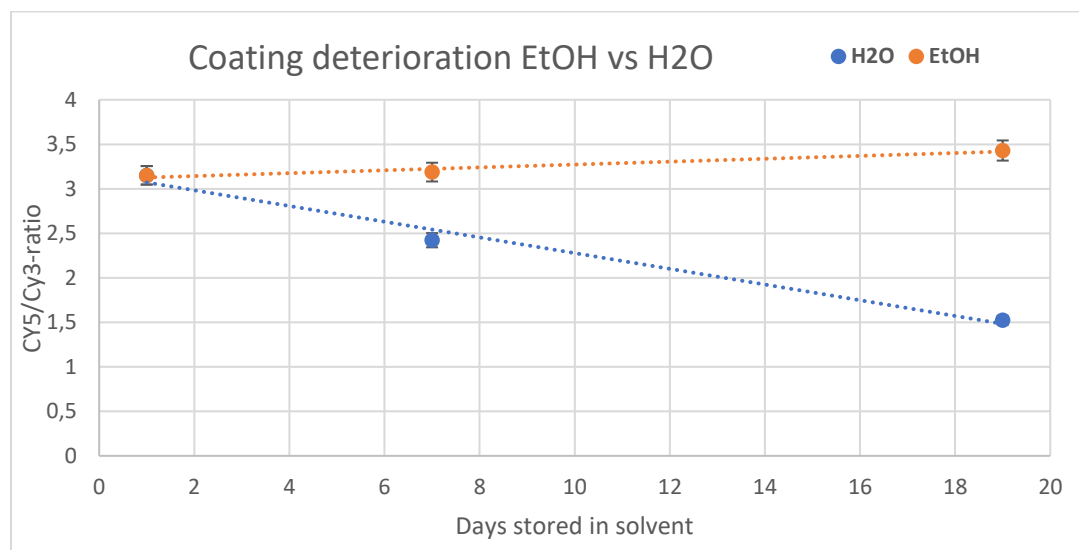


Figure 14: Cy5/Cy3 ratio representing density of azide groups on the surface of a single nanoparticle batch plotted against number of days stored in the solvent. Aliquots of the sample were made at day 1, 7 and 19 following azide quantification using the azide quantification protocol described in methods (1.3.4).

1.3.6 Evaluation of stabilizing ligands

The stability of the three coating types was evaluated by diluting the dispersed nanoparticle sample in hybridization buffer 1x and imaging the sample in hybridization chambers following the protocol described in methods. The buffer concentration was chosen with the purpose of evaluating the NP stability in conditions used for RCP labelling by hybridization of oligos. The buffer concentration is required for the DBCO-oligo to bind to RCPs facilitating NP to RCP binding by utilizing click chemistry. Coating 1 exhibited highest stability of the three coating types and was stable in 1x hybridization buffer,

the fluorescent signal was homogenous in the range of the entire sample indicating no presence of aggregated NPs. Coatings 2 and 3 displayed instability in hybridization buffer 1x, both samples had a speciation of aggregated NPs of different sizes indicating that a relatively high percentage of the NPs was in an aggregated state. These results indicate that coatings 2 and 3 perform poorly in buffer conditions suitable for DNA hybridization and will result in poor binding to RCPs with a high concentration of aggregated NPs that are not bound to RCPs. The images of the stability control are displayed in figure 15.

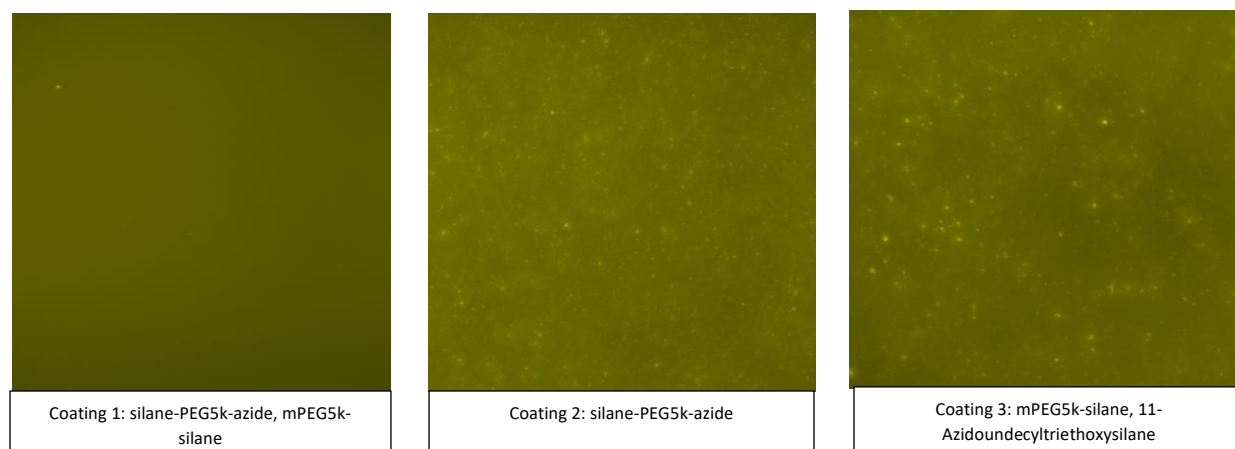


Figure 15: Coating 1 (Silane-PEG5k-azide, mPEG5k-silane), coating 2(silane-PEG5k-azide) and coating 3(mPEG5k-silane, 11-azidoundecyltriethoxysilane) diluted [2:100] and imaged in hybridization chambers following the protocol described in methods. All samples were imaged using 100ms exposure time in the Cy3 channel.

The relative azide density of the three coatings was evaluated using the developed quantification method following the protocol described in methods. Coating 3 yielded the highest azide density indicating that the reaction kinetics of 11-undecyltriethoxysilane is significantly higher than of mPEG5k which is supported by the stability testing conducted in the previous experiment. Coating 1 resulted in a low azide density and a stable dispersion indicating that the majority of the ligand density was comprised of mPEG5k-silane. Coating two yielded relatively high azide density and was not stable in the buffer conditions indicating low success rate of subsequent NP to RCP binding. The instability of coating 2 and 3 is believed to be caused by higher azide density on the surface of the NPs. There is a correlation of azide density on the surface of NPs and stability in aqueous buffers. This represents a complex problem to solve for successfully binding NPs to RCP by utilizing click chemistry. For efficient NP to RCP binding there must be a minimum azide density on the surface of NPs which is not known. The destabilizing effect of the azide groups combined with variables introduced by other ligands increases the difficulty of evaluating this problem. If the NP dispersion is not stable it is not possible to isolate which variable is causing the NP to RCP binding to fail. The next step of evaluating the coatings was confirming that the DBCO oligos are hybridized to the RCPs using sulfo-Cy5-azide. The Cy5/Cy3 ratios are plotted in figure 16.

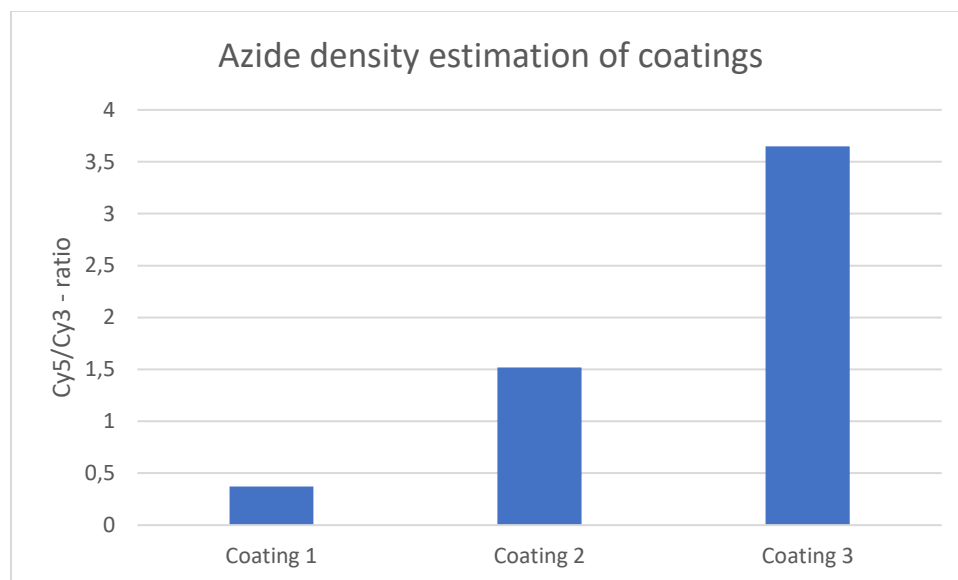


Figure 16: Cy5/Cy3 ratio of Coating 1 (Silane-PEG5k-azide, mPEG5k-silane), coating 2(silane-PEG5k-azide) and coating 3(mPEG5k-silane, 11-azidoundecyltriethoxysilane) measured following the azide quantification protocol. All samples were imaged using 100ms exposure in both channels.

1.3.7 Confirmation of DBCO groups on labelled RCPs using CY5-azide

In order to confirm the presence of the DBCO groups on the RCPs the method described in the introduction (1.1.9) was evaluated. An experiment was designed with three samples of different sulfo-Cy5-azide concentrations and 0.1 μM DBCO oligo incubated in hybridization buffer 0.8x in order to fluorescently modify the DBCO oligo. The composition of hybridization buffer is listed under methods (1.2.1.10). After incubation, the Cy5 conjugated oligo was used to co-label RCPs with Cy3-detection oligo. The purpose of the co-labelling was to confirm that the Cy5 signal is co-localized with the Cy3-detection oligo that is known to hybridize successfully.

Evaluation of Cy5-azide to RCP binding		
	Cy5-azide concentration	Incubation time
Sample 1	0,1 μM	6 hours
Sample 2	0,33 μM	5 hours
Sample 3	0,5 μM	4 hours

Table 12: Sample list of the experiment evaluating the use of click chemistry conjugation using Cy5-azide.

After conjugation of the sulfo-Cy5-azide to the DBCO-oligo the oligo was used to co-label RCPs with standard cy3-detection oligo following the labelling protocol described in methods. The resulting images of the samples were manually analyzed using Zeiss software by measuring the max intensity of RCPs subtracted by the background using line profile. The co-labelling experiment yielded co-localized signal of the standard Cy3-detection oligo and the DBCO-oligo conjugated to sulfo-Cy5-azide. The intensities of the co-labelled detection oligos in figure 17 show a clear correlation of the sulfo-Cy5-azide concentration in the conjugation step and the resulting intensity. With the results of this experiment the presence of DBCO oligo on the RCPs and the click conjugation in hybridization buffer were confirmed. with the DBCO oligo present on the RCPs and the click conjugation **working** in hybridization buffer the next step was to evaluate the NP to RCP binding.

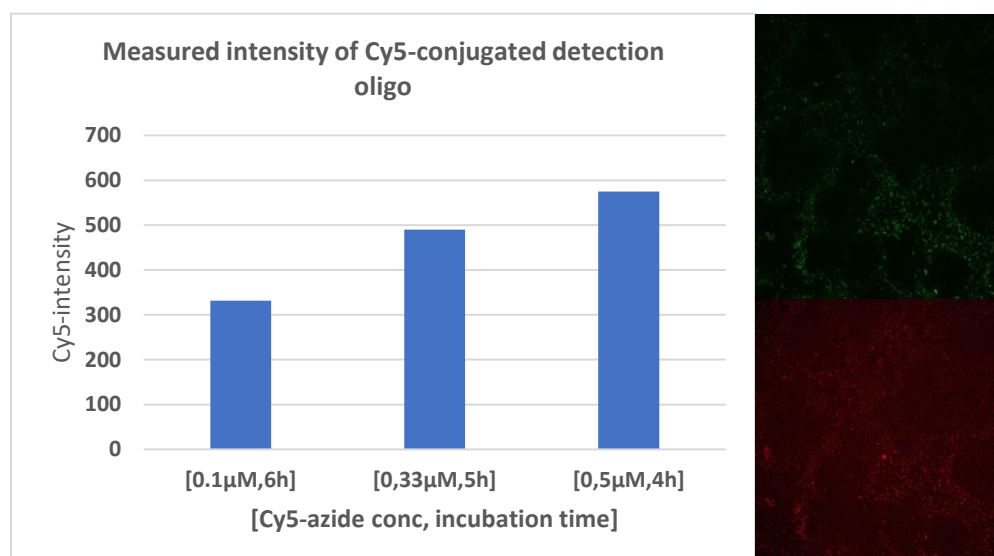


Figure 17: measured RCP intensities labelled with DBCO-oligo conjugated with sulfo-Cy5-azide in the previous experiment. All images were acquired using the 20x objective, 5 μm Z-stack height and 0,25 μm slice thickness. 100ms exposure time was used for both channels.

1.3.8 Nanoparticle to RCP binding using coating 1,2,3

The NP to RCP binding using click conjugation was evaluated using nanoparticles functionalized with Coating 1 (Silane-PEG5k-azide, mPEG5k-silane), coating 2(silane-PEG5k-azide) and coating 3(mPEG5k-silane, 11-azidoundecyltriethoxysilane). The NP to RCP binding was performed with mobile RCPs in hybridization buffer 0.25x following the method described in the introduction (1.1.8). The RCPs were co-labelled with AF750-detection oligo displayed in green and nanoparticles (displayed in red). The nanoparticle to RCP binding was unsuccessful and no significant co-localized signal was detected. The experiment was repeated, and the buffer concentration varied with no successful results. There can be several potential causes for the unsuccessful results of the nanoparticle to RCP binding. The NPs in the sample showed signs of aggregation indicating instability of the NP dispersion likely caused by a combination of the destabilizing azide groups and hydrolysis of the siloxane bonds by which the stabilizing ligands are bound. The incubation time for the experiment is 1 hour which is significantly lower compared to the previous experiment confirming the hybridization of the DBCO oligo to RCP, the incubation time has an effect on to what extent the click conjugation is completed but the cause is most likely due to instability of the NP dispersion as there were high number of NP aggregates present in the samples. As a means of decreasing the destabilizing factor of the azide groups the next step was to vary the solvent composition of the NP to RCP binding step. Varying the solvent can have an effect on DNA hybridization, decreasing the polarity in the solvent can reduce the degree of deprotonation of DNA and cause hybridized ssDNA to denature. Before evaluating the NP to RCP binding in modified solvent conditions the stability of hybridized oligos has to be evaluated in the modified solvent conditions. The next step of this chapter was to evaluate the stability of fluorescent detection oligos hybridized to RCPs in a series of solvent conditions. Coating 1 resulted in a stable dispersion in the stability test performed in (1.3.6), the likely cause of coating 1 failing to bind to the RCPs by click conjugation was the lower azide density of that coating. The following evaluations of NP to RCP binding was performed using coating 2,3. The resulting images of the samples are displayed in figure 18.

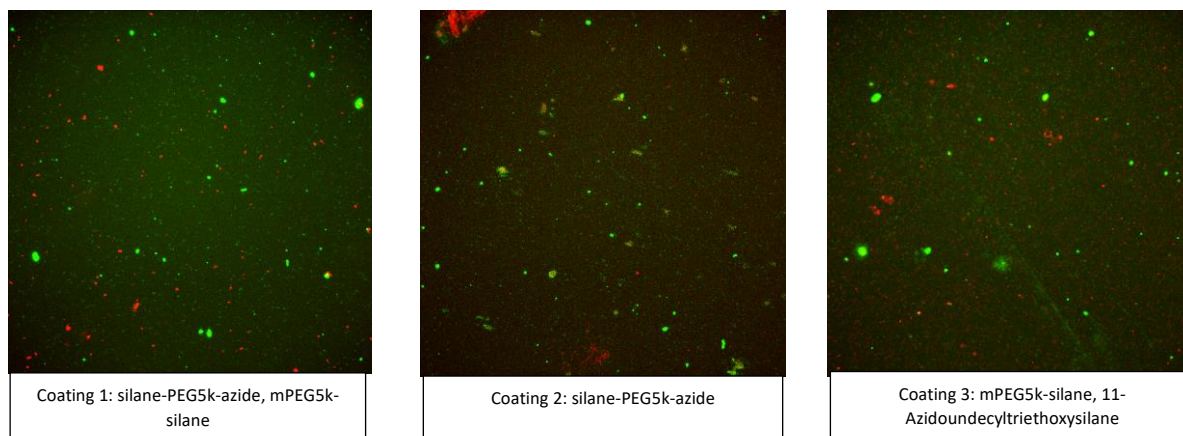


Figure 18: Images of nanoparticle to RCP binding using the protocol described in methods. The Images were acquired using the 20x objective with 5 μm Z-stack height and 0,25 μm slice thickness. 100ms exposure time was used for both channels.

1.3.9 Denaturation of hybridized detection oligo in polar solvents

To evaluate the stability of hybridized oligos the following experiment was designed. RCPs were labelled with Cy3-detection oligo following the labelling protocol described in methods(1.2.1.10). The labelled RCPs were immobilized on superfrost slides and hybridization chambers were attached. The hybridization chambers were then filled with the solvent and the slides were incubated at 37°C for 1hour. The evaluated solvents were chosen to cover a range of polarity with different solvent compositions. Hybridization buffer 1x was used as a reference to estimate the loss of signal intensity due to denaturation of the Cy3-detection oligo from the RCPs. After the incubation the solvent was removed and imaging performed in slowfade for all samples. The measured intensities showed a clear correlation of solvent polarity and reduction in signal intensity of labelled RCPs due to denaturation of detection oligo. The denaturation occurs due to change in dielectric constant of the solvent which effects the pKa of deprotonation for the nucleic acid bases of DNA. The degree of deprotonation of nucleic acid bases have significant effect on the ability of ssDNA to hybridize and form dsDNA. The ethanol sample yielded approximately 33% reduction of intensity after 1 hour incubation. The intensity decrease is significant but there were still detection oligo hybridized to the RCPs. The detection oligo signal in the 100% ethanol sample indicate that ethanol could be used in the NP to RCP binding step without denaturing all of the hybridized DBCO oligos from the RCPs. The next step of the chapter was to evaluate the NP to RCP binding in 50% ethanol. The experimental data is plotted in figure 19. [11]

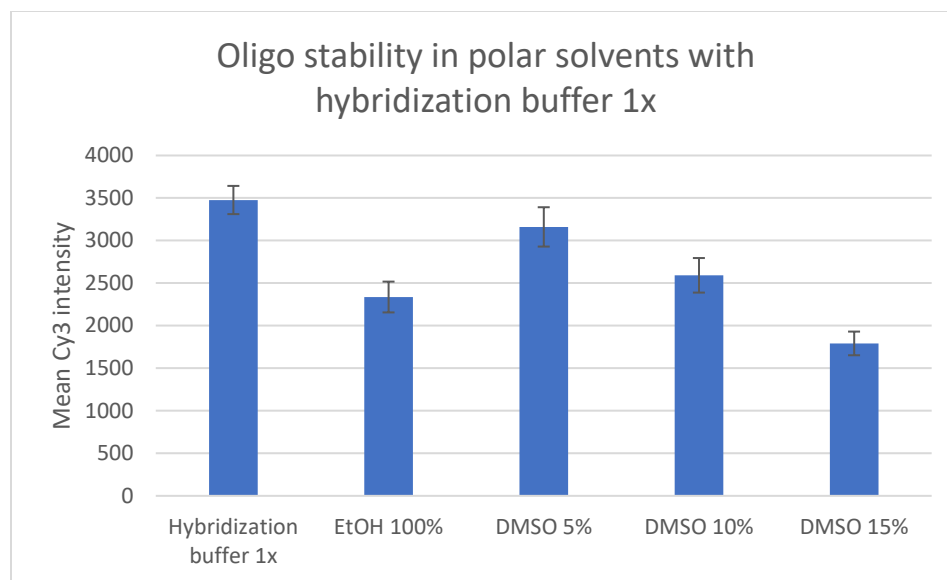


Figure 19: Measured Cy3 intensity of RCPs (prelabelled with Cy3-detection oligo) incubated for 1 hour at 37°C in various solvent conditions. The mean intensities were measured by using line profile in Zeiss software.

1.3.10 Nanoparticle to RCP binding using coating 2,3 with modified solvent conditions

In the previous experiment the stability of oligo hybridized to RCPs in 100% ethanol was evaluated, the next step of developing the NP to RCP binding was repeating the NP to RCP binding experiment with modified solvent conditions. Coating 2 and 3 were chosen for the evaluation of NP to RCP binding. Coatings 2 and 3 were chosen due to their higher azide density, with 50% ethanol in the solvent the aim was to increase the stability of the NP dispersion enabling the high azide density coatings to form a stable dispersion facilitating the click reaction used to bind NPs to the DBCO oligo hybridized to the RCPs. In the experiment a negative control consisting of bare NPs was included, the bare NPs are not functionalized and have no coating. Images of all samples are displayed in figure 20.

All samples of the experiment yielded co-localized signal of the NP channel (Cy3) and the detection oligo channel (AF750). The colocalized signal in the negative control excludes the click reaction as the binding mechanism. The likely cause of the colocalized signal in all samples could therefore be formation of aggregated complexes of NPs and RCPs. The formation of aggregated complexes is facilitated due to the solvent containing 50% ethanol. The ethanol in the solvent weakens the hydrogen bonding that stabilizes the structure of the RCPs. The weakened structure of the RCPs can interact with the charges present on the surface of NPs and form complexes containing multiple NPs and RCPs. To better understand the cause of the colocalized signal further investigation has to be conducted. A series of NP to RCP binding experiments with multiple solvent conditions has to be performed to determine the range of solvent polarity and dielectric constant that yields colocalized signal in all samples. The evaluated range of solvent conditions can then be complemented with existing data on DNA stability on polar solvents for further investigation of the NP and RCP complex formation. The NP to RCP complex formation can be used for the evaluation of the NP emission by comparing signal intensity of fluorescently labelled detection oligos to the NP signal. The main purpose of performing the NP to RCP binding is to enable measurement of NP emission from aggregates of similar size to RCPs. Comparing the signal intensity of

NPs to RCPs enables estimations of minimum exposure time necessary for the detection of RCPs and a general understanding of the intensity increase NP probes can provide.

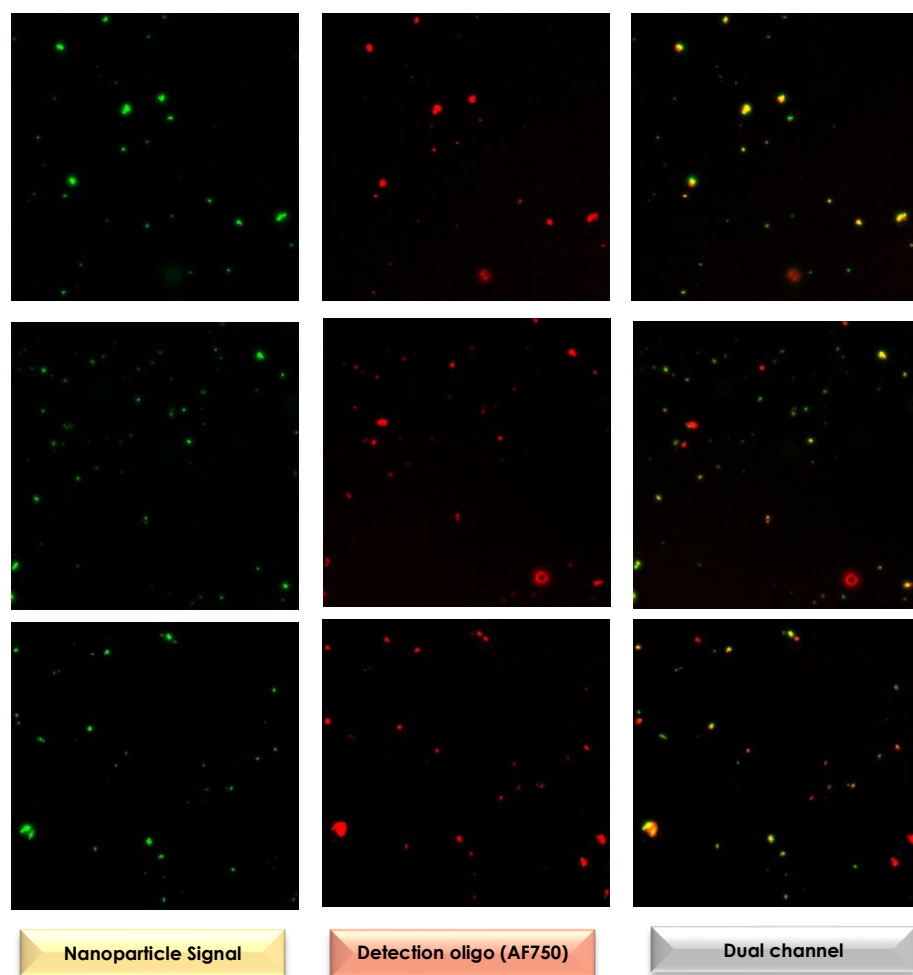


Figure 20: Images of nanoparticle to RCP binding using the protocol described in methods with the solvent changed to 50% ethanol, 50% MilliQ water. The Images were acquired using the 20x objective with 5 μm Z-stack height and 0,25 μm slice thickness. 100ms exposure time was used for both channels.

1.3.11 Evaluation of nanoparticle emission using aggregation method

For this part of the chapter a specific nanoparticle batch was supplied by ‘Aplex Bio’. The previous nanoparticles used for the development of the quantification methods were fluorescent in the Cy3 channel with relatively low intensity. For this experiment, a batch of high intensity nanoparticles was analyzed and compared to standard detection oligo based on intensity. The signal is highly co-localized and can be analyzed by image processing, the aggregates are slightly larger compared to standard RCPs but the method is highly useful for measuring the emission of nanoparticles. The aggregation method of forming complexes of NPs with RCPs is highly useful as it is a method of evaluating emissions that does not require any stabilization of functionalization prior to the analysis. The method has the benefit of

performing rapid evaluation of NP emission directly after synthesis reducing the required time for performing measurements by several days

The bare NP stock of the high intensity NPs was used to evaluate the fluorescent signal intensity of the NPs. The procedure was identical to the previous experiment performed with 50% ethanol. The resulted images was similar to the previous experiment yielding colocalized NP and detection oligo (AF750) signal. The intensity of the NP emission was analyzed by zeiss software using line profile in the next section. Images of the sample are displayed in figure 21.

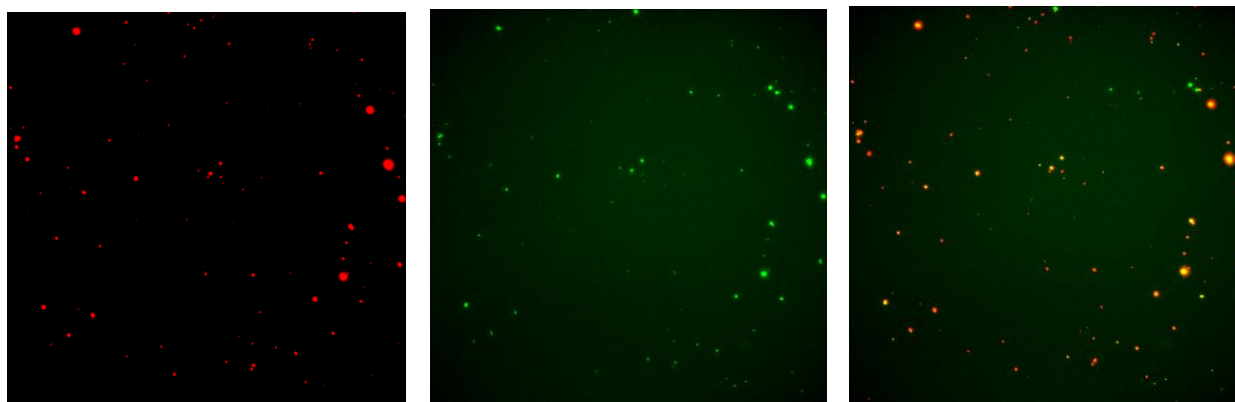


Figure 21: RCPs labelled with AF750-detection oligo followed by aggregation with high intensity nanoparticles using protocol described in methods. Nanoparticles are imaged in CY3 channel using 100msm exposure, detection oligo channel is acquired using 500ms exposure time.

The nanoparticle emission of the high intensity NP batch was analyzed with Zeiss software using line profile to measure the maximum value subtracted by the local background for the aggregates. The high intensity nanoparticle batch has significant advantage compared to standard detection oligos. The measured intensity cannot be directly interpolated to NPs bound to RCPs as the size of the aggregates deviates slightly from standard RCP size. The intensity of the NP signal was significantly higher by a factor of 15 using 5 times lower exposure time in the detection oligo channel (AF750). The advantages of such a large increase in intensity are significant, imaging times can be reduced by using lower exposure times for imaging and the higher intensity can enable the detection of RCPs synthesized with lower amplification time, which in theory will result in a lower limit of detection by using high intensity fluorescent probes. The intensities are displayed in figure 22.

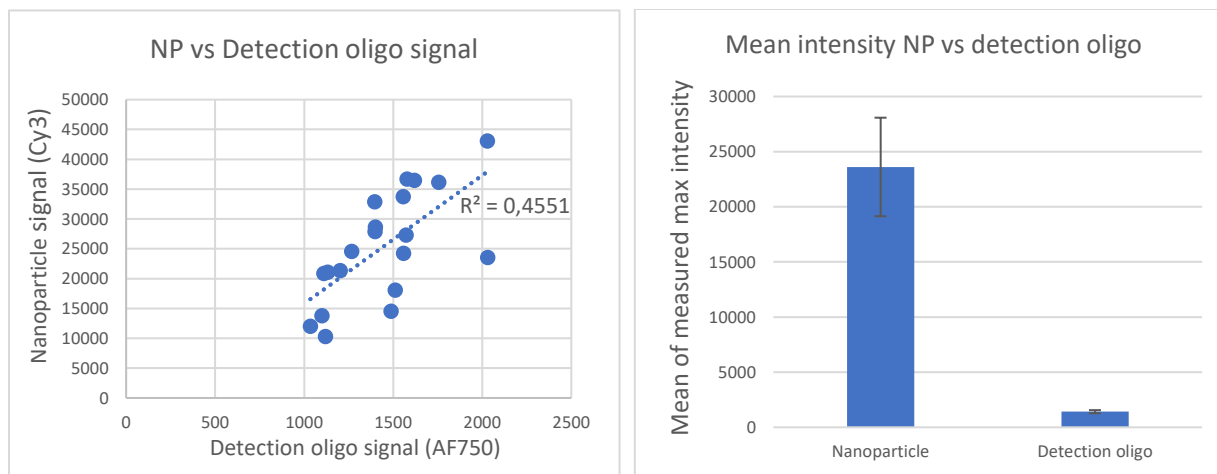


Figure 22: Nanoparticle emission analyzed using Zeiss software. The intensity of the signal was measured using line profile with background subtraction. Nanoparticle signal was measured in Cy3 channel using 100ms exposure time, detection oligo channel is acquired using 500ms exposure time.

1.4 Conclusions

There were several goals in this chapter, quantifying and optimizing the azide density on the surface of the particles. Evaluating stabilizing ligands by functionalizing nanoparticles with three types of coating and evaluating their ability to bind to RCP by conjugation utilizing click chemistry. Developing a method for measuring nanoparticle emission and characterizing the emission of a high intensity nanoparticle batch supplied by “Aplex Bio”.

1. Nanoparticles were successfully functionalized and a method of quantifying the relative azide density on the nanoparticles was developed by utilizing Cy5-DBCO and fluorescent quantification.
 2. combinations of mPEG5k-silane, silane-PEG5k-azide and 11-azidoundecyltriethoxysilane were evaluated based on stability and azide density. The subsequent binding of the functionalized nanoparticles to RCPs was unsuccessful.
 3. A method of evaluating nanoparticle emission was developed utilizing nonspecific aggregation of nanoparticles with RCPs forming aggregates of slightly larger size compared to standard RCPs.
 4. The emission of the high intensity nanoparticle batch was analyzed using the developed aggregation method. The emission was significantly higher than standard detection oligos indicating promising applications in areas where amplification time of target and exposure time during imaging is of importance.
-

2. Oligo functionalization of nanoparticles for efficient probing

2.1 Introduction

In this chapter, the click chemistry evaluated in chapter 2 was used to functionalize a batch of nanoparticles supplied by Apex Bio. The supplied nanoparticles have been stabilized and azide functionalized by surface modification using proprietary technology developed by Apex Bio. In chapter 2 a method of evaluating NP emissions was developed using aggregation of NPs and RCPs to mimic nanoparticle to RCP binding. A method was developed for the quantification of oligo density on the surface of the particles. The hybridization efficiency and specificity were evaluated by designing experiments with matching and mismatching sequences of detection oligo functionalized to the surface of NPs, the NPs were then hybridized to amplified synthetic targets of HIV and SARS-COV-2.

2.1.1 Oligo functionalization

The functionalization of the NPs was performed using click chemistry evaluated in chapter 1 of the thesis. Conjugation of biomolecules can be achieved using a variety of functional groups. The main advantages of using click chemistry are selectivity and kinetics of the click reaction. The NPs were functionalized with oligo by using a detection oligo with DBCO modification on the 5-prime end of the oligo. The DBCO molecule reacts selectively with azide groups resulting in a stable triazole compound. The reaction requires no catalyst due to the ring strain of the DBCO molecule reducing the energy gap between the original state of the molecule and its transition state. With conjugation using DBCO and azide crosslinkers, use of conjugation chemistry susceptible to hydrolysis can be avoided. The functionalization of the NPs using DBCO oligo, facilitates high reaction control in water-based buffers. This is beneficial for developing probes for biological application, which requires high salt concentrations for the stability and function of DNA. The schematic of the reaction used for the functionalization is illustrated in figure 23. [13]

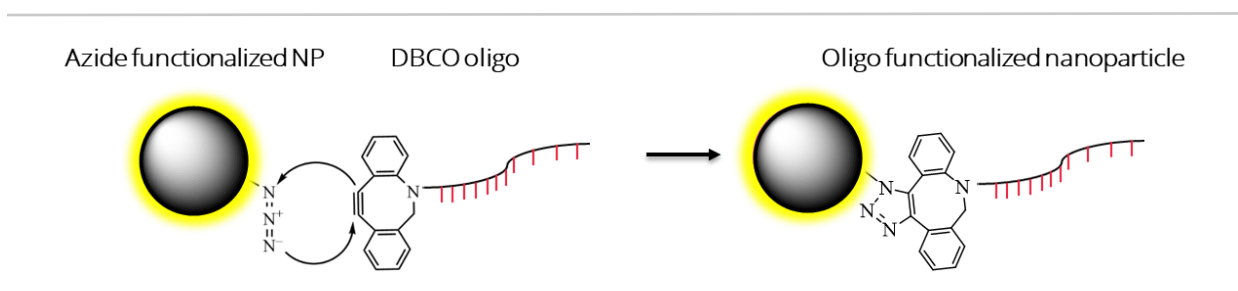


Figure 23: Schematic overview of the click reaction used for functionalization of nanoparticles.

For the nanoparticle functionalization performed in chapter 3, two DBCO oligos with sequences complementary to HIV and SARS-COV-2 were used. The DBCO oligos were ordered from IDT which provides custom modification of oligos and purification by HPLC. The oligos used in this chapter are listed in table 13. The oligos were designed with a spacer separating the DBCO molecule and oligo sequence that targets the RCPs. The spacer is comprised of 11 thymine molecules and its purpose is to

separate the oligo sequence from the surface of the particles. The purpose of separating the oligo from the NP surface is to allow the part of the oligo that binds to its target to come close enough to the RCPs to facilitate binding. This reduces the risk of nanoparticles not being able to bind to their target because of repulsion occurring between nanoparticles and RCPs at small distances.

2.1.3 Nucleic acid hybridization of functionalized nanoparticles to RCPs

Nucleic acid hybridization is the process of joining two complementary ssDNA strands to form dsDNA. The process is facilitated by the formation of hydrogen bonds between complementary nucleotide bases which is dependent on the degree of deprotonation of nucleic acid bases. The deprotonation of a nucleic acid sequence is dependent on pH of the solvent, the subsequent salt concentration of the required pH buffer has a significant impact on the colloidal stability of nanoparticle dispersions. The nanoparticles used for this chapter have been provided by Apex Bio and are stable for use in SSC 1x buffer which facilitates efficient nucleic acid hybridization. There are several prerequisites for successful NP to RCP hybridization, the nanoparticle dispersion must be stable in the buffer conditions suitable for nucleic acid hybridization. The surface density of nucleic acid sequences used for the hybridization to the RCPs must be high enough to enable efficient hybridization to the target. The hydrodynamic diameter of the nanoparticles cannot be too large, if the hydrodynamic diameter is too large the distance between the nanoparticles and the RCPs will be too large which inhibits the hybridization of complementary strands. The specificity of the binding is an important factor, the nucleic acid sequence used to functionalize the nanoparticles must be dissimilar to other targets present in tested sample to enable specific binding to the target. The hybridization specificity is highly dependent on the stringency of DNA hybridization, the stringency is dependent on the buffer conditions and incubation temperature used for the hybridization. High temperatures and low salt concentrations result in high stringency which permits only permits hybridization between nucleic acid sequences that are highly similar. Low temperature and high salt concentration results in low stringency which permits hybridization between dissimilar strands, choosing the right reaction conditions is crucial for the enabling specific hybridization between two nucleic acid sequences. The hybridization of NPs to RCPs will result in a complex of several NPs bound to RCPs by hybridization and the aim in this chapter is to develop NPs that bind with high specificity. The nucleic acid sequence used to functionalize the NP should only bind to RCPs amplified from synthetic targets and PLPs that have complementary nucleic acid sequence. In the case of a RCP with mismatching nucleic acid sequence the NPs should not bind to the target, the schematic of specific NP binding is illustrated in figure 24. [13][14]

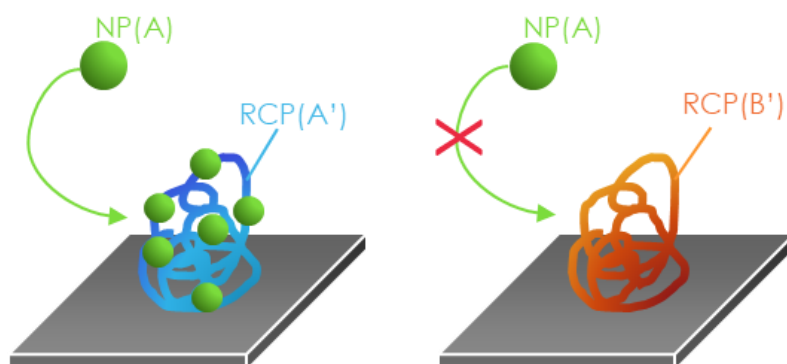


Figure 24: Schematic overview of nanoparticle to RCP binding.

2.2 Materials and methods

2.2.1 Materials

The DBCO oligos used for functionalization of NPs were ordered from IDT with DBCO modification on the 5-prime end. The oligos are listed in table 13.

Oligo type	Nucleic acid sequence
DBCO oligo (SARS-COV-2)	5'DBCO-TTTTTTTTTTTGCGTCTATTAGTGGAGCC-3'
DBCO oligo (HIV)	5'-/5DBCO/TTTTTTTTTTTCCTCAGTAATAGTGTCTTAC-3'

Table 13: DBCO oligos used for the functionalization of NPs in chapter 2.

List of synthetic targets and PLPs used in chapter 2, all synthetic targets and PLPs were ordered from IDT. The synthetic targets and PLPs are listed in table 14.

Type	Nucleic acid sequence
Synthetic target	
HIV	CTCTCTCTCTCTACTATA TGTTTATGTTTATTTGTTCTTTCCOCTGGCCTTAA CCGAA TTTTTCCTCA TTTATCTAA TTCTCCCCGCT
Padlock probe	
HIV	AAGGCCAGGGGAAAG AGTAGCCGTGACTATCGACT TCGCTCTATTAGTGGAGCC TTAAATGGGAAAAAATTCGGTT
Synthetic target	
SARS-COV-2	5'Biotin-CTCTCTCTCTCTCTCTCTCTCTCTCTCTCTCGGTGTGACAA GCTACAACA CGTTGTA TGTTCGAGCAA
Padlock probe	
SARS-COV-2	TGTTGTAGCTTGTCA CACCGGTGTATGCAGCTCCTCAGTAATAGTGCTTACGGCATCACTGGTTACGTCTGTTGCTCGCAA ACATACAACG

Table 14: List of synthetic targets and padlock probes used for RCA in chapter 2.

The following oligos were used for the detection of RCPs, the AF750 complementary oligo was used to quantify oligo density on the surface of NPs. All oligos were ordered from IDT. The oligos are listed in table 15.

Type	Nucleic acid sequence
AF750 Oligo (HIV)	5'AF750-AGTAGCCGTGACTATCGACT
AF750 Oligo (SARS-COV-2)	5'AF750-TGTAAGACACTATTACTGAAGA
AF750 Oligo (complementary)	5'/5Alex750N/TTT GGAGTCATTATCACAGAATG

Table 15: list of detection oligos used in chapter 2.

The chemicals and reagents used in this chapter are listed in table 16.

Chemical	CAS	Ordered from
Hybridization buffer 2x	-	Prepared by Scilife
Phi29 polymerase	-	supplied by Scilife
TTh (Dansk) ligase	-	supplied by Scilife
BSA	-	Supplied by Scilife
dNTPs	-	Supplied by Scilife
Amplification buffer	-	Supplied by Scilife
Phi29 buffer	-	Supplied by Scilife
Click buffer (Aplex Bio)	-	Supplied by Aplex Bio

Table 16: chemicals and buffers used in chapter 2.

2.2.2 Methods

2.2.2.1 Functionalization of nanoparticles with DBCO-oligo

1. **Sample preparation and incubation**, the nanoparticle stock was sonicated for 30 seconds prior to pipetting. 50 μL of the nanoparticle stock was pipetted to an Eppendorf tube (1,5 mL) following by 112,6 μL of the buffer solution provided by Aplex Bio. 4 μL of DBCO oligo [100 μM] was pipetted to the solution followed by vortexing for 10 seconds at setting 7-8. The sample was incubated for 2hours at 37 $^{\circ}\text{C}$ and 1000 RPM mixing, Eppendorf thermomixer (Thermomixer comfort 5355) was used for the incubation. Reaction conditions are listed in table 17.

Oligo functionalization	Concentration	Volume to add	Final concentration
Nanoparticle stock (bare)	-	50 μL	-
Click buffer provided by Aplex Bio	1x	112,6 μL	0,675x
DBCO oligo	100 μM	4 μL	3,43 μM
Total volume		166,6 μL	
Incubation		37 $^{\circ}\text{C}$ 2h	
2. Washing	Centrifugation: 3x	15 min at 21350 RPM	
Redispersion volume	50 μL	Absolute Ethanol	

Table 17: protocol conditions, reaction parameters of the nanoparticle functionalization step.

2.2.2.2 Quantification of oligo density on nanoparticle surface

Sample preparation steps. The nanoparticle stock was sonicated 30 seconds and added (20 μ L) to an Eppendorf tube (1.5mL). MilliQ water (128 μ L) was added to the Eppendorf tube followed by 50 μ L [4x] SSC buffer, reaction tube vortexed for 10 seconds at max setting. 2 μ L of Alexa Fluorophore [100 μ M] labeled detection oligo complementary to the sequence of the nanoparticles was added to the Eppendorf tube followed by 10 seconds vortex at max setting. The sample was incubated 1 hour at 37°C. Protocol conditions are listed in table 18.

1. Hybridization	Stock concentration	Volume to add (stock)	Final concentration
Oligo-NP stock	Stock	20 μ L	[1:10]
SSC buffer	4x	50 μ L	1x
Water (MilliQ)	-	128 μ L	-
AF750 Detection oligo	100 μ M	2 μ L	1 μ M
Total volume		200 μ L	
Incubation		37°C 1h	
2. Washing	Centrifugation: 3x	15 min at 21350 RPM	
Redispersion volume	20 μ L	SSC 1x buffer	

Table 18: Protocol conditions for the oligo density quantification of nanoparticles by hybridization with AF750 detection oligo.

Washing. After incubation, the sample was washed three times by centrifugation at 21350 RPM for 15 minutes, followed by removal of supernatant and redispersion in 200 μ L SSC buffer [1x]. Upon completed washing procedure the sample was redispersed in 20 μ L absolute ethanol.

2.2.2.3 Solid phase hybridization

Immobilization of RCPs. Circles approximately 0.5 cm in diameter were marked on superfrost slides using a diamond tip pen. 4-5 μ L of RCP solution was pipetted to the marked circles followed by drying in a 37°C oven for 5 minutes. The schematics of the immobilization process are shown in figure 25.

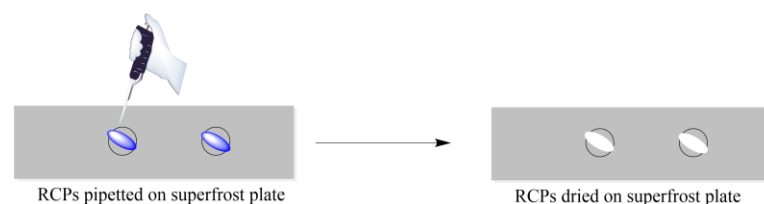


Figure 25: Schematic overview, the immobilization of RCPs on superfrost slides.

Preparation of labelling solution. Following the protocol in table 19, 130.7 μ L MilliQ water was pipetted to an Eppendorf tube (1.5 mL) followed by 45 μ L SSC [4x] buffer. The Eppendorf tube was vortexed for 10 seconds at max setting. 2,5 μ L of the nanoparticle stock was pipetted to the Eppendorf tube followed by 1,8 μ L of AF750 Detection oligo [1 μ M].

Solid phase hybridization	Concentration	Volume to add	Final concentration
Oligo-NP stock	-	2,5 μL	-
AF750 Detection oligo	1 μM	1,8 μL	5 nM
Water (MilliQ)	-	130,7 μL	-
SSC buffer	4x	45 μL	1x
Total volume		166,6 μL	
Incubation after chambers filled		37°C 1h	

2. Washing

Washed with PBS-Tween buffer using pipette

Table 19: protocol conditions of preparation labelling solution for dual labelling of RCPs with detection oligo and functionalized nanoparticles.

Attachment and filling of hybridization chambers. After immobilization of RCPs on the superfrost slides hybridization chamber (specify) were attached covering the marked circles on the slides. 45-50 μL of the labelling solution prepared in the previous steps was pipetted to the hybridization chambers followed by sealing of the chamber using circular plastic covers.

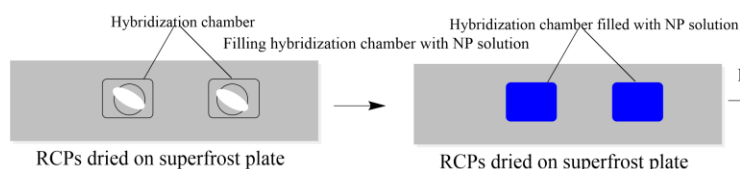


Figure 26: Schematic overview, attachment of hybridization chambers to superfrost slides and filling of attached hybridization chamber with labelling solution.

Incubation and washing. After the filling and covering of hybridization chambers the slides were incubated for 1 hour in a 37°C oven. Once the incubation is complete the slides were removed from the oven and the labelling solution removed by pipette. The hybridization chamber was then washed 3x times with PBS-Tween buffer by pipette.

Detachment of hybridization chamber and preparation of sample for imaging. After the washing step the hybridization chamber are removed by slowly pipetting 2 μL of absolute ethanol around the edges of the hybridization chambers following detachment using tweezers. Before imaging of the samples 6-7 μL of slowfade was pipetted to the marked circles and covered with coverslip glass followed by imaging.

2.2.2.4 Liquid phase hybridization

Preparation of labelling solution. Following the protocol in table 20, MilliQ water (130 μL) was pipetted to an Eppendorf tube (1.5 mL) followed by 45 μL SSC [4x] buffer. The Eppendorf tube was vortexed for 10 seconds at max setting. 2,5 μL of the nanoparticle stock was pipetted to the Eppendorf tube followed by 1,8 μL of AF750 Detection oligo [1 μM].

Liquid phase hybridization	Concentration	Volume to add	Final concentration
Oligo-NP stock	-	2,5 μL	-
AF750 Detection oligo	1 μM	1,8 μL	5 nM
Water (MilliQ)	-	130,7 μL	-
SSC buffer	4x	45 μL	1x
Total volume		166,6 μL	
Incubation after chambers filled		37°C 1h	

Table 20: protocol conditions, preparation of labelling solution for dual labelling of RCPs with detection oligo and functionalized nanoparticles

Sample preparation and incubation. After the preparation of the labelling solution 10 μL of RCP solution was pipetted to a PCR tube (200 μL) followed by 10 μL of the labelling solution prepared in the previous step. The sample is then incubated in a PCR thermo cycler for 1h at 37°C. After incubation the 10 μL of the sample is pipetted on a superfrost slide and covered with a coverslip glass followed by imaging.

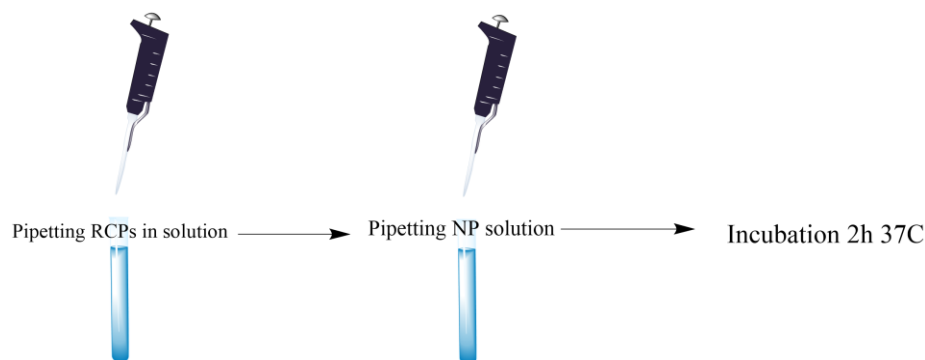


Figure 27: Schematic overview, hybridization of nanoparticles to mobile RCPs in solution

2.2.2.5 Imaging of nanoparticle solution in hybridization chambers

- Preparation of imaging slide,** two hybridization chamber (Grace Bio-labs, Secure-seal hybridization chamber 8-9mm Diameter x 0,8mm depth) were attached to a coverglass (Menzel-Gläser 24 x 50 mm #1,5).
- Filling of hybridization chambers,** The desired nanoparticle solution was diluted [2:100] in MilliQ water, 50 μL of the diluted solution was pipetted to the hybridization chambers. The circular holes of the hybridization chambers were covered with circular plastic covers (3M VHB). The prepared cover glass with the attached and filled hybridization chambers was placed on a superfrost slide with the hybridization chambers oriented towards the glass.
- Imaging,** After the slide preparation the samples were imaged using the microscope setup described under methods in section 1 of the thesis. The imaging were acquired with the 5x (0.16NA, air, 420630-9900) objective. The imaging parameters used 50 μm total Z-height with 2,5 μm slice thickness.

2.3 Results and discussion

2.3.1 Developing method of oligo density quantification

Enabling reproducible oligo functionalization of nanoparticles requires a method of quantifying the relative amount of oligo on the surface of the particles. The method of oligo quantification evaluated for this project was based on hybridization of the oligo functionalized particles to a complementary oligo sequence labelled with the fluorophore Alexa Fluor. 750, measuring the relative intensity of the internal fluorescence of the particles and the hybridized labelled oligo provides relative values of oligo density on the surface of the particles. The NP concentration in the stock was not known for this project, absolute intensities could not be used to quantify the relative oligo density on the NPs. For this reason the intensity ratio of complementary AF750 oligo and NP fluorescence was necessary. The NP fluorescence is a bulk solution is directly correlated to the concentration of NPs in the solution. The internal fluorescence was used as a reference to quantify the relative oligo density on the NPs. The signal produced by the NPs can be measured in the Cy3 channel and is defined as Cy3 signal for discussion purposes. The hybridization was performed in SSC 1x buffer using 1 hour incubation at 37°C, the schematic overview of the hybridization control is illustrated in figure 28.

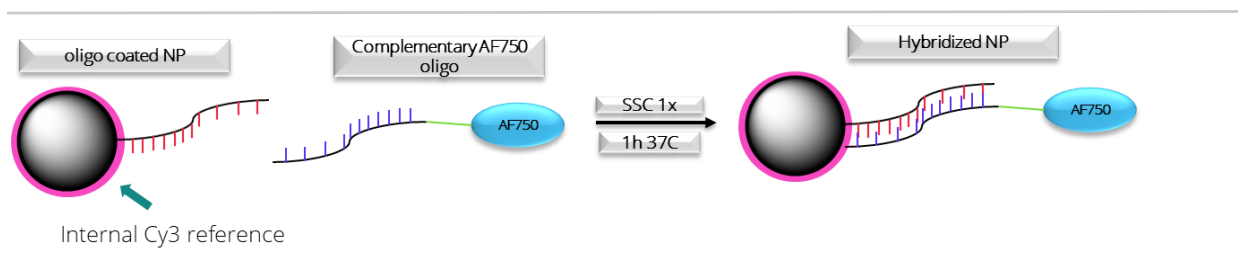


Figure 28: Schematic overview of the quantification process consisting of hybridization of complementary detection oligo labelled with fluorophore Alexa Fluorophore 750.

The hybridization method of quantifying oligo density on the surface of nanoparticles was evaluated using a series of oligo functionalized nanoparticles with oligo concentrations in the functionalization step ranging from 0 to 4.8 μM . The quantification method used is described in methods (2.2.2), all samples are quantified using identical conditions. The resulting plot of oligo concentration and AF750/Cy3-ratio exhibits a linear correlation with a high R-square value validating the method of quantifying relative oligo density. The measured value is a ratio between the internal cy3 fluorescence of the particles, and the labelled detection oligo hybridized to the particles. The quantification method is limited to measuring relative values of oligo density which can be used for reproducing oligo functionalized nanoparticles. The plotted graph is illustrated in figure 29. The main purpose of the developed quantification method was to ensure reproducibility of the functionalization step yielding successful hybridization of NPs to RCPs. To further evaluate the effect of the oligo density the batches of NPs that were used to quantify oligo density should be hybridized to RCPs. The resulting data can then be used to determine the optimal oligo density on the surface of NPs for efficient hybridization.

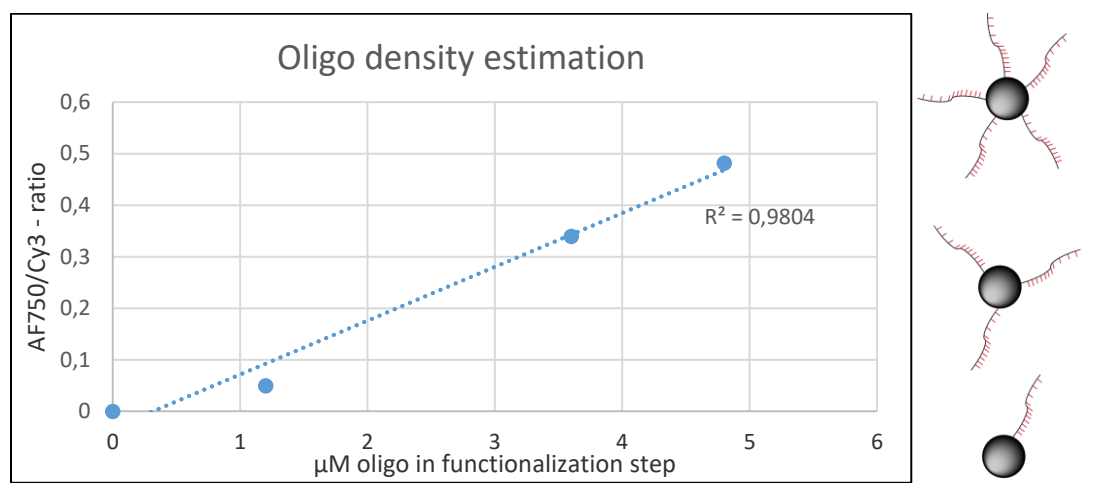


Figure 29: Measured AF750/Cy3 ratio plotted against the oligo concentration in the functionalization step. The intensity ratios are obtained by imaging the nanoparticle solution in hybridization chambers with 100ms exposure the Cy3 channel and 2000ms exposure in the AF750 channel.

2.3.2 Evaluation of nanoparticle to RCP hybridization efficiency

For the evaluation of NP to RCP hybridization efficiency two hybridization methods were chosen. The first method was NP hybridization to immobilized RCPs following the protocol described in methods (2.2.2.3). The second method was NP hybridization to mobile RCPs in solution following the protocol described in methods (2.2.2.4). To quantify the hybridization efficiency of the NP to RCP binding a combination of two methods was used. The RCPs were co-labelled with fluorescently labelled detection oligo with the purpose of measuring relative intensities of nanoparticle signal to detection oligo signal. The measured intensity ratios can be compared for the two chosen methods estimating a relative value of hybridization efficiency with the aim of drawing a conclusion on which method yields the highest hybridization efficiency. Measurement of the intensity ratios of the hybridized nanoparticles and detection oligo cannot fully estimate the hybridization efficiency because it lacks information of unspecific signal and degree of colocalization, the intensity ratios of both methods can indicate how many nanoparticles binds to each RCP relative the other method. The degree of colocalization in both channels was the second chosen parameter for the efficiency evaluation. To estimate the colocalization degree of the NP binding, Image J software with the JaCob plugin was used. The plugin uses mathematical correlation of coordinates and intensity of the signal in both channels to estimate a correlation factor of 0-1. With measured intensity ratios and calculated colocalization degree a conclusion on which method yields the highest relative hybridization efficiency can be drawn.

2.3.2.1 Hybridization efficiency to Immobilized RCPs

In order to evaluate the hybridization efficiency of nanoparticles to immobilized RCPs hybridization tests were performed following the protocol for solid phase hybridization listed in methods (3.2.3). The experiment included a negative and positive control. The positive control was a stabilized nanoparticle batch functionalized with DBCO oligo complementary to the RCPs of sequence SARS-COV-2 and yielded co-localized signal between nanoparticle and detection oligo channel. The negative control consisted of a nanoparticle batch with no oligo conjugated to the particles. Based on the images a

qualitative conclusion was drawn, the colocalized signal in the positive control arose from hybridization of the oligo functionalized to the surface of the NPs. The conclusion was supported by the lack of colocalized signal in the negative control. The nucleic acid sequences for the SARS-COV-2 target are listed in methods(2.2.1). The RCPs are amplified using the RCA protocol listed in method (chapter 1). Images of the samples are displayed in figure 30.

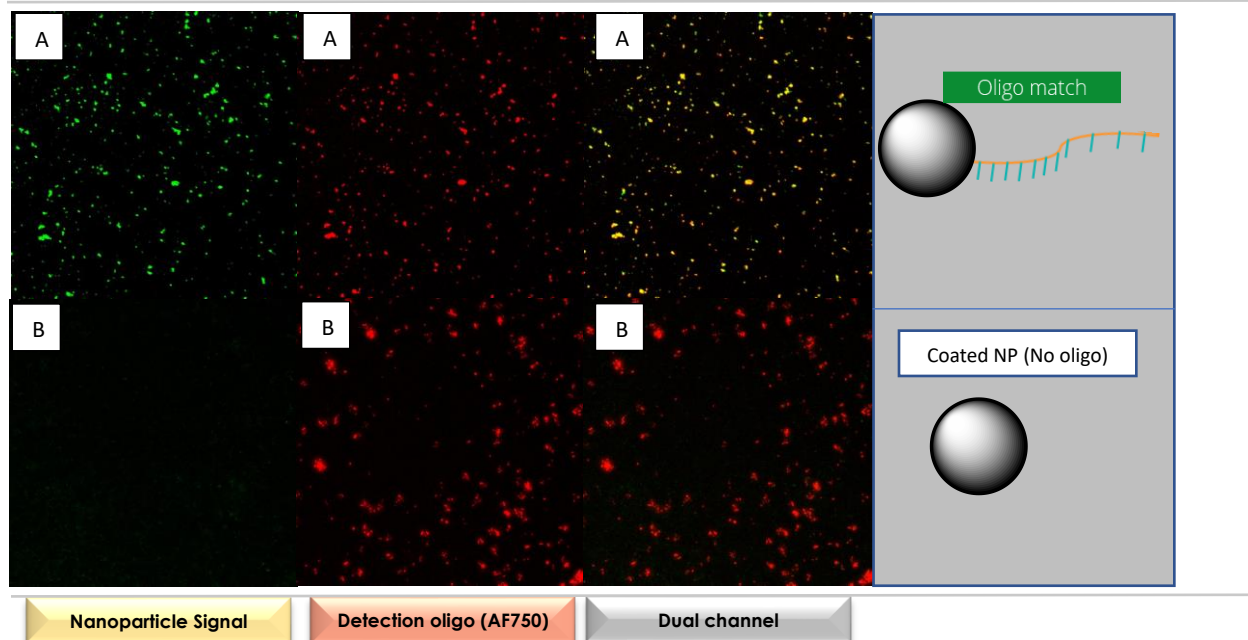


Figure 30: Fluorescent microscopy images of the negative and positive controls for hybridization of nanoparticles to immobilized RCPs with sequence SARS-COV-2. Sample A was the positive control and was comprised of nanoparticles functionalized with DBCO oligo with sequence complementary to the RCP. The negative control was comprised of NPs coated NPs without oligo. The images were acquired using 100ms exposure in the AF750 channel and 100ms exposure in the Cy3 channel. Both samples were co-labelled with AF750-detection oligo. The images were acquired using the 20x (0.8 NA, air, 420650-9901) objective. All images are presented with normalized histograms.

To compare the hybridization efficiency to immobilized RCPs and RCPs in solution the intensities of the positive controls were analyzed using Zeiss software. The maximum intensity in the AF750 channel (detection oligo) and the Cy3 channel (nanoparticles) was measured and a mean intensity was calculated, the intensities were measured using line profile to measure the maximum intensity value of individual RCPs and subtract the local background value from the measured maximum value. The obtained data was calculated from 20 RCPs. The intensity of the nanoparticles signal compared to the detection oligo signal is displayed in figure 31. The purpose of the intensity measurements of the nanoparticle and detection oligo signal was the comparison of the hybridization efficiency to mobile and immobilized RCPs. Comparing the measured intensity ratio of NPs and fluorescently labelled detection oligo bound to RCPs can be used to quantify the hybridization efficiency of one method relative to the other. The measured values are compared to the second method in the next section (3.3.3.2). The experiment was repeated following the same procedure to ensure that the result of the experiment was reproducible and to increase the certainty of the measured values.

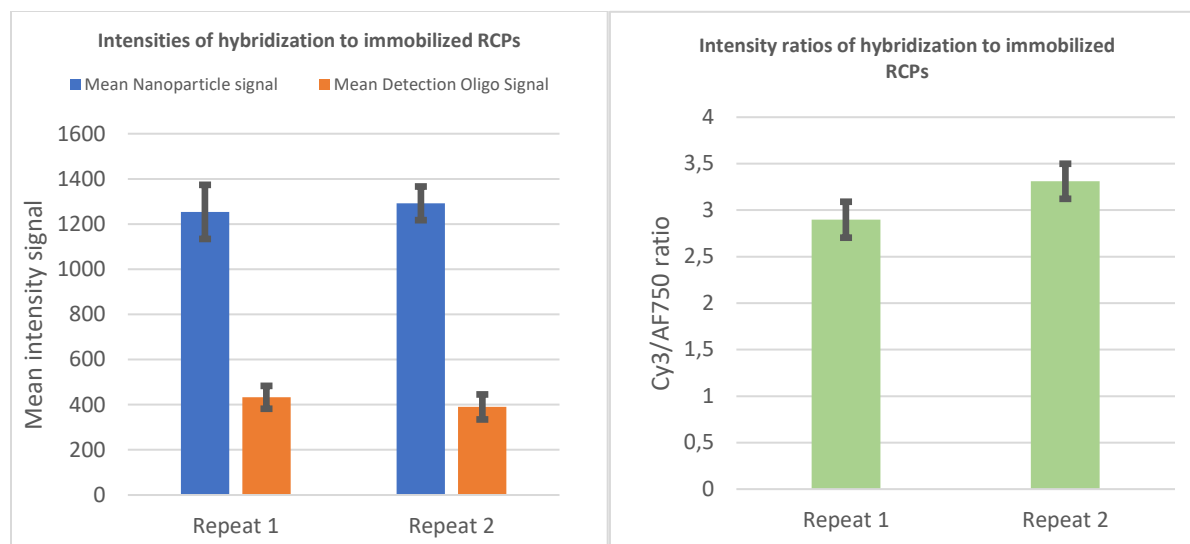


Figure 31: Data analysis of the hybridization of nanoparticles to immobilized RCPs by manual measurement using Zeiss software. The mean intensity is calculated from a sample population of 20 RCPs.

In order to fully evaluate the hybridization efficiency, the colocalization of nanoparticle signal and detection oligo signal was analysed using Image J software with JaCob plugin. The colocalization was calculated using the Manders colocalization method which calculates the degree of colocalization of each channel relative to the other channel. The coefficient M1 represents the degree of colocalization of the detection oligo signal to the nanoparticle signal. The coefficient M2 represents the degree of colocalization of the nanoparticle signal to the detection oligo signal. The results of the colocalization analysis performed on the images of nanoparticle to immobilized RCP hybridization are displayed in figure 32. The colocalization coefficient for the detection oligo signal was 0,9125 and 0,046 for the negative control. The high coefficient value of 0,9125 indicated that the detection oligo signal was almost fully colocalized with the nanoparticle signal. The coefficient of the negative control was 0,046 which is negligible compared to the positive control and supports the conclusion that the degree of colocalization is solely caused by the hybridization of nanoparticles to RCPs. The coefficient M2 was 0,536 for the positive control which is significantly lower compared to M1. A possible factor effecting the overlap value of M1, nanoparticles have higher signal intensity and have a lower theoretical limit of detection than fluorescently labelled detection oligos. The nanoparticles can thus in theory detect smaller RCPs which can explain the difference of the colocalization coefficients. The second factor is the adsorption of the particles to the superfrost slides which can yield signal that is not colocalized with the detection oligo signal. It is believed to be a combination of both factors causing the difference in colocalization of one channel to the other.

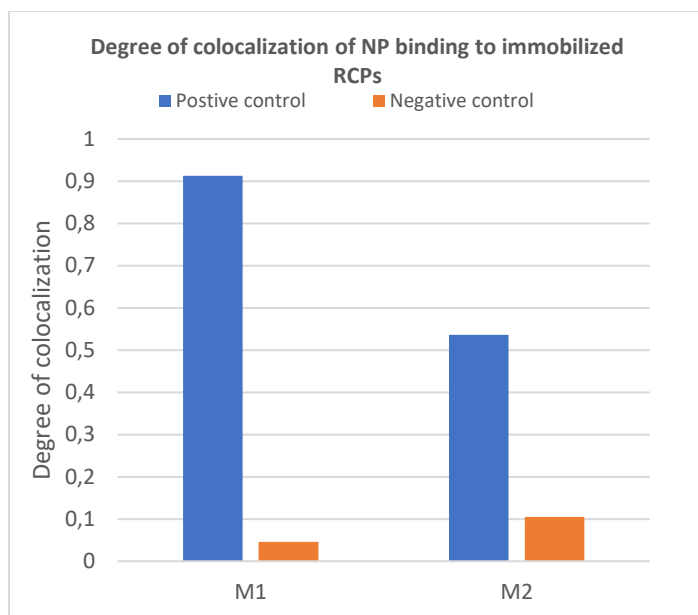


Figure 32: Degree of colocalization calculated using Image J software with JaCob plugin. The calculated values M1 and M2 corresponds to the colocalization degree each channel, M1 is the colocalization of detection oligo signal and M2 is the colocalization of the nanoparticle signal. The colocalization calculation were performed using Manders colocalization method on the sample hybridized to immobilized RCPs.

2.3.2.2 Hybridization efficiency to mobile RCPs in solution

The second method of hybridization was to mobile RCPs in solution using the protocol listed in methods (3.3.4). The positive control of this experiment was a nanoparticle batch functionalized with oligo sequence complementary to the RCPs used. The positive control yielded co-localized signal of the nanoparticles with the detection oligo. The overlapping signal of the nanoparticles was significantly dimmer compared to hybridization of the immobilized sample, the lower signal intensity is due to a lower number of NPs bound to each RCP. The negative control yielded no co-localized signal indicating specific binding to the target. Images of the samples are displayed in figure 33.

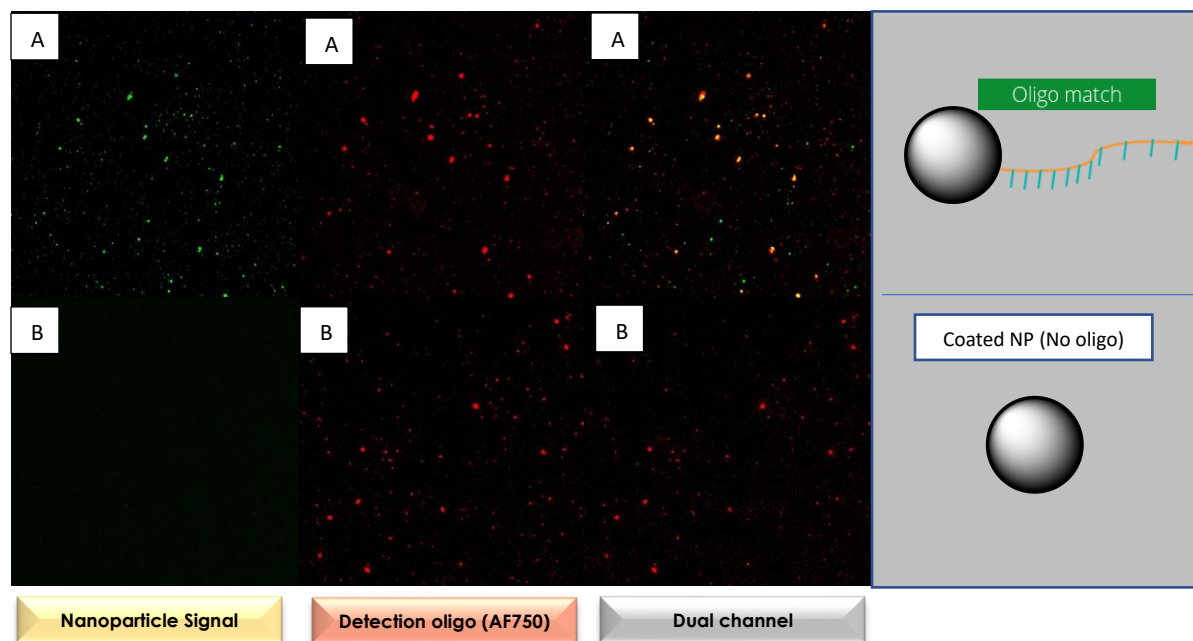


Figure 33: Fluorescent microscopy images of the negative and positive controls for hybridization of nanoparticles to mobile RCPs in solution with sequence SARS-COV-2. Sample A was the positive control and was comprised of

nanoparticles functionalized with DBCO oligo with sequence complementary to the RCP. The negative control was comprised of core nanoparticles. The images were acquired using 100ms exposure in the AF750 channel and 100ms exposure in the Cy3 channel. Both samples were co-labelled with AF750-detection oligo. The images were acquired using the 20x (0.8 NA, air, 420650-9901) objective.

To compare the hybridization efficiency between the mobile and immobilized samples the intensities of the co-localized signal was measured with Zeiss software using the same settings and population size of RCPs. The signal intensity of the nanoparticles was significantly lower in the sample with mobile RCPs and the intensity ratio was approximately a third compared to the immobilized sample. This indicates that there are fewer NPs per detection oligo bound to the RCPs in hybridization experiment using mobile RCPs. The intensity ratio was the first measurement designed to estimate the relative hybridization efficiency, combined with the colocalization analysis a conclusion of the efficiency can be drawn. The intensities were plotted in figure 34.

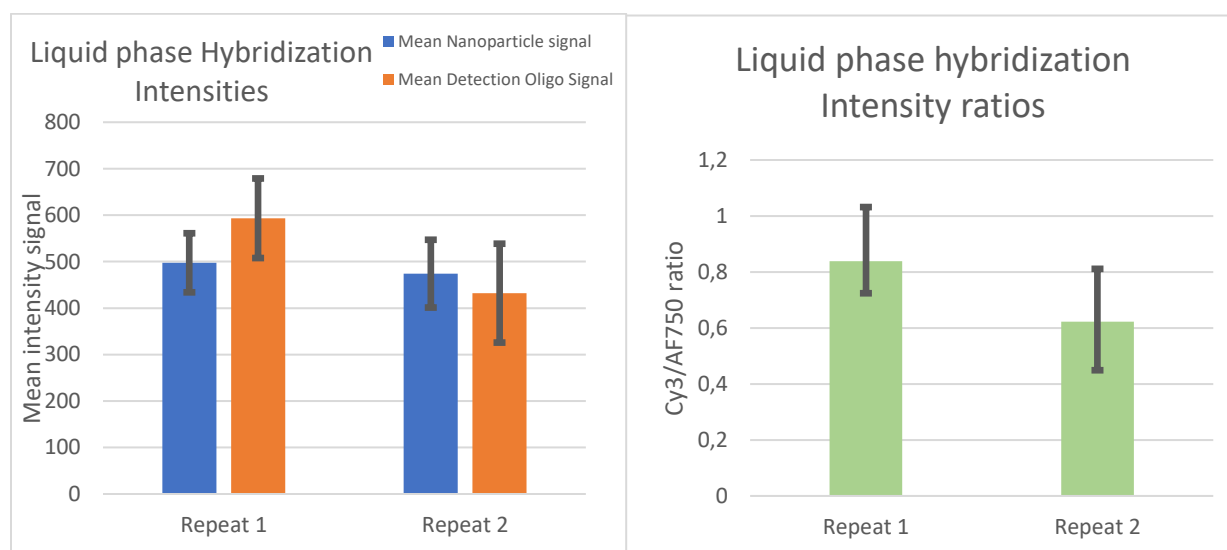


Figure 34: Data analysis of the hybridization of nanoparticles to mobile RCPs in solution by manual measurement using Zeiss software. The mean intensity is calculated from a sample population of 20 RCPs.

The colocalization of the hybridization to mobile RCPs in solution was analyzed using Image J following the same method as in (3.3.1), the colocalization coefficients are plotted in figure 35. The resulting colocalization coefficients were significantly lower compared to ones calculated for hybridization to immobilized RCPs. The coefficients for nanoparticles hybridized to immobilized RCPs were larger by a factor of 2 indicating that the hybridization efficiency to immobilized RCPs was significantly higher compared to mobile RCPs in solution. With the results from the intensity ratios and the colocalization analysis the following conclusion was drawn. For the immobilized sample the relative number of nanoparticles hybridized to RCPs was approximately 3 times higher, the degree of colocalization was 2 times higher. This concludes that the hybridization to NPs to immobilized RCPs is significantly higher compared to mobile RCPs in solution. All future hybridization experiments using NPs were performed with immobilized RCP.

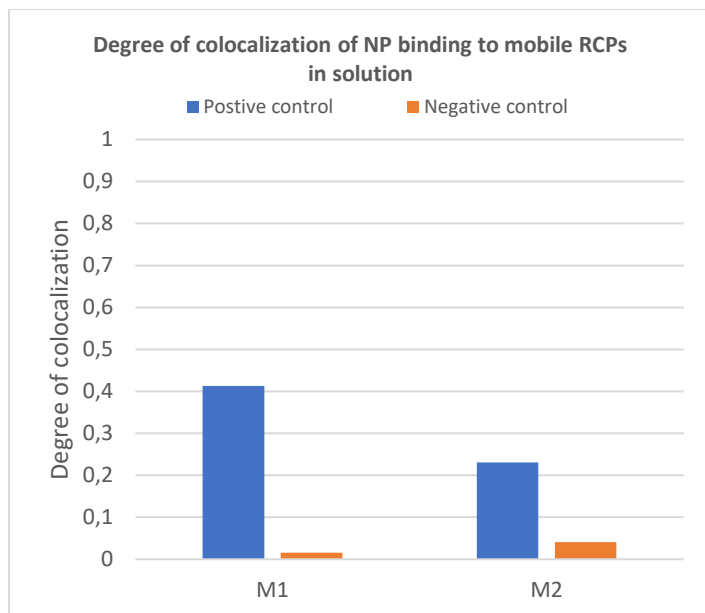


Figure 35: Degree of colocalization calculated using Image J software with JaCob plugin. The calculated values M1 and M2 corresponds to the colocalization degree each channel, M1 is the colocalization of detection oligo signal to NP signal and M2 is the colocalization of the NP signal to detection oligo signal. The colocalization calculation were performed using Manders colocalization method on the sample hybridized to mobile RCPs in solution.

2.3.3 Hybridization specificity

The previous experiment confirmed the hybridization of the nanoparticle to RCPs and concluded that immobilization of RCPs prior to hybridization yielded significantly improved hybridization efficiency. The efficiency was quantified by intensity analysis of RCPs and colocalization of NP and detection oligo signal. The next step of optimizing the hybridization method was evaluating the specificity of the NP to RCP hybridization. In order to evaluate the specificity of the NPs, two batches of NPs and RCPs were prepared. The first NP batch consisted of NPs functionalized using DBCO oligo with the nucleic acid sequence complementary to the HIV target, the second NP batch was functionalized using the DBCO oligo complementary to the SARS-COV-2 target, both NP batches were functionalized following the protocol describe in methods (3.2.1). The synthetic targets of HIV and SARS-CoV-2 were amplified using the RCA protocol listed in methods in chapter 1. Two nanoparticle batches were functionalized with DBCO oligo complementary to respective HIV and SARS-COV-2 synthetic targets, the DBCO oligos are listed in table 13.

The results of the hybridization test showed highly co-localized signal in the positive control and no co-localized signal in the negative control. The nanoparticles functionalized with oligo complementary to the RCPs with HIV sequence resulted in specific binding to their target while the negative control containing NPs functionalized with DBCO oligo with the sequence complementary to SARS-COV-2 yielded no colocalized signal. The results of the negative and positive control indicated that the hybridization of the NPs was highly specific, the images of the specificity test are displayed in figure 36.

Target sequence HIV

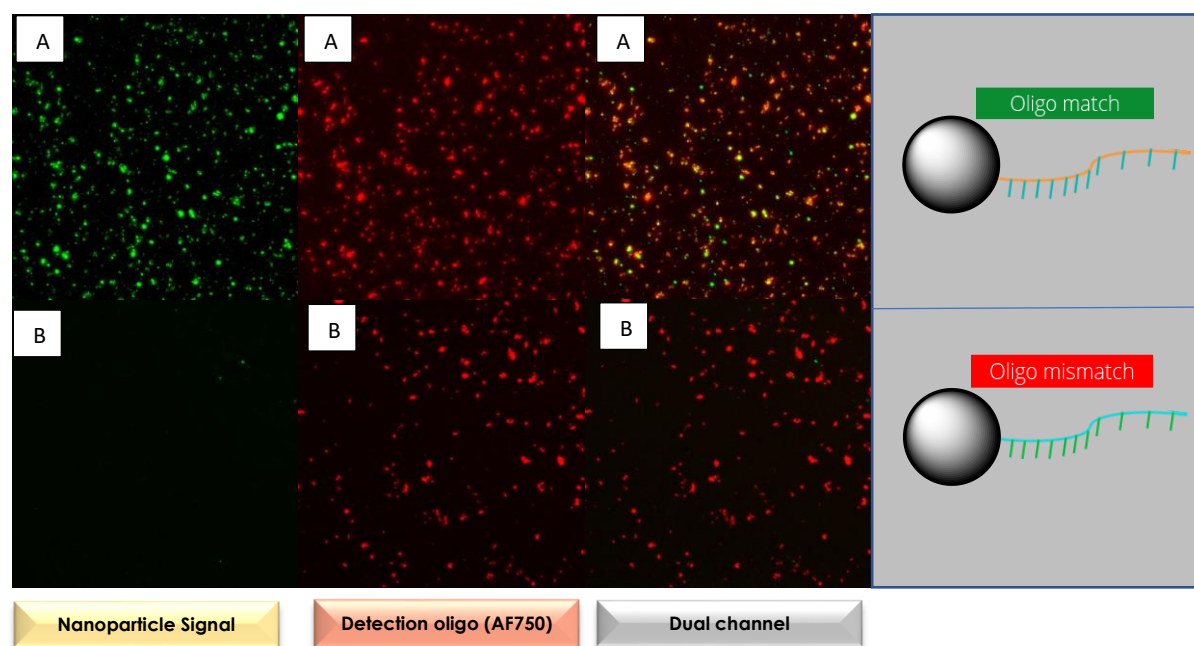


Figure 36: Fluorescent microscopy images of the negative and positive controls for hybridization of nanoparticles to immobilized RCPs with sequence HIV. Sample A was the positive control and was comprised of nanoparticles functionalized with DBCO oligo with sequence complementary to the RCP. The negative control was comprised of nanoparticles functionalized with DBCO oligo with sequence HIV. The images were acquired using 100ms exposure in the AF750 channel and 100ms exposure in the Cy3 channel. Both samples were co-labelled with AF750-detection oligo. The images were acquired using the 20x (0.8 NA, air, 420650-9901) objective.

The same experiment was performed with RCPs amplified using the synthetic target of SARS-COV-2. The positive control B yielded highly co-localized signal between the nanoparticle and detection oligo channel. The experiment concludes that both nanoparticle batches yielded successful hybridization to their target with high specificity, the microscopy images of this experiment are displayed in figure 37.

Target sequence SARS-COV-2

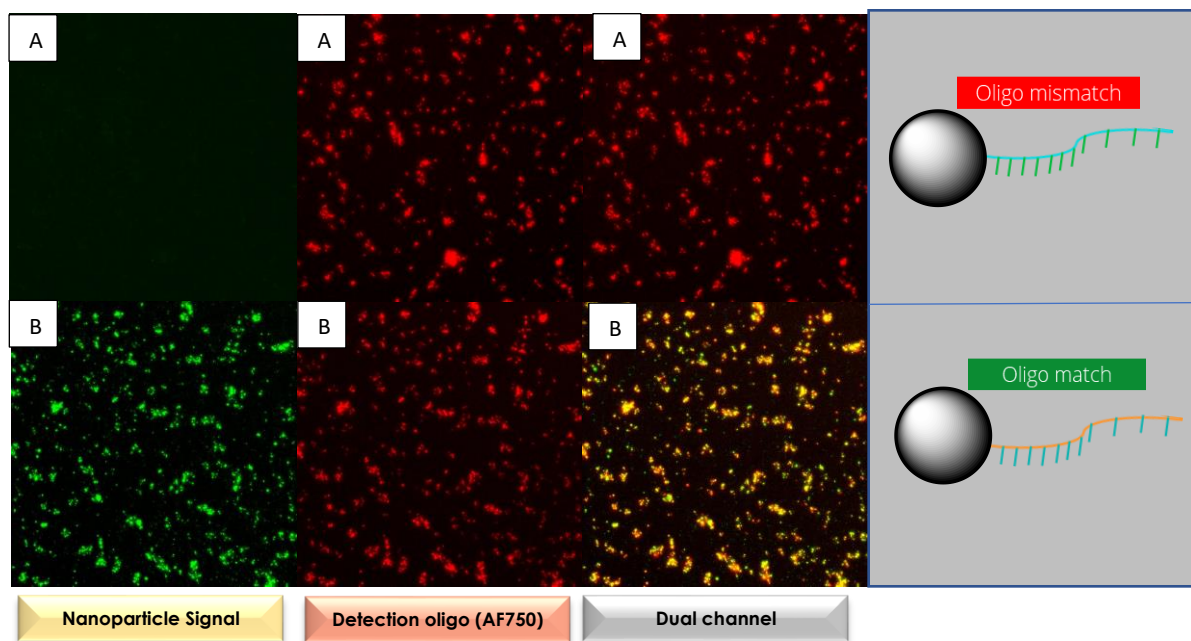


Figure 37: Fluorescent microscopy images of the negative and positive controls for hybridization of nanoparticles to immobilized RCPs with sequence SARS-COV-2. Sample A was the positive control and was comprised of nanoparticles functionalized with DBCO oligo with sequence complementary to the RCP. The negative control was comprised of nanoparticles functionalized with DBCO oligo with sequence HIV. The images were acquired using 100ms exposure in the AF750 channel and 100ms exposure in the Cy3 channel. Both samples were co-labelled with AF750-detection oligo. The images were acquired using the 20x (0.8 NA, air, 420650-9901) objective.

The images of the hybridization specificity experiment were analyzed using “Image J” software. The degree of colocalization was quantified using “JACOB” plugin with Manders colocalization analysis. Coefficient M2 corresponds to the overlap value of AF750 channel to Cy3 channel, yielding a 94,7 % overlapping signal. The coefficient are plotted in figure 38, M1 corresponds to the overlap of the Cy3 channel to the AF750 channel and is significantly lower than M2. A possible factor effecting the overlap value of M1, nanoparticles have higher signal intensity and have a lower theoretical limit of detection than fluorescently labelled detection oligos. The nanoparticles can thus in theory detect smaller RCPs which can explain the difference of the colocalization coefficients. The second factor is the adsorption of the particles to the superfrost slides which can yield signal that is not colocalized with the detection oligo signal. It is believed to be a combination of both factors causing the difference in colocalization of one channel to the other.

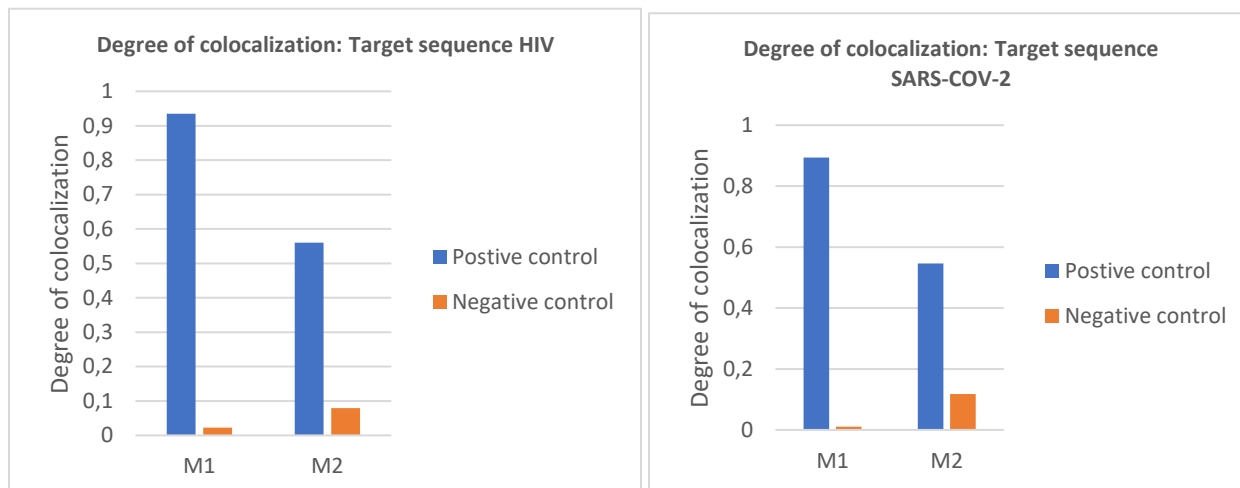


Figure 38: Colocalization analysis of nanoparticle hybridization to mobile and immobilized RCPs of sequence HIV and SARS-COV-2. The analysis was performed Fiji (Image J) software with Jacob plugin. M1 was the coefficient quantifying the overlap of the nanoparticle signal to the detection oligo signal. M2 was the coefficient quantifying the overlap of the detection oligo signal with the nanoparticle signal. The background was removed by the adjustment of the threshold setting.

2.4 Conclusions

There were several goals in this chapter, developing a method of quantifying oligo density on the surface of nanoparticles, proving evaluating hybridization efficiency of nanoparticles to mobile and immobilized RCPs and evaluating the specificity of nanoparticle to RCP hybridization. Based on the results of this chapter following conclusions were drawn.

1. Oligo density of the nanoparticles can be quantified by hybridizing fluorescently labelled detection oligo to the nanoparticles and measuring the bulk intensity ratios of the internal fluorescence of the nanoparticles and the fluorescently labelled oligo hybridized to the particles.
2. Hybridization of nanoparticles to RCPs has been confirmed.
3. The hybridization efficiency of nanoparticles to immobilized RCPs was significantly higher compared to mobile RCPs.
4. The specificity of the nanoparticle to RCP hybridization was confirmed concluding that the nanoparticles only bind to nucleic acid sequences complementary to the detection oligo used to functionalize the nanoparticles.

3. Development of 14 plex pathogen panel

The aim of the 14 plex pathogen panel was to develop a molecular assay with the capability of detecting and discriminating between 14 pathogenic targets in a single step without the use of sequencing or complex detection methods. The developed panel can be used with existing epifluorescent microscopy systems and will not require any specialized apparatus. The NPs have been oligo functionalized and characterized with respect to oligo density on the surface of the particles in previous steps of the thesis. The NPs have been oligo functionalized and characterized with respect to oligo density on the surface of the particles in previous steps of the thesis. The nanoparticle-RCP binding has been evaluated by analyzing intensity of the particles and colocalization, evaluating the overlap of detection oligo signal to nanoparticle signal in RCPs dual labelled with detection oligos and nanoparticles. As the specific hybridization of the nanoparticles to RCPs has been confirmed the next step of developing the pathogen panel was the choice of targets. The targets were chosen based on the relevance to the current needs in viral diagnostics. Early and rapid diagnosis of respiratory viruses is of particular importance as current methods being used for rapid diagnosis are limited in regards of multiplexity. The implementation of a 14 plex assay would provide significant benefit in point of care as well as tracking and preventing pathogen outbreaks. [15]

The focus of this chapter was the evaluation of chosen synthetic targets and padlock probes ordered for each target. To enable the detection of 14 targets in one test the specificity of the padlock probes and synthetic targets were evaluated. For every chosen pathogen a negative control and a positive control was designed. The negative control consisted of 13 mismatching targets and 1 padlock probe matching the chosen pathogen. The positive control consisted of the matching synthetic target and PLP for each pathogen.

3.1 Pathogen targets for development of 14 plex panel

Targets 1-5 (table 21) were chosen with the purpose of distinguishing between the most common subgroups of human coronaviruses. The implementation of these targets in the panel will allow an initial detection of the COVID-19 virus with discrimination of the most common subgroups. Distinguishing between different strains of corona virus will significantly increase the accuracy of transmission chain tracking and outbreak mapping. [2] Current methods of COVID-19 detection does not include the detection of respiratory viral infections with similar symptoms, several influenza viruses have symptoms similar to COVID-19. Implementing influenza virus targets in the pathogen panel will allow the tracking of multiple viral infections with similar symptoms using one single step rapid diagnostic test. The advantage of implementing such a test in point of care is significant as the targets of the test can be adjusted to detect pathogens with similar symptoms which are commonly misdiagnosed, improving quality of care. Targets 6-9 (table 21) are the most common influenza viruses of subtype A and B. with the chosen targets the panel can detect a set of the most common viruses that are in continuous global circulation and constantly spreading through temporary geographically overlapping epidemics. Targets 1-9 were chosen based of previously developed molecular assay. [15][16][17][18][19][20]

Bacterial infection is a growing global concern with lack of quick and simple diagnostic tools to prevent arising issues from overuse of broad-spectrum antibiotics. The need for rapid diagnostic tools for identifying bacterial subtypes is crucial for the improvement of point of care and reducing the use of broad-spectrum antibiotics which contributes to the global increase of antibiotic resistant bacteria. Targets

10-11 (table 21) are genetic markers for antibiotic resistance in bacteria and are chosen for the purpose of early detection of antibiotic resistant bacteria. The use of broad-spectrum antibiotics on bacterial infections with antibiotic resistance is a common issue in patient care. Being able to detect these genetic markers can change the prescribed antibiotics for such patients. Target 12-14 (table 21) are chosen with the purpose of complementing the antibiotic resistance targets with the detection of three types of bacteria, including these targets will allow the panel to detect different types of bacteria as well as antibiotic resistance markers.

No.	target organism	Type
1	SARS-CoV-2_ORF1ab	RNA corona virus
2	CoV-NL63	RNA corona virus
3	CoV-229E	RNA corona virus
4	CoV-OC43	RNA corona virus
5	CoV-HKU1	RNA corona virus
6	Influenza H3N2_NP	RNA influenza virus
7	Influenza H1N1_NP	RNA influenza virus
8	Influenza Victoria_NP	RNA influenza virus
9	Influenza Yamagata_NP	RNA influenza virus
10	mecA AMR gene	Antibiotic resistance marker
11	OXA-48 AMR gene	Antibiotic resistance marker
12	E. coli	Bacteria
13	S. aureus	Bacteria
14	P. aeruginosa	Bacteria

Table 21: table of pathogenic organisms chosen as targets for the development of the 14 plex panel.

3.2 Synthetic targets

To develop and evaluate the pathogen panel with the 14 chosen targets, synthetic targets were ordered for each pathogen. For each of the pathogens a sequence of a segment in the genome was chosen as the target sequence and synthetic single stranded DNA was ordered. The specificity and sensitivity of the chosen sequences was evaluated by amplification tests using complementary PLPs. All targets were ordered with biotin tails to allow the option of immobilization using the protein streptavidin. The immobilization utilizing the biotin tails will not be used in this chapter, it is a tool for future work to allow the evaluation of further applications, one of which is the use of microfluidic systems for the immobilization, amplification and detection of amplified targets. Nucleic acid sequences of the synthetic targets were chosen based on previously developed molecular assays. [15][16][17][18][19][20]

To develop and evaluate the pathogen panel a sequence of a segment in the genome of each organism was chosen. The chosen sequences must be unique for each pathogenic target allowing for discrimination of each target by the ligation step of the amplification and the specific detection using the functionalized nanoparticle probes. All targets were ordered with biotinylated tails. The sequences for the targets are illustrated in table 22.

target organism	Nucleic acid sequence of target
SARS-CoV-2_ORF1ab	TCTCTCTCTCTCTCCGGTGTGACAAGCTACAACACGTTGTATGTTTTCGAGCAA
CoV-NL63	TCTCTCTCTCTCTCTCTATCTGTTGCAGTACAACAATTAACATGCTTAGAGCCCA
CoV-229E	TCTCTCTCTCTCTCTTATCACTAGCCGTACAACATGTGACATGCTTAGAACCTA
CoV-OC43	TCTCTCTCTCTCTCTCTATCGCTTTCGAACAACATGTCTCATGTTTCGGGCTA
CoV-HKU1	TCTCTCTCTCTCTCTCTATCACCATGTGAACAACAAAATTCATGTTTACGAGCCA
Influenza H3N2_NP	TCTCTCTCTCTCTCTCAATCTGGCGCCAAGCCAACAATGGTGAGGATGCTACAT
Influenza H1N1_NP	TCTCTCTCTCTCTCTCAGTTTGGCGCCAAGCAAACAATGGCGAAGATGCAACAG
Influenza Victoria_NP	TCTCTCTCTCTCTCTCAGTCCCCAGAAGATCAGGCGCAACTGGTGTTGCAAT
Influenza Yamagata_NP	TCTCTCTCTCTCTCTCAGTCCCCAGAAGATCAGGTGCGACTGGTGTTGCAAT
mecA AMR gene	TCTCTCTCTCTCTCTCAGGTGAATTATTAGCACTTGTAAGCACACCTTCATATG
OXA-48 AMR gene	TCTCTCTCTCTCTCTCGAAGGATTTACCAATAATCTTAAACGGGCGAAC
E. coli	TCTCTCTCTCTCTCTCGTCAATGAGCAAAGGTATTAACCTTTACTCCCTTC
S. aureus	TCTCTCTCTCTCTCTTACACCTGAAACAAAGCATCCTAAAAAAGGTGTAGAGA
P. aeruginosa	TCTCTCTCTCTCTCTCTCACTTTCTCCCTCAGGACGTATGCGG

Table 22: Table of biotinylated nucleic acid sequences of all targets in the 14 plex panel. The biotin tails are displayed in green text and the nucleic acid sequence in normal text.

3.3 Padlock probes

To enable the amplification of the chosen synthetic targets using RCA, padlock probes complementary to the nucleic acid sequences of the chosen targets were ordered. Padlock probes were chosen based on previous amplification test of these targets “paper x,y,z”. The padlock probes were designed with left and right-side arms specific to the complementary synthetic target with two barcodes sequences implemented in the linker between the left and right-side arm. The barcodes are the sequences that will be used for the detection of the amplified targets. Barcode one was the sequence that the functionalized highly multiplexed nanoparticles supplied by “Aplex Bio” will hybridize to, while the barcode 2 will be the used for hybridization of detection oligos to enable colocalization analysis of the detection oligo signal and the nanoparticle signal. The padlock probe design using two barcodes allows the discrimination of specific binding of nanoparticles to amplified targets and unspecific adsorption of nanoparticles to the glass slides used for immobilization of the amplified rolling product. The padlock probes have a restriction sites which are necessary only for circle to circle rolling amplification (CTCA). CTCA will not be used for the evaluation of the pathogen panel, the purpose of the restriction site was to enable CTCA to reach higher copy numbers and sensitivity once the panel was completed. The padlock probes for each target are listed in table 23.

Target organism	Left arm	Code 1	Restriction Site	Code 2	Right arm
SARS-CoV-2_ORF1ab	TGTTGTAGCTTGTACACCG	AGTAGCCGTGACTATCGACT	GTGTATGCAGCT	TGCGTCTATTAGTGGAGCC	TTGCTCGCAACATACAACG
CoV-NL63	TGTTGTACTGCAACAGATAG	CCTCAATGCTGCTGCTACTAC	GTGTATGCAGCT	TGCGTCTATTAGTGGAGCC	TGGGCTCTAAGCATGTTAAT
CoV-229E	TGTTGTACGGCTAGTGATAA	CTCAGCCGATGCAGTGAAT	GTGTATGCAGCT	TGCGTCTATTAGTGGAGCC	TAGGTCTTAAGCATGTCACA
CoV-OC43	TGTTGTTCCGAAAGCGATAG	AGAGAGTAGTACTCCGACT	GTGTATGCAGCT	TGCGTCTATTAGTGGAGCC	TAGCCCGAAAACATGAGACA
CoV-HKU1	TGTTGTTACATGGTGATAG	CAATCTAGTATCAGTGGCGC	GTGTATGCAGCT	TGCGTCTATTAGTGGAGCC	TGGCTCGTAAACATGAATTT
Influenza H3N2_NP	TGTTGGCTTGGCGCCAGATT	GGGCCTTATCCGGTGCTAT	GTGTATGCAGCT	TGCGTCTATTAGTGGAGCC	ATGTAGCATCCTCACCAT
Influenza H1N1_NP	TGTTTGCTTGGCGCCAACT	CTGATTCCTTGACTCACAT	GTGTATGCAGCT	TGCGTCTATTAGTGGAGCC	CTGTTGCATCTCGCCAT
Influenza Victoria_NP	CCTGATCTTCTGGGGACTGT	AGTAGCCGTGACTATCGACT	GTGTATGCAGCT	CCTCAGTAATAGTGCTTAC	ATTGCAACACCAGTTGCG
Influenza Yamagata_NP	CCTGATCTTCTGGGGACTGT	CCTCAATGCTGCTGCTACTAC	GTGTATGCAGCT	CCTCAGTAATAGTGCTTAC	ATTGCAACACCAGTCGCA
mecA AMR gene	AGTGCTAATAATCACCTGT	CTCAGCCGATGCAGTGAAT	GTGTATGCAGCT	CCTCAGTAATAGTGCTTAC	CATATGAAGGTGTGCTTACA
OXA-48 AMR gene	ATTATTGGTAAATCCTTGC	AGAGAGTAGTACTCCGACT	GTGTATGCAGCT	CCTCAGTAATAGTGCTTAC	GTTCCGCCGTTTAAG
E. coli	TTAATACCTTTGCTCATTGAC	CAATCTAGTATCAGTGGCGC	GTGTATGCAGCT	CCTCAGTAATAGTGCTTAC	GAAGGGAGTAAAG
S. aureus	TGCTTTGTTTCAGGTGTA	GGGCCTTATCCGGTGCTAT	GTGTATGCAGCT	CCTCAGTAATAGTGCTTAC	TCTCTACACCTTTTTTAGGA
P. aeruginosa	AGGGAGAAAGTGAGA	CTGATTCCTTGACTCACAT	GTGTATGCAGCT	CCTCAGTAATAGTGCTTAC	CCGCATACGTCCTG

Table 23: Table of nucleic acid sequences of the padlock probes used for the amplification of the target sequences for the 14 plex panel.

3.4 Padlock probe specificity

The 14 plex panel requires specific amplification and detection of the nucleic acid sequence of each target to ensure that the developed assay based on the chosen synthetic targets and padlock probes does not yield false positive results. The ligation step in RCA is highly specific and will only ligate the padlock probe to the complementary synthetic target, the amplification of the circularized target by Phi-29 polymerase can only amplify circular DNA. The specificity of the amplification is due to the ligation specificity, it will be evaluated based on the PLP to synthetic target interaction. The experimental design included one positive and one negative control per pathogenic target. The negative control consisted of standard concentration (RCA protocol, chapter 1.2.1.4) of the 13 synthetic targets not complementary to the padlock probe, listed in table 22, 23. The positive control consists of only one synthetic target and its complementary padlock probe. The negative and positive control will be amplified with the same RCA protocol (chapter 1.2.1.4). If the PLP is specific, it will only generate a signal in the positive control and not in the negative control, as the latter contains targets that the PLP does not bind to, unless it does so nonspecifically. If the PLP does not bind to a target, then the ligation step will step will yield no circular targets and subsequently no nucleic acid amplification will occur. Schematics of the designed experiment are illustrated in figure 39.

After the amplification of the negative and positive control each sample was labelled with detection oligos and imaged using epifluorescent a fluorescent microscope. The successfully amplified samples were analyzed using Cell-Profiler software to determine the RCP count and measure mean intensity in each sample. Targets 1-7 were labelled with detection oligo AF750, targets 8-14 were labelled with detection oligo Atto425. Cell profiler is a software designed to identify, count and measure mean intensities of RCPs.

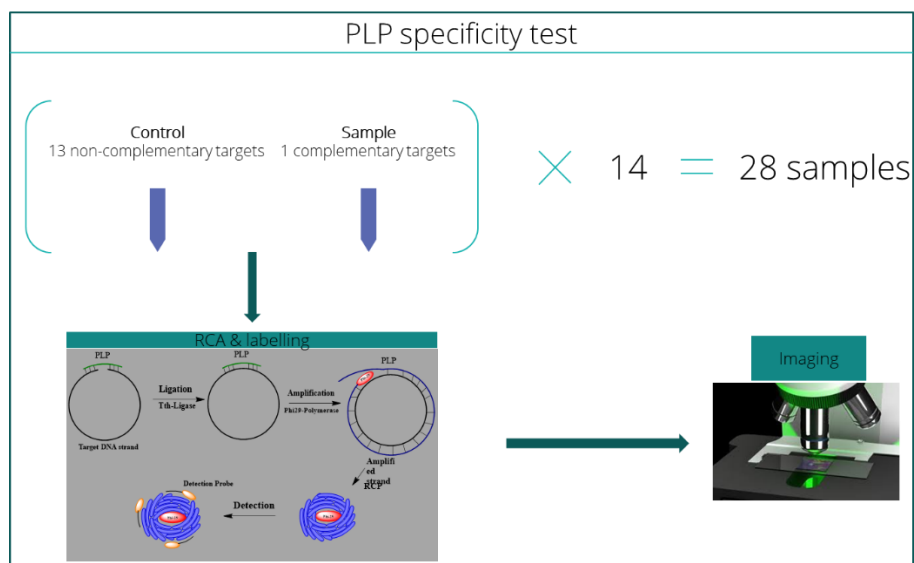


Figure 39: Schematic overview of the experimental design of the padlock probe specificity evaluation

3.5 Materials and methods

3.5.1 Materials

3.5.1.1 Chemicals and oligos

Chemical	CAS	Ordered from
Hybridization buffer 2x	-	Prepared by Scilife
Phi29 polymerase	-	supplied by Scilife
TTh (Dansk) ligase	-	supplied by Scilife
BSA	-	Supplied by Scilife
dNTPs	-	Supplied by Scilife
Amplification buffer	-	Supplied by Scilife
Phi29 buffer	-	Supplied by Scilife

Table 24: list of chemicals used for in chapter 3.

Detection oligos

Detection Oligos	
Detection oligo AF750	AF750-TTTTTTTTTTTTTCGTCTATTTAGTGGAGCC
Detection oligo Atto425	Atto425-TTTTTTTTTTTCCTCAGTAATAGTGTCTTAC

Table 25: Detection oligos used for in chapter 3.

3.5.1.2 Synthetic targets and padlock probes

All synthetic targets and padlock probes were ordered from IDT and are listed in figure 22, 23.

3.5.2 Methods

3.5.2.1 RCA and labelling protocol for the evaluation of padlock probe specificity

To amplify the negative and positive controls in the experiment designed to evaluate the padlock probe specificity a standard protocol for RCA was used. The first step of the amplification was the ligation of the padlock probe to the synthetic target with the reaction conditions listed in table 26. The first step of the ligation was the preparation of the ligation mix. All the components of the ligation mix were pipetted to an Eppendorf tube with the enzyme Tth (Gdansk) pipetted as the last component followed by mixing with pipette. Once the ligation mix was prepared and put on ice the complementary synthetic target was pipetted to the positive control in a PCR tube followed by pipetting equal volume of the ligation mix containing the Tth (Gdansk) enzyme. For the negative control, the 13 non-complementary synthetic targets were pipetted to a PCR tube followed by equal volume of the ligation mix. After sample preparation all tubes were incubated for 30 minutes at 60°C. The reaction conditions are listed in table 26.

During the incubation time of the ligation the RCA mix was prepared by pipetting all components with the enzyme Phi-29 being the last component, the RCA mix was mixed using a pipette and stored on ice until the ligation step was completed.

After the first incubation 10 [ul] of the prepared RCA mix was pipetted all PCR tubes following by incubation for 2 hours at 37°C. To deactivate the polymerase enzyme the RCA incubation ends with a 15 min heating step at 85°C.

Once the ligation and RCA step of the procedure was completed targets 1-7 were labelled with detection oligo-AF750 and targets 8-14 were labelled with detection oligo-Atto425 using the labelling procedure listed in Table 26. After the procedure, all samples were stored in the fridge at 4°C.

1.Ligation	Stock Concentration	Final Concentration	In each tube [μl]	Ligation mix
Synthetic target (S03923)	10 nM	1 nM	10	0
Padlock probe (S03877)	1 nM	100 pM	2	12
BSA	20 μg/μl	0.2 μg/μl	0,2	1,2
Ampl Buffer	10 ×	1 ×	2	12
Tth (Gdansk)	5 U/μl	0.125 U/uL	0,5	3
H2O mQ	-		5,3	31,8
		Mix to add	10	60
		Total with mix	20	Total Mix
Reaction time	30 min. 60°C			

2.RCA (in solution)	Stock conc	Final Concentration	In each tube [μl]	RCA mix
dNTP's	2.5 mM	125uM	1,5	9
phi 29 buffer	10x	1 x	3	18
BSA	20 μg/μl	0.2 μg/μl	0,1	0,6
phi 29 polymerase	10 U/uL	400mU/uL	1,2	7,2
H2O mQ			4,2	25,2
		Mix to add	10	60
		Total with mix	30	Total Mix
Reaction Time	37 °C 2 h,	85°C 15 min.		
3. Labeling	Stock Conc.	Final Concentration	Volume	6
Detection Oligo-AF750 Detection Oligo-Atto425	1 μM	5 nM	0,3	1,8
Hybridization buffer	2x	1x	15	90
H2O mQ			14,7	88,2
		Mix to add	30	180
		Total volume	60	Total Mix
Reaction Time	> 75°C 2 min, 55°C 15 min			

Table 26: Rolling circle amplification protocol used for the padlock probe specificity evaluation. Step 1 is the reaction conditions for the ligation step creating the circular target. Step 2 is the amplification step which amplifies the ligated circular target. Step 3 is the labelling procedure used for the labelling and detection of the RCs.

3.5.2.2 Sample preparation prior to imaging

For the analysis of the negative and positive controls for each sample of the padlock probe specificity experiment 10[ul] of each sample was pipetted on to a superfrost slide and covered with glass coverslips. Schematics of the slide preparation is illustrated in figure 40. Once the slides were prepared all samples were imaged using fluorescent microscopy.

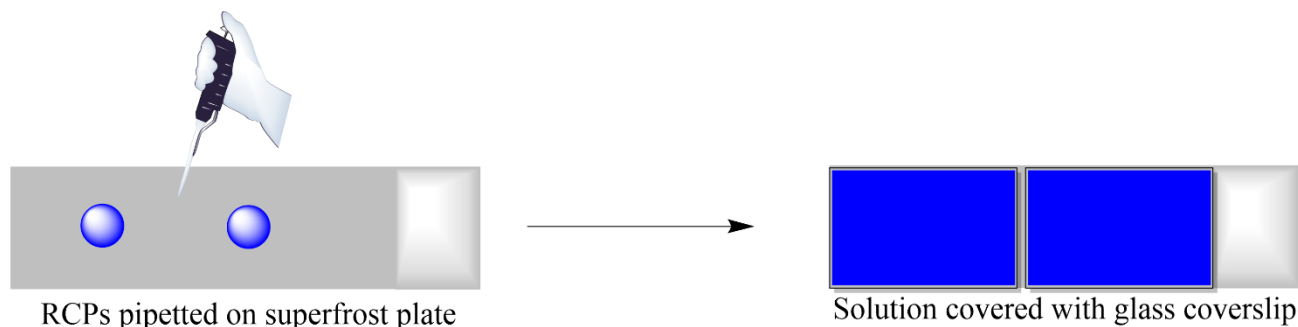


Figure 40: Schematic overview of the slide preparation prior to imaging of the samples.

3.5.2.3 Imaging

All fluorescent microscopy imaging performed during the thesis used a standard epifluorescent microscope (Zeiss Axio Imager.Z2) with an external LED light source (Lumencor SPECTRA X light engine). The microscope setup used a light engine with filter paddles (395/25, 438/29, 470/24, 555/28, 635/22, 730,50). Images were obtained with a sCMOS camera (2048 x 2048, 16bit, ORCA-Flash4.0LT Plus, Hamamatsu) using objectives 20x (0.8 NA, air, 420650-9901) and 5x (0.16NA, air, 420630-9900). The setup used filtercubes for wavelength separation including quad band Chroma 89402 (DAPI, Cy3, Cy5) and quad band Chroma 89403 (Atto425, TexasRed, AlexaFluor750). All samples were mounted on an automatic multi-slide stage (PILine, M-686K011).

3.6 Results and discussion

3.6.1 Imaging of amplified and labelled targets: SARS-COV-2, NL63, 229E

Targets SARS-COV-2, NL63 and 229E shows successful detection of RCPs in the positive controls and only background fluorescence in the negative control. The amplification results for these targets indicate that the padlock probes were successfully ligated to their complementary targets and subsequently amplified. The lack of signal in the negative controls indicate that no unspecific ligation has occurred. The acquired images were analysed in the following section, using Cell profiler software to quantify the specificity by comparing RCP count and mean intensity of all samples. The images of the samples acquired using the epifluorescent microscope are displayed in figure 41.

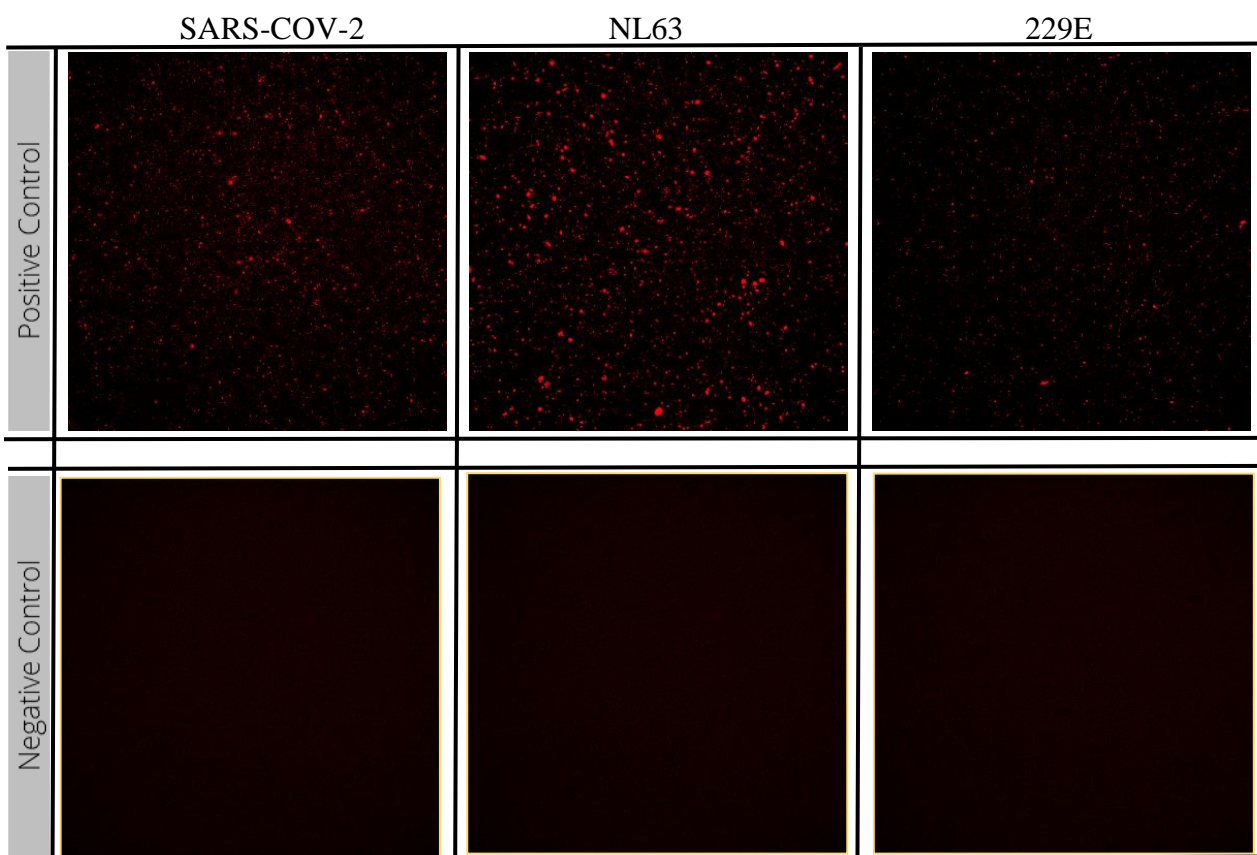


Figure 41: Fluorescent microscopy images of the negative and positive controls for SARS-COV-2, NL63 and 229E. The positive control contains amplified product of the synthetic target and its complementary padlock probe, the negative control contains amplified product of the same padlock probe with the 13 non-complementary synthetic targets of the pathogen panel. All images within the same fluorophore channel have normalized histograms and the samples were imaged in the AF750 channel using 20 times magnification and 100ms exposure time.

3.6.2 Imaging of amplified and labelled targets: OC43, HKU1, Inf.H3N2

Targets OC43, HKU1 and Influenza H3N2 shows similar results as SARS-COV-2, NL63 and 229E. The positive controls yield successful ligation and amplification, while the negative controls show only background signal. The results of the negative and positive control for samples OC43, HKU1, Influenza H3N2 formed the following conclusion, the PLPs of these targets ligate their complementary synthetic targets with high specificity. The acquired images were analysed in the following section, using Cell profiler software to quantify the specificity by comparing RCP count and mean intensity of all samples. The images of the samples acquired using the epifluorescent microscope are displayed in figure 42.

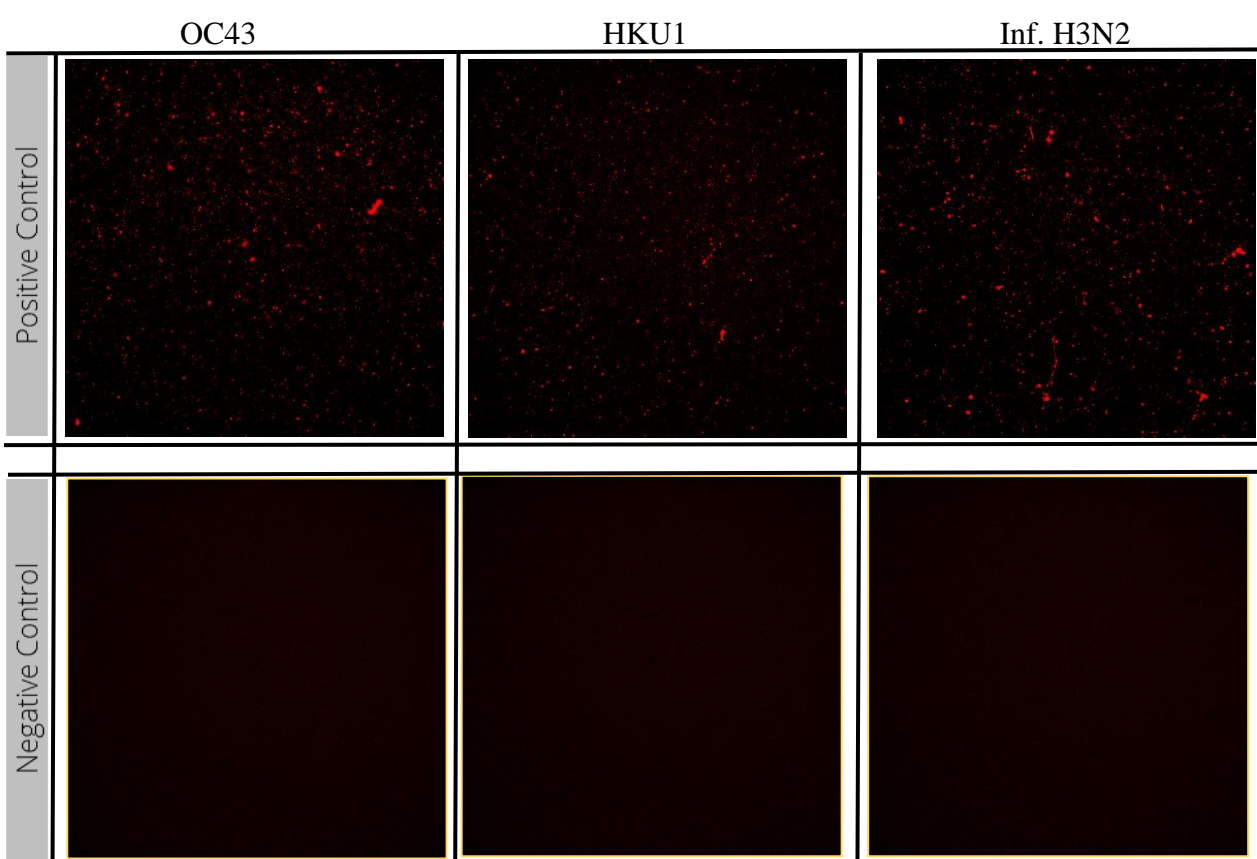


Figure 42: Fluorescent microscopy images of the negative and positive controls for OC43, HKU1 and Influenza H3N2. The positive control contains amplified product of the synthetic target and its complementary padlock probe, the negative control contains amplified product of the same padlock probe with the 13 non-complementary synthetic targets of the pathogen panel. All images within the same fluorophore channel have normalized histograms and were imaged in the AF750 channel using 20 times magnification and 100ms exposure time

3.6.3 Imaging of amplified and labelled targets: Influenza H1N1, Influenza Victoria, Yamagata

Targets Influenza H1N1 and Yamagata shows similar results as the previous targets. The positive controls yield successful ligation and amplification, while the negative controls show only background signal. These results indicate that the padlock probes of targets Influenza H1N1 and Yamagata ligate their complementary synthetic targets with high specificity. Target Influenza Victoria shows successful ligation and amplification in the positive control, but the negative control yields some unspecific signal indicating that some degree of unspecific ligation. The images will be analysed in the following data analysis section. The images of the samples acquired using the epifluorescent microscope are illustrated in figure 43.

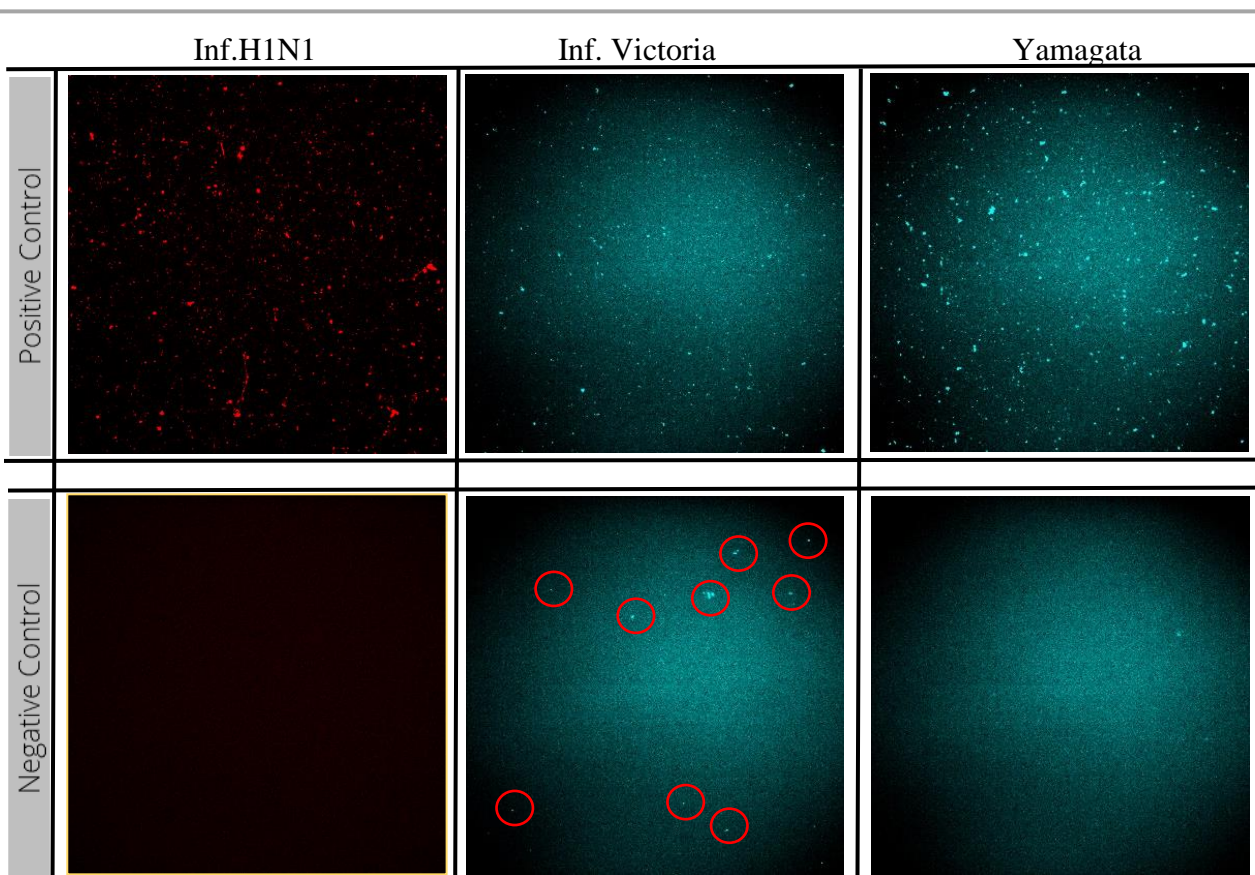


Figure 43: Fluorescent microscopy images of the negative and positive controls for Influenza H1N1, Influenza Victoria and Yamagata. The positive control contains amplified product of the synthetic target and its complementary padlock probe, the negative control contains amplified product of the same padlock probe with the 13 non-complementary synthetic targets of the pathogen panel. All images within the same fluorophore channel have normalized histograms. Target Influenza H1N1 was imaged in the AF750 channel using 100ms exposure time, Influenza Victoria and Yamagata was imaged in the Atto425 channel using 100ms exposure time, all samples were imaged using 20 times magnification. Signal obtained in the negative controls is marked with red circles showing unspecific ligation and amplification.

3.6.4 Imaging of amplified and labelled targets: OC43, HKU1, Inf.H3N2

The positive controls of targets Mec-A, Oxa-48 and Ecoli were successfully amplified. The negative control showed no significant signal. These results indicate that the padlock probes of targets Influenza OC43, HKU1 and Influenza H3N2 ligate their complementary synthetic targets with high specificity. The acquired images were analysed in the following section, using Cell profiler software to quantify the specificity by comparing RCP count and mean intensity of all samples. The images of the samples acquired using the epifluorescent microscope are displayed in figure 44.

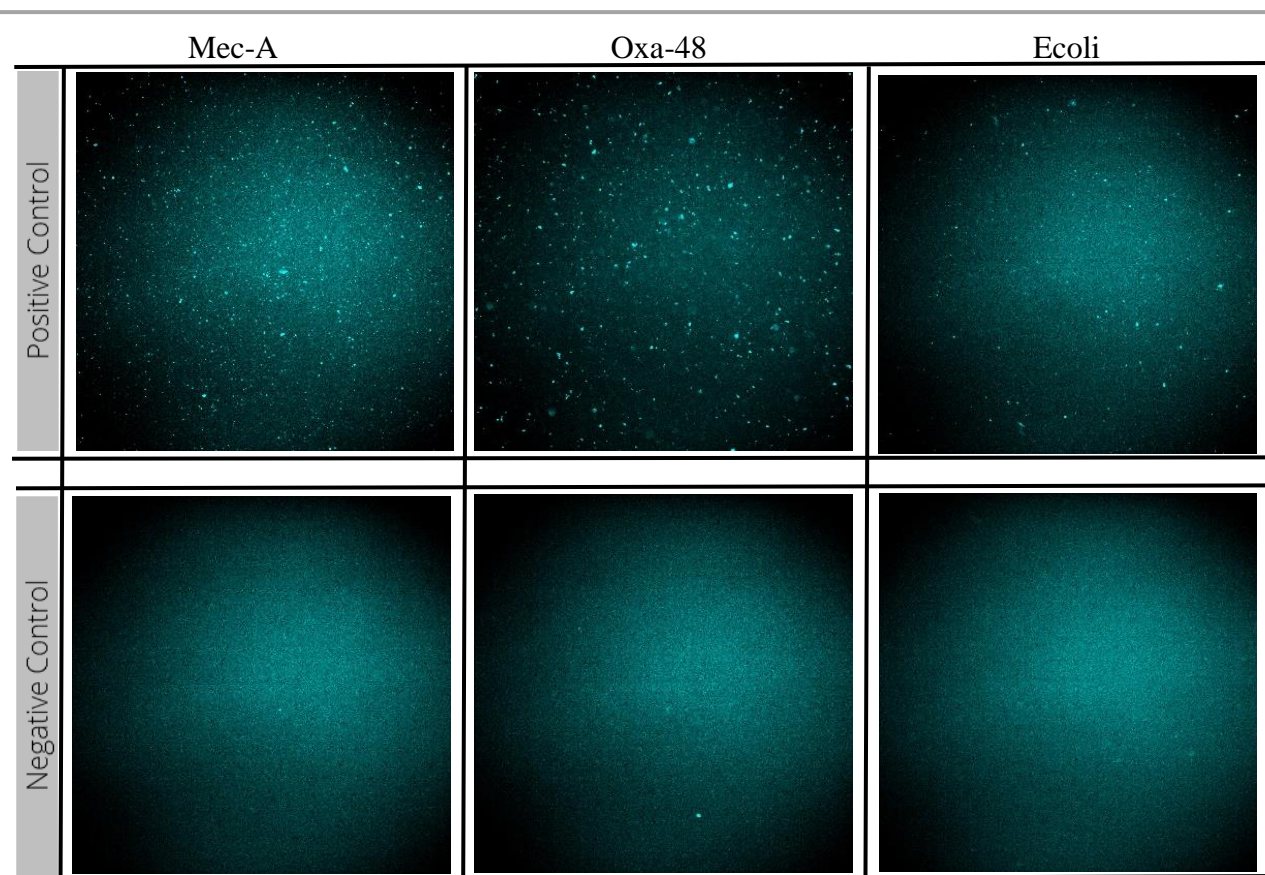


Figure 44: Fluorescent microscopy images of the negative and positive controls for Mec-A, Oxa-48 and Ecoli. The positive control contains amplified product of the synthetic target and its complementary padlock probe, the negative control contains amplified product of the same padlock probe with the 13 non-complementary synthetic targets of the pathogen panel. All images within the same fluorophore channel have normalized histograms. The images were acquired in the Atto-425 channel using 20 times magnification with 100ms exposure time.

3.6.5 Imaging of amplified and labelled targets: Saureus, Paeroginosa

Targets Saureus and Paeroginosa shows similar results as SARS-COV-2, NL63 and 229E. The positive controls yield successful ligation and amplification, while the negative controls show only background signal. These results indicate that the padlock probes of targets Saureus and Paeroginosa ligate to their complementary synthetic targets with high specificity. The acquired images were analysed in the following section, using Cell profiler software to quantify the specificity by comparing RCP count and mean intensity of all samples. The images of the samples acquired using the epifluorescent microscope are displayed in figure 45.

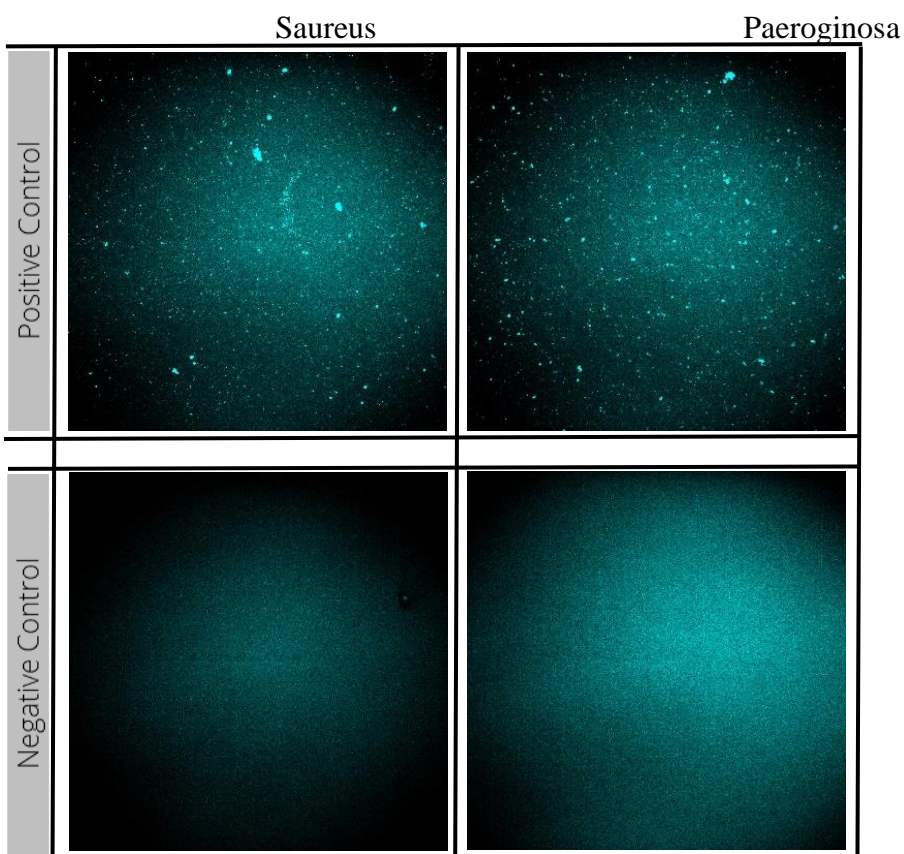


Figure 45: Fluorescent microscopy images of the negative and positive controls Saureus and Paeroginosa. The positive control contains amplified product of the synthetic target and its complementary padlock probe, the negative control contains amplified product of the same padlock probe with the 13 non-complementary synthetic targets of the pathogen panel. All images within the same fluorophore channel have normalized histograms. The images were acquired in the Atto-425 channel using 20 times magnification and 100ms exposure time.

3.6.6 Data analysis of padlock probe specificity

The images of the negative and positive controls for each target were analysed using Cell Profiler software. The software counted the RCPs in the images of all samples and measures the mean intensity. The acquired data is analysed in the following sections.

3.6.6.1 Data analysis of targets: SARS-COV-2, NL63, 223E, OC43, HKU1, Influenza H3N2, Influenza H1N1

The mean intensity of the RCPs in the positive controls for targets SARS-COV-2, NL63, 223E, OC43, HKU1, Influenza H3N2 and Influenza H1N1 was analysed using ‘‘Cell profiler’’, the intensities are listed in figure 47. The RCP count in figure 46 was deviating for different targets which was believed to be caused by mobile RCPs in some of the samples. The mean intensities of those samples ranged from 400-450 which was consistent for all samples labelled with AF750-detection oligo. This was a further indication that the inconsistent RCP count was caused by the focus offset of the mobile RCPs in the samples. The intensity of the RCPs is directly correlated to their size, larger RCPs have more sites available for the detection oligo binding meaning that larger RCPs have a higher number of detection-oligos hybridized to them. This indicates that the amplification has yielded RCPs of similar size in all samples validating the conclusion that the amplification of the synthetic targets was consistent in these samples.

While the deviation in RCP count is a potential error in the data the RCP count between the positive and negative controls could still be compared. For targets SARS-COV-2, NL63, 223E, OC43, HKU1, Influenza H3N2 and Influenza H1N1 ‘‘Cell Profiler’’ counted 0-1 RCPs in all negative controls. The difference in the positive and negative controls was significant enough to form the conclusion that there is no unspecific ligation and amplification, confirming the specificity of the padlock probes for these targets.

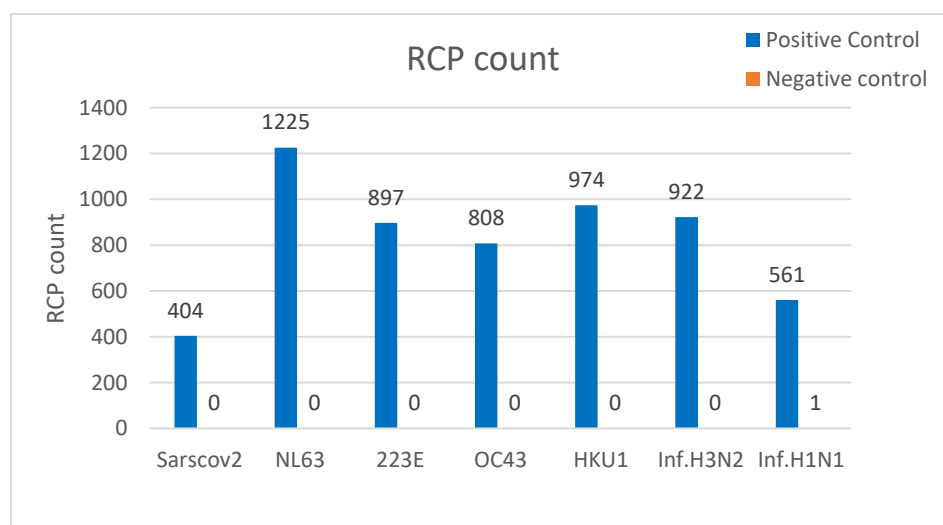


Figure 46: RCP count of the positive and negative controls for targets SARS-COV-2, NL63, 223E, OC43, HKU1, Influenza H3N2 and Influenza H1N1. The RCP count for these targets was acquired using ‘‘Cell Profiler’’ with the identical settings of size and intensity threshold.

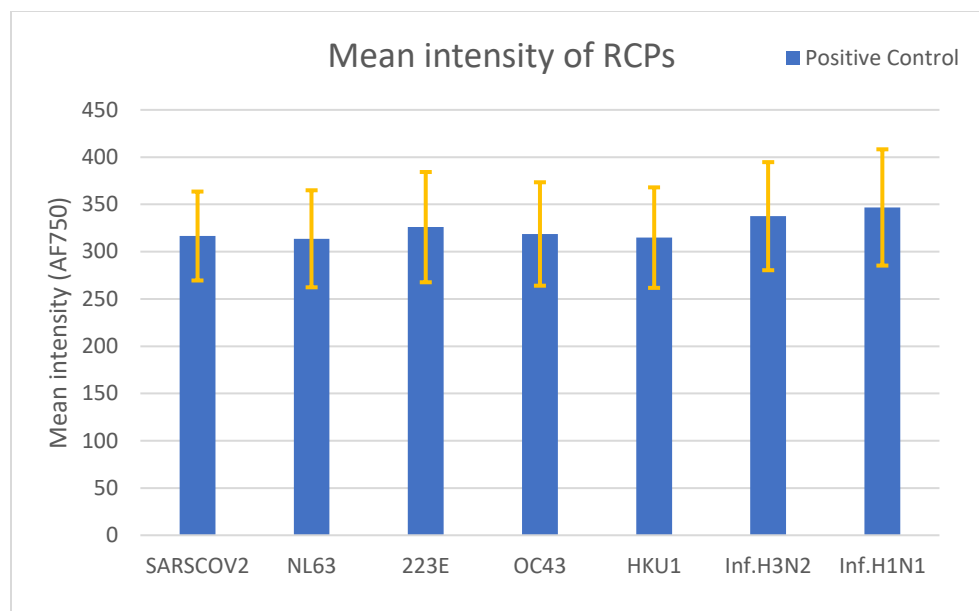


Figure 47: Mean intensity per RCP in samples SARS-COV-2, NL63, 223E, OC43, HKU1, Influenza H3N2 and Influenza H1N1. The RCP intensity was measured using "Cell Profiler" with the identical settings of size and intensity threshold.

3.6.6.2 Data analysis of targets: Influenza Victoria, Yamagata, Mec-A, Oxa-48, Ecoli, Saureus, Paeroginosa

Targets Yamagata, Mec-A, Oxa-48, Ecoli, Saureus and Paeroginosa showed similar results to the previously analysed targets. A deviating RCP count was measured which was believed to be caused by mobile RCPs floating in and out of the focus plate of the microscope, the RCP count is listed in figure 48. The negative control of target Influenza Victoria showed some signal indicating unspecific ligation and amplification. "Cell Profiler" counted 29 RCP in the negative control which was approximately 5% of the RCP in the positive control. This was a source of error in the panel but does not necessarily exclude the use of the padlock probe and synthetic target for Influenza Victoria. RCA is an isothermal linear method of amplification meaning that the amplification of the target is linearly correlated to the time of incubation making it a highly quantitative method. By implementing quantification of the amplified target, the unspecific ligation will result in a lower sensitivity of target in the designed panel but enabling the use of chosen padlock probe and synthetic target despite the 5% unspecific signal.

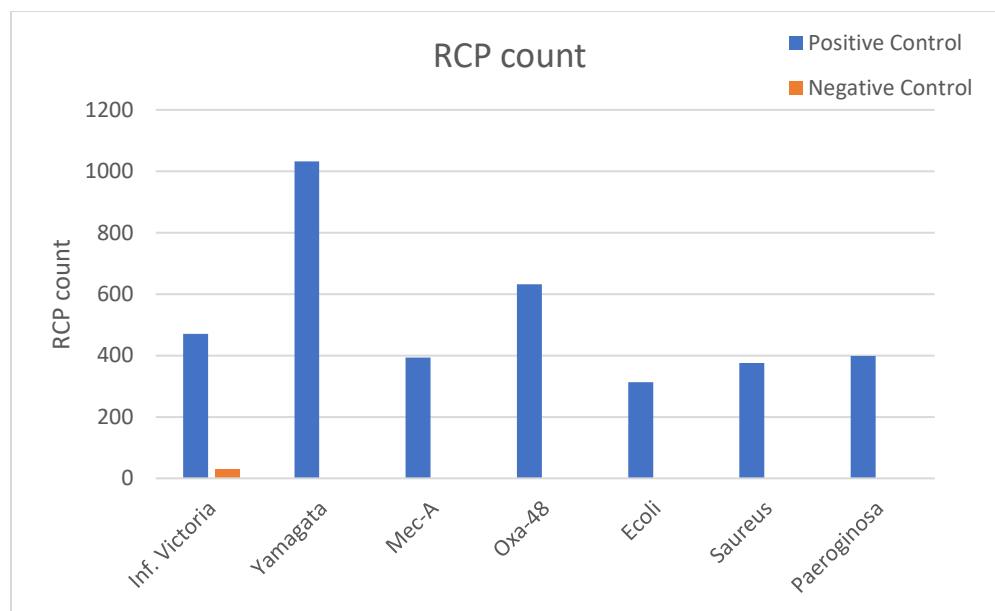


Figure 48: RCP count of the amplified negative and positive controls for targets Influenza Victoria, Yamagata, Mec-A, Oxa-48, Ecoli, Saureus and Paeroginosa of the pathogen panel. The RCP count was acquired using "Cell Profiler" with the identical settings of size and intensity threshold.

The mean intensity of targets Influenza Victoria, Yamagata, Mec-A, Oxa-48, Ecoli, Saureus and Paeroginosa yielded similar results compared to the previous targets, the intensities are listed in figure 49. The consistent intensities of the RCPs validate the conclusion that the padlock probes are specific to their synthetic target and yields consistent amplification of the synthetic targets with the exception of Influenza Victoria which yielded approximately 5% unspecific signal.

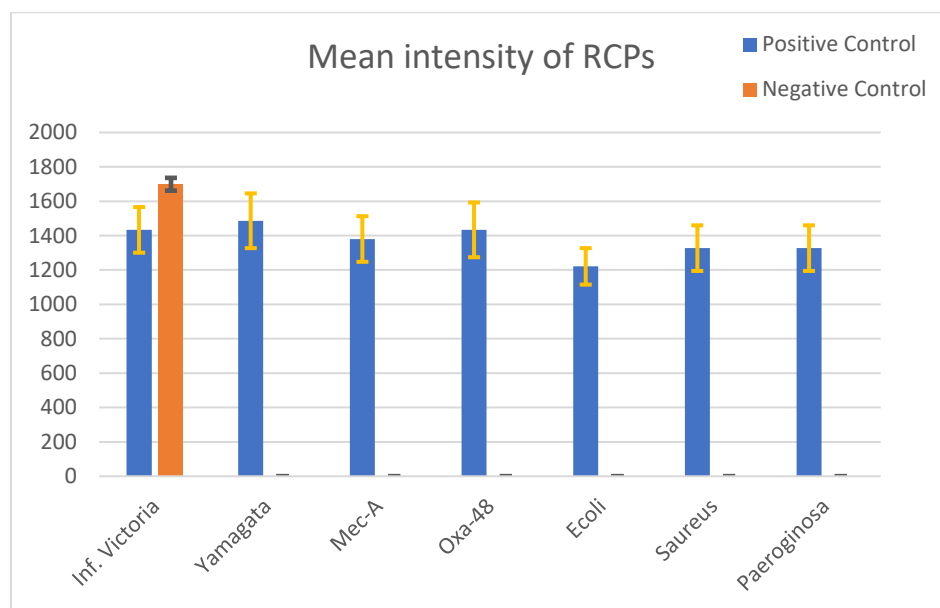


Figure 49: Mean intensity per RCP in samples Influenza Victoria, Yamagata, Mec-A, Oxa-48, Ecoli, Saureus and Paeroginosa. The RCP intensity was measured using "Cell Profiler" with the identical settings of size and intensity threshold.

3.7 Conclusions: padlock probe specificity

The amplification of the positive controls yielded successful ligation and amplification of all targets with deviating RCP count. The deviation of the RCP count was believed to be caused by mobile RCPs that failed to immobilize on the positive surface of the superfrost slide used for the imaging. Mobile RCPs move in and out of the focus plane during imaging and results in inaccurate intensities and sizes of the mobile RCPs which causes the ‘‘Cell Profiler’’ software to exclude the RCPs in the image analysis. The evaluated padlock probes were ligated to their targets with high specificity with the exception of Influenza Victoria, in which the negative control yielded 5% unspecific ligation and subsequent amplification. The results of the padlock probe evaluation are illustrated in figure 50.

Padlock probe specificity overview														
Padlock Probes	SARS-COV-2	NL63	229E	OC43	HKU1	Inf.H3N2	Inf.H1N1	Inf.Victoria	Yamgata	Mec-A	OXA-48	Ecoli	Saureus	Paeroginosa
Targets	SARS-COV-2													
	NL63													
	229E													
	OC43													
	HKU1													
	Inf.H3N2													
	Inf.H1N1													
	Inf.Victoria													
	Yamgata													
	Mec-A													
	OXA-48													
	Ecoli													
	Saureus													
	Paeroginosa													
		Successful Ligation			No ligation			Low-No Ligation						

Figure 50: schematic overview of the padlock probe specificity to each target of the pathogen panel. Green boxes indicate successful ligation of the padlock probe to the synthetic target, red boxes indicate no ligation and orange boxes indicate ligation with low yield.

The specificity of the padlock probes for each target has been confirmed. The next step of developing the pathogen panel was functionalizing 14 nanoparticle batches supplied by ‘‘Aplex Bio’’ with detection oligos complementary to their respective targets. The functionalization procedure and hybridization of the nanoparticles to RCPs have been confirmed in previous steps of the thesis, the main obstacle to achieve this was the cost of the DBCO oligos required for the functionalization of the nanoparticles. DBCO modified oligos have approximately 20 times higher cost compared to oligos with standard modifications. The cost of the project was not feasible and a cost-effective method of functionalizing the nanoparticles with detection oligo must be developed for further evaluation the pathogen panel.

4. Oligo modification for cost effective nanoparticle functionalization

The cost of DBCO modified oligos is approximately 20 times higher compared to amine modified oligos. The high cost of the DBCO oligo was a non-ideal cost that could be reduced by developing a protocol for DBCO modification of oligos. This chapter evaluates oligo modification using amine oligos and DBCO-NHS-ester reagents for the development of a cost-effective NP functionalization enabling NP to RCP hybridization. In order to develop a method for DBCO modification of oligos two approaches were evaluated during this chapter. The modification utilized the substitution reaction of amine modified oligos and ester reagents. The first approach was to perform the modification using an excess of amine oligo. The goal of this approach was to push the reaction yield of the DBCO-ester reagent close to 100%, if successful this approach can eliminate the need of purification after the modification and will reduce the required time for preparing a NP batch that hybridizes to RCPs. The second approach was to use DBCO-ester reagent in excess and purify the oligo after the reaction

4.1 Introduction

4.1.1 Oligo modification by formation of covalent bonds

Modification of oligos requires functional groups that can react with each other to form covalent bonds which is the basis of oligo modification. There are multiple functional groups that are commonly used for these types of modifications. This chapter will evaluate oligo modification using amine and activated ester groups for the conjugation of DBCO molecules to amine modified oligos. The solubility of the DBCO group in polar solvents is poor and no specific data on the solubility was found during the research conducted for the thesis. Two types of NHS-ester reagents were evaluated, DBCO-NHS-ester and Sulfo-DBCO-NHS-ester. The NHS-ester reagents are listed in figure 51.

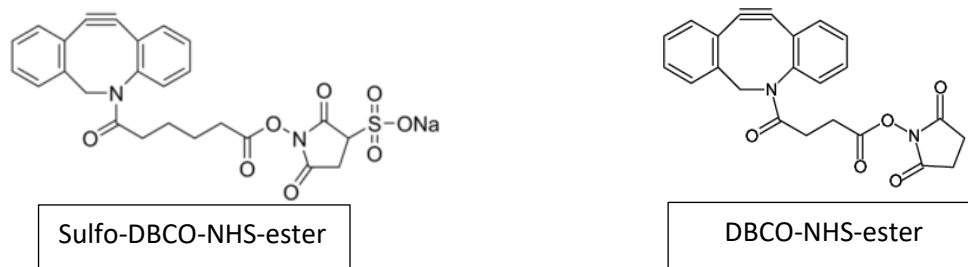


Figure 51; List of NHS-ester molecules evaluated for this project

The reaction utilized for the modification of the amine oligo was a nucleophilic substitution comprised of nucleophilic addition of the amine to the carbonyl carbon followed by the elimination of the NHS group by the dissociation of the ester bond. The dissociation of the ester bond is favoured as the NHS-ester group is a better leaving group under basic and acidic conditions. The substitution reaction was catalysed by boric acid buffer at PH 8,5. The reaction is illustrated in figure 52.

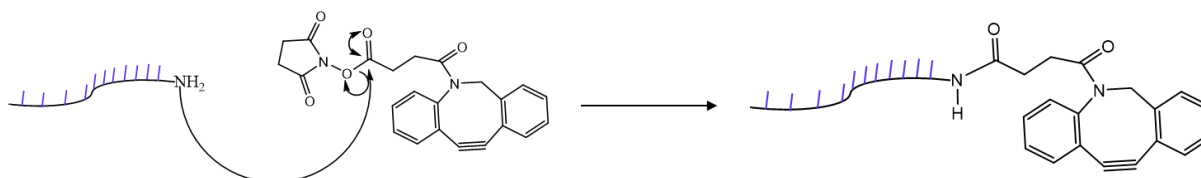


Figure 52: Schematic overview of the modification reaction using Amine modified oligo and DBCO-NHS-ester reagent

4.1.2 Concentration measurement of oligos and DBCO-NHS-ester in solution

A Part of this chapter was to estimating oligo loss following the modification and UV absorbance as quantification method was used. DNA oligos are essentially nucleic acid sequences which is comprised of nucleic acid bases adenine, guanine, cytosine and thymine connected by a phosphate backbone. Oligos contain multiple double bonds causing the molecule to absorb UV light. The wavelength of maximum absorbance for oligos is 260 nm (add source).

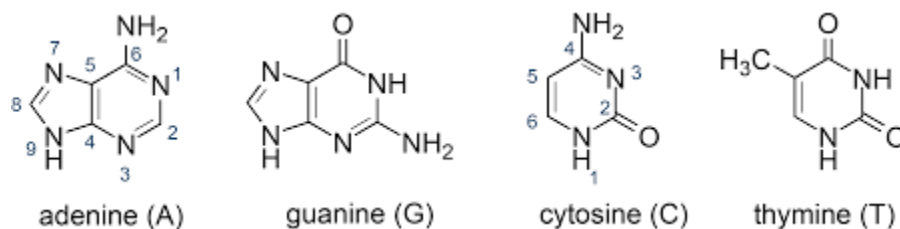


Figure 53: List of nucleotide bases of DNA, Adenine, Guanine, Cytosine, Thymine

The DBCO molecule contains a triple bond (SP-SP) and 6 double bonds (SP²-SP²) which allows detection of the molecule using UV absorbance. The wavelength of maximum absorbance for the DBCO molecule is 290 nm.

4.1.3 Goal of experiments

1. Evaluate the two described methods of oligo modification. The first method of the modification was performing the reaction with amine-oligo in excess. To enable NP functionalization using oligo modified by this approach several variables must be evaluated. The yield of the reaction must be quantified, the yield of the reaction has to be high. If the yield is sufficient there will be free DBCO-NHS-ester molecules in the solution. Free DBCO-NHS ester in the solution will have a significant impact on the functionalization process, the molecule is smaller compared to the modified oligo and will react faster with the azide groups on the NPs. This will result in a percentage of the azide groups reaction with DBCO-NHS-ester molecules instead of modified oligo.

2. The goal of the second approach was to quantify the reaction yield and loss of oligo in the purification step. If these factors can be quantified the modified oligo concentration can be adjusted and used for the functionalization of NPs

4.2 Materials and methods

4.2.1 Materials

The Oligos listed in table 27 were used in chapter 4. All oligos were ordered from IDT.

Oligo type	Nucleic acid sequence
Amine oligo (SARS-COV-2)	5'NH ₂ -TTTTTTTTTTTCCTCAGTAATAGTGTCTTAC
DBCO oligo (SARS-COV-2)	5'DBCO-TTTTTTTTTTTTCCTCAGTAATAGTGTCTTAC

Table 27: List of oligos used in chapter 4.

All chemicals used in chapter 4 are listed in table 28.

Chemical	CAS	Ordered from
Hybridization buffer 2x	-	Prepared by Scilife
Dibenzocyclooctyne-sulfo-N-hydroxysuccinimidyl ester	-	Sigmaaldrich
Dibenzocyclooctyne-N-hydroxysuccinimidyl ester	-	Sigmaaldrich
Boric acid	10043-35-3	Sigmaaldrich
Sodium hydroxide	1310-73-2	Sigmaaldrich
Phi29 polymerase	-	supplied by Scilife
TTh (Dansk) ligase	-	supplied by Scilife
Ethanol (absolute)	64-17-5	Sigmaaldrich
BSA		Supplied by Scilife
dNTPs		Supplied by Scilife
Amplification buffer	-	Supplied by Scilife
Phi29 buffer	-	Supplied by Scilife

Table 28: List of chemicals used in chapter 4.

4.2.2 Methods

4.2.2.1 Oligo modification protocol

1. **Boric acid buffer preparation**, 89,7 mg of boric acid was weighed in a falcon tube (40 mL) followed by the addition of 9,4 ml MilliQ water, mixed until completely dissolved. pH was adjusted by addition of 350 μ L NaOH solution (0.9M) in 50 μ L aliquots until PH was measured to $8,5 \pm 0,1$.

2. **Preparation of DBCO-NHS ester stock**, the stock is prepared fresh before every reaction as the ester hydrolyzes in aqueous solutions. 0,2-0,6 mg of DBCO-NHS ester is weighed in an Eppendorf tube and dissolved in DMSO (1,24ml/mg)

3. **Sample preparation**, Boric acid buffer and MilliQ water was pipetted to an Eppendorf tube, volumes according to protocol in table 29, 30. Amine oligo was pipetted to the Eppendorf tube followed by DBCO-NHS ester, volumes following the protocols in table 29, 30. Sample was incubated at room temperature with 700RPM mix.

Oligo modification		
Reagents	Stock concentration	Volume
DBCO NHS ESTER	0,002M	12,5µL
Amine Oligo	0,004M	5µL
Boric acid buffer (PH 8,5)	0,1538M	32,5µL
Total volume		50µL
Incubation		RT

Table 29: Protocol conditions used for the DBCO modification of amine oligo using DBCO-NHS-ester excess.

Oligo modification		
Reagents	Concentration	Volume
DBCO NHS ESTER	0,002M	2µL
Amine Oligo	0,004M	5µL
Boric acid buffer (PH 8,5)	0,1538M	32,5µL
Water (Milli Q)		10,5µL
Total volume		50µL
Incubation		RT

Table 30: Protocol conditions used for the DBCO modification of amine oligo using Amine oligo excess.

Oligo modification		
Reagents	Concentration	Volume
Sulfo DBCO NHS ESTER	0,04M	7µL
Amine Oligo	0,004M	2µL
Boric acid buffer (PH 8,5)	0,1538M	32,5µL
Water (Milli Q)		8,5µL
Total volume		50µL
Incubation		RT O.N

Table 31: Protocol conditions used for the DBCO modification of amine oligo with Sulfo-DBCO-NHS-ester excess.

4.2.2.2 Ethanol precipitation wash

1. **Precipitation**, The oligo was precipitated by the addition of 1/10 of the volume (5 µL) of 3M NaCl solution and half of the reaction volume (25 µL) -20°C Absolute ethanol. Solution mixed by pipette and incubated at -20°C for 30 minutes.

2. **Centrifugation, rinsing and redispersion**, After incubation the Eppendorf tube was centrifuged at 12000g for 30 minutes. Following the centrifugation step the supernatant was removed by pipette and

the precipitated oligo pellet was rinsed with -20°C 70% ethanol. The pellet was redispersed in MilliQ water according to the desired concentration.

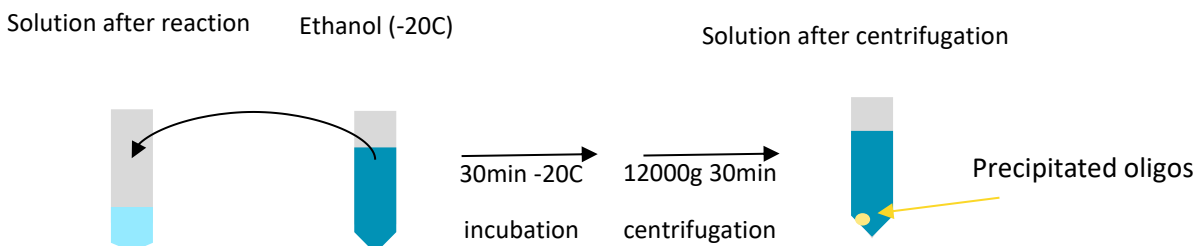


Figure 54: Schematic overview of the oligo precipitation method

4.2.2.3 HPLC

The HPLC system used for this project was, Waters ACQUITY UPLC I-Class PLUS System (with a binary solvent pump (BSM), fixed loop injector (FL) and a column manager). The column you used was a: ACQUITY UPLC BEH C18 Column, 130\AA , $1.7\text{ }\mu\text{m}$, $2.1\text{ mm} \times 50\text{ mm}$.

Measurement, $10\text{ }\mu\text{L}$ of the reaction mixture is directly aliquoted to a HPLC container followed by analysis. The HPLC setup used was comprised of a UV-vis dual wavelength detector measuring absorbance at 260 nm and 290 nm . The column used for the analysis was a C18, 50 mm .

4.2.2.4 Nanodrop

Dilution, the samples were diluted [1:100] in MilliQ water prior to concentration analysis. The samples were measure 3x times by pipetting $1\text{ }\mu\text{L}$ of the diluted sample to the nanodrop detector. The concentration measurement was performed on the nanophotometer N60 (IMPEN).

4.3 Results and discussion

4.3.1 Yield estimation of oligo modification with oligo excess

The first step of this chapter was evaluating yield measurement of the modification using HPLC with UV detection. The experiment was performed with amine-oligo in excess with the purpose of minimizing the need of purification assuming that the yield would be high enough. The experiment is described in detail in the following section.

4.3.1.1 HPLC analysis of modification using amine oligo excess

with a large excess of amine-oligo we tried to push the consumption of the DBCO-ester to 100%. If this is successful, the reaction mixture will contain the reaction product DBCO-oligo, the unreacted NH₂-oligo, but no unreacted DBCO-NHS-ester, which means that this reaction mixture can directly be used to subsequently functionalize the nanoparticles without the need for further purification. The reason no purification is needed is because there would be no unreacted DBCO-ester present. If there was, these would cause an unwanted side reaction with the N3-sites of the nanoparticle surface thereby inhibiting the spots from binding the DBCO-modified oligos. In addition, if there is a large excess of free DBCO-ester compared to DBCO-oligo, the functionalization of the nanoparticle surface with oligo could be completely inhibited due to the smaller DBCO-ester having faster reaction kinetics than the larger DBCO-oligo. It is therefore important to make sure that there are no free DBCO-esters (or hydrolyzed DBCO-esters) remaining in the reaction mixture before using it for the nanoparticle functionalization in order to achieve high control of the functionalization reaction.

The reaction was performed following the oligo excess protocol described in methods with 5x excess of oligo, with concentrations of oligo [400 μM] and DBCO-NHS-ESTER [80 μM]. The reaction was performed in 0.1M of Boric acid buffer with PH 8,5. with a large excess of amine-oligo we tried to push the consumption of the DBCO-NHS-ester to 100%. If this is successful, the reaction mixture will contain the reaction product DBCO-oligo, the unreacted NH₂-oligo, but no unreacted DBCO-NHS-ester, which means that this reaction mixture can directly be used to subsequently functionalize the nanoparticles without the need for further purification. The reason no purification is needed is because there would be no unreacted DBCO-NHS-ester present. If there was, these would cause an unwanted side reaction with the N3-sites of the nanoparticle surface thereby inhibiting the spots from binding the DBCO-modified oligos. In addition, if there is a large excess of free DBCO-ester compared to DBCO-oligo, the functionalization of the nanoparticle surface with oligo could be completely inhibited due to the smaller DBCO-NHS-ester having faster reaction kinetics than the larger DBCO-oligo. It is therefore important to make sure that there are no free DBCO-NHS-esters (or hydrolyzed DBCO-NHS-esters) remaining in the reaction mixture before using it for the nanoparticle functionalization in order to achieve high control of the functionalization reaction.

Samples of the reaction mixture were aliquoted every 2 hours of incubation and analysed using the described HPLC method with UV detection. The resulting data obtained from the HPLC analysis yielded a significantly higher absorption of oligo compared to the DBCO-NHS-ESTER. No direct correlation of peak area and incubation time was measured. No reaction yield could be estimated, the most probable

cause is that the excess of oligo is not enough for the reaction to have a measurable yield. The HPLC graphs are displayed in Figure 55.

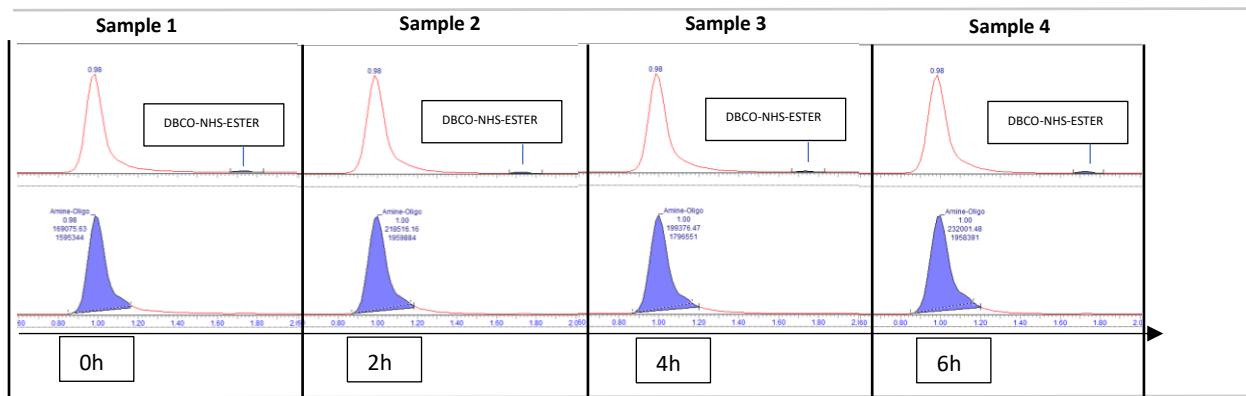


Figure 55: HPLC analysis of the oligo modification reaction using oligo in excess. The samples were analysed using a C18, 50mm column and UV-vis detection. The Oligo peaks displayed in the second row were measured using 260 nm wavelength and the DBCO-NHS-ESTER was measured using 290nm wavelength.

The peak data was analysed and yielded a high deviation of the peak area for both DBCO-NHS-ESTER and the amine oligo. The DBCO-NHS-ester had a retention time of 1,72 minutes and the amine oligo had a retention time of 1 minute. No clear correlation could be identified in the obtained data concluding that the experiment had to be redesigned and repeated to determine if the deviation in the measurement was too high for the yield to be measured or if the reaction yield was too low.

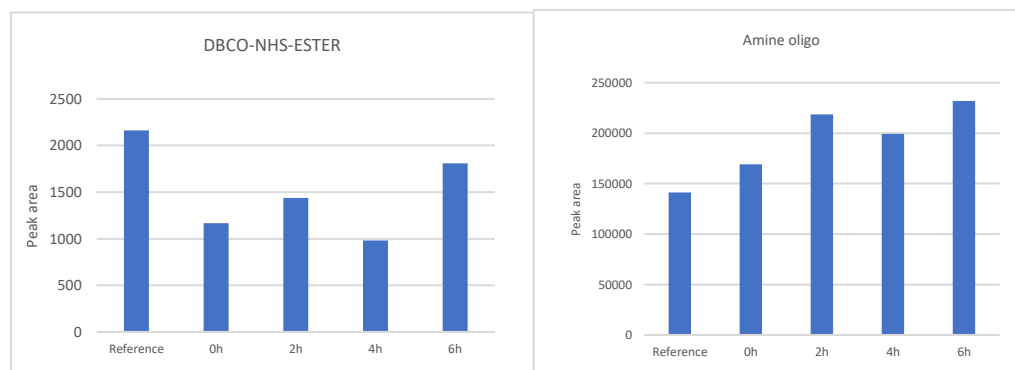


Figure 56: HPLC peak area of the experiment using amine oligo excess calculated using HPLC software provided by "Waters". The software used automatic peak recognition with manual adjustment. The data is calculated from the HPLC analysis of the oligo modification using 200 μ M amine oligo and 40 μ M DBCO-NHS-ESTER

4.3.1.2 Yield estimation of oligo modification with DBCO-NHS-Ester excess

In order to further evaluate the yield estimation method a second experiment was designed with concentration of oligo [400 μ M] and DBCO-NHS-ESTER [500 μ M] with all other parameters kept constant. Samples of the reaction mixture were aliquoted in 45 minute intervals and analysed by HPLC with UV detection. The obtained peaks for the amine oligo and DBCO-NHS-ESTER showed no qualitative correlation with incubation time indicating that the reaction yields was low. The HPLC graphs are displayed in figure 57.

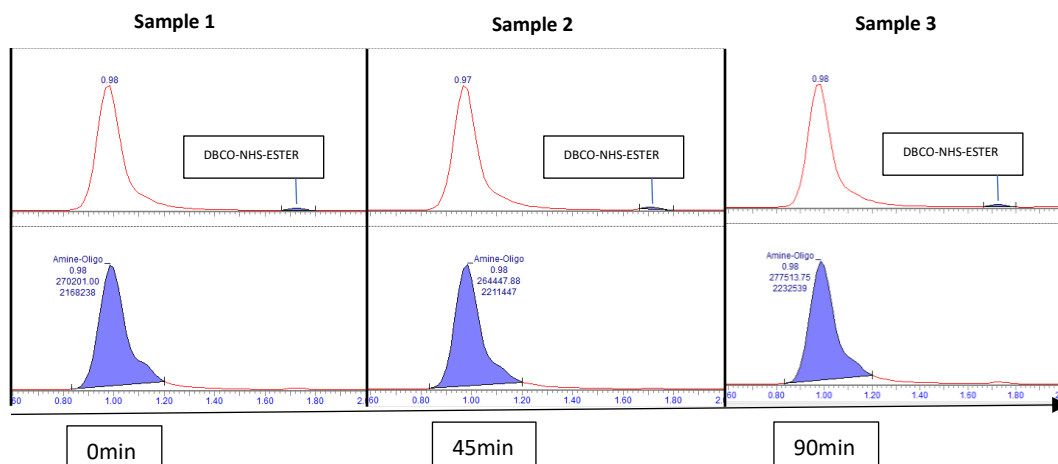


Figure 57: HPLC analysis of the oligo modification reaction using oligo in excess. The samples were analysed using a C18, 50mm column and UV-vis detection. The Oligo peaks displayed in the second row were measured using 260 nm wavelength and the DBCO-NHS-ESTER was measured using 290nm wavelength.

The peak data of the second experiment was analyzed in figure 58 showing a lower deviation of measurement compared to the first experiment. No clear correlation of peak area and incubation time was measured indicating that the reaction yield was, or that the hydrolysis of the DBCO-NHS-ester has faster kinetics inhibiting the reaction. The yield was too low to implement the evaluated method of oligo modification for the functionalization of nanoparticles. The low yield reaction is believed to be caused by either the hydrolysis of the DBCO-NHS-ester or due to the DBCO-NHS-ester being insoluble at the chosen concentrations. The second conclusion drawn from the HPLC analysis of the modification experiments was that the sensitivity of the UV measurement was too low, a more sensitive detection method has to be implemented to accurately measure the yield of the modification at tested concentrations. To improve the sensitivity of the detection method a mass spectrometer could be used to detect the consumption of DBCO-NHS-ester. A quadrupole detector has higher sensitivity compared to UV detection, implementing detection by mass would increase the ability to quantify lower yields. The solubility of DBCO-NHS-ester was not evaluated prior to these experiments and was an unknown variable which can be one of the factors causing the low yield of the modification. If the solubility of the DBCO-NHS-ester is lower than the concentration used in the experiment, it will result in a percentage of the DBCO-NHS-ester not being able to react with the amine-oligo. The areas of the peaks in figure 57 are listed in figure 58.

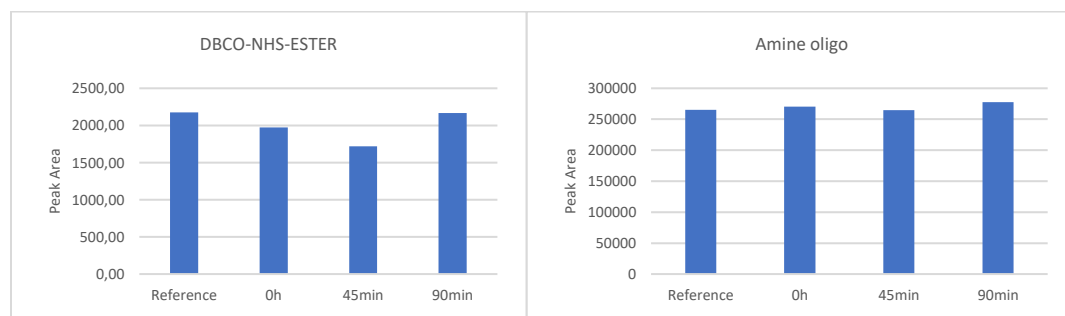


Figure 58: HPLC peak area of the modification experiment using DBCO-NHS-ester in excess calculated using HPLC software provided by "Waters". The software used automatic peak recognition with manual adjustment. The data is calculated from the HPLC analysis of the oligo modification using 200 μ M amine oligo and 40 μ M DBCO-NHS-ESTER

4.3.1.3 Oligo modification using Sulfo-DBCO-NHS ester

The previous experiments aimed to measure the yield of the modification reaction were unsuccessful and the time limitation of the thesis prevented further HPLC analysis. The previous experiment failed due to either hydrolysis or solubility issues of DBCO-NHS-ester.

The aim of this chapter was to evaluate two ester reagents, DBCO-NHS-ester and Sulfo-DBCO-NHS-ester. The previous modification experiment was unsuccessful and could not estimate the reaction yield. The cause of the low yield was either the hydrolysis of the DBCO-NHS-ester or its solubility in aqueous solutions. To eliminate one of the factors the following experiment was performed with sulfo-DBCO-NHS-ester as the sulfo group on the molecule will increase its solubility in aqueous solutions. To decrease the risk of low yield the sulfo-DBCO-NHS-ester was used in high excess and purified using ethanol precipitation of the oligo after incubation, the purification is described under the methods section of this chapter. As the time limit of the thesis hindered further HPLC analysis we proceeded with attempting to functionalize NPs with the oligo modified using sulfo-DBCO-NHS-ester in high excess and purified using ethanol precipitation. The modification using sulfo-DBCO-NHS-ester in high excess cannot be easily quantified using UV detection. The ester reagent is used in 35 times excess, even with 100% yield the relative peak area will be 97% of the initial peak requiring very high accuracy to enable UV measurement. The modification was evaluated by functionalizing nanoparticles using the modified oligo and performing subsequent hybridization tests.

Oligo modification and concentration measurement

The modification was performed following the protocol using the Sulfo-DBCO-NHS-ester listed in the methods section of this chapter. The concentrations used in the reaction were 160 μM amine oligo and 5600 μM Sulfo-DBCO-NHS-ester with overnight incubation at room temperature. The modified oligo was washed using ethanol precipitation described in the methods section of this chapter. The concentration loss resulting from the ethanol precipitation of the modified oligo was measured to 16% using the nanodrop, the measurement method is described under the method section. The concentration loss is plotted in figure 59.

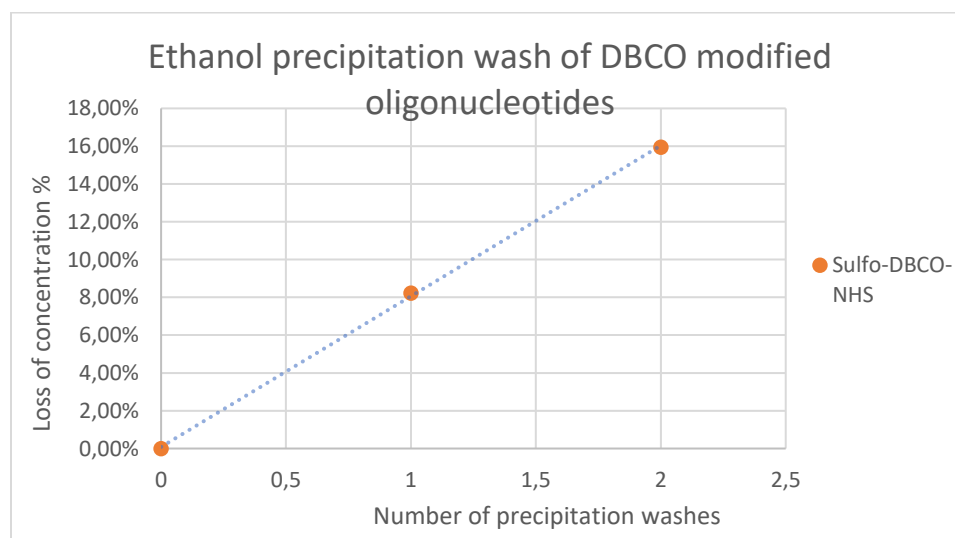


Figure 59: Measurement of oligo loss using the nanodrop set to oligo measurement of 20-30 base pairs. The measurement was performed on (specify instrument)

4.3.1.4 Nanoparticle functionalization using modified oligo

After the modification procedure an experiment was designed to evaluate the hybridization efficiency of nanoparticles functionalized with the oligo modified in the previous experiment. The yield of the modified oligo was unknown and total concentration of modified oligo was comprised of successfully modified DBCO oligo and unreacted amine oligo.

The modified oligo stock was diluted to 200 μM and the functionalization of the nanoparticles was performed with oligo concentrations ranging from 7,2 μM to 28,8 μM . The concentrations for this reaction were chosen to cover a range of possible yields of the modification experiment. The oligo concentration range of 7,2 μM to 28,8 μM covers a modification yield of 12,5%-50% as the previous experiments resulted in low or immeasurable yields. The chosen concentrations are listed in figure 60, the control of the experiment was NPs functionalized with DBCO oligo ordered from IDT using the oligo concentration that resulted in successful hybridization in chapter 2.

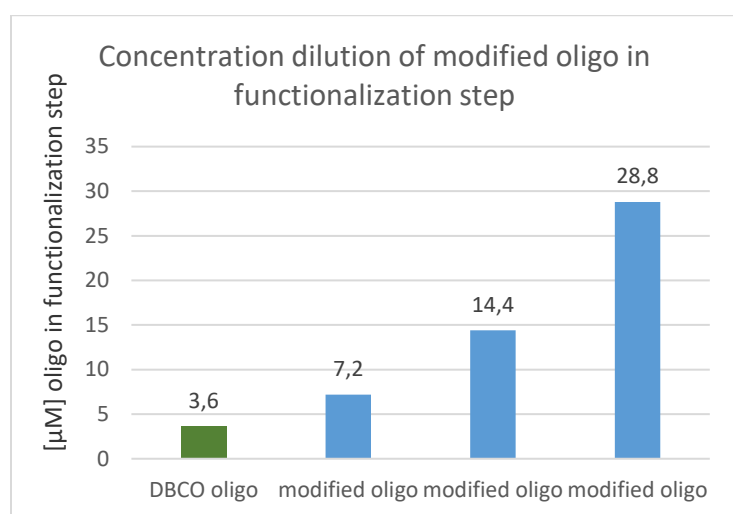


Figure 60: Concentrations used in the experiment designed to evaluate the hybridization efficiency of nanoparticles functionalized with the modified oligo. The yield of the modified oligo is unknown and the total concentration is comprised of DBCO modified oligo and unreacted amine oligo.

4.3.1.5 Evaluation of hybridization efficiency using nanoparticles functionalized with modified oligo.

The hybridization of the nanoparticles functionalized with the modified oligo was performed on immobilized RCPs with SARS-COV-2 sequence. The RCPs used for the hybridization were amplified using the standard protocol of RCA described under methods in chapter 2. The hybridization experiment resulted in overlap in samples corresponding to 14,4 μM and 28,8 μM oligo concentration, indicating that the yield of the reaction is relatively low.

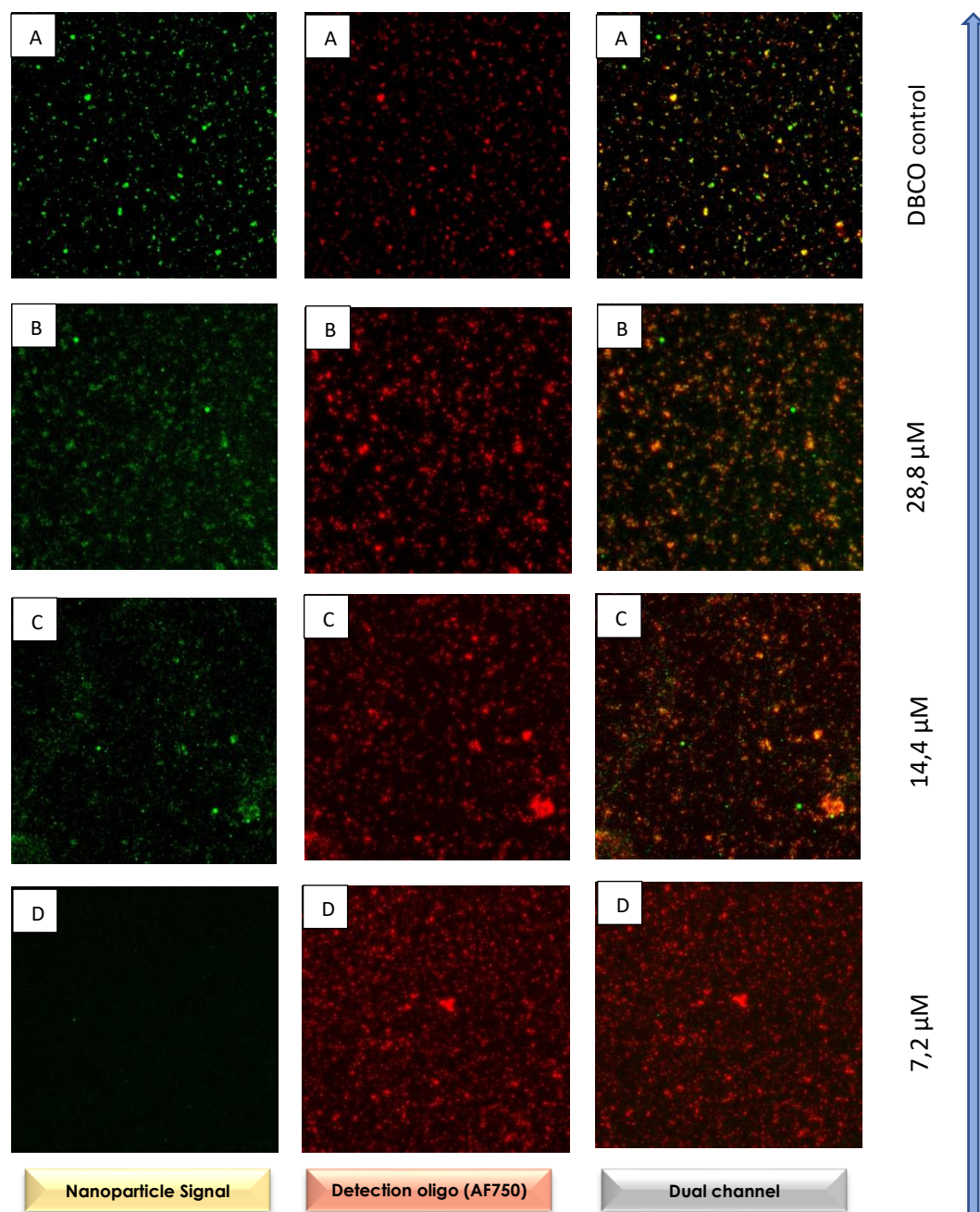


Figure 61: Images of the hybridization experiment acquired with the epifluorescent microscope using 100ms exposure in the Cy3 channel (nanoparticle channel) and 100ms exposure in the AF750 channel (detection oligo)

channel). Sample A was the hybridization of NPs (DBCO control) functionalized with 3,6 μM DBCO oligo, sample B was the hybridization sample of NPs functionalized with 28,8 μM of modified oligo, Sample C was the hybridization sample of NPs functionalized with 14,4 μM modified oligo and sample D was the hybridization sample of NPs functionalized with 7,2 μM sample. In all samples RCPs were co-labelled with NPs & Detection oligo AF750 to determine if the signal is co-localized.

In order to evaluate the hybridization efficiency, the intensity ratio of the nanoparticle signal to the background signal was measured for all of the hybridized samples with colocalized signal in both channels. The max intensity ratios were measured manually in zeiss software by taking a line profile of colocalized signal and measuring the max value and the local background for 20 RCPs. The resulting ratios indicate that the hybridization efficiency of the nanoparticles functionalized with the modified oligo is significantly lower because 14,4 μM of modified oligo was needed in the functionalization step to yield subsequent colocalized signal compared to 3,6 μM of DBCO oligo ordered from IDT. Samples 14,4 μM and 28,8 μM yielded approximately 43% of the signal to background ratio compared to the control. The colocalization of the NP in both channels was analyzed using Image J software with Jacob plugin. The colocalization was analyzed using Manders colocalization method. The Mander coefficient M1 representing the overlap of detection oligo signal to NP signal was used to evaluate the hybridization efficiency. The colocalization coefficient of the DBCO oligo control was approximately 70 % higher compared to samples 14,4 μM and 28,8 μM indicating a significant difference in degree of colocalization. The conclusion drawn from this experiment was that there are multiple factors effecting the hybridization efficiency. The yield of the modification is low requiring 4-8 times higher concentration of the modified oligo to yield hybridization to the RCPs. The signal to background ratio did not exhibiting a clear correlation with the concentration of oligo in the functionalization step. There are many unknown variables in this experiment. The efficiency of the purification method for the modification step was unknown and the yield of the oligo modification was unknown. To further optimize the oligo modification the reaction yield has to be quantified with HPLC coupled to mass spectroscopy. The stock of modified oligo has to be analyzed with mass spectroscopy as well to estimate the efficiency of the purification method. Once these factors are known the oligo modification can be optimized to result in high hybridization efficiency of functionalized NPs.

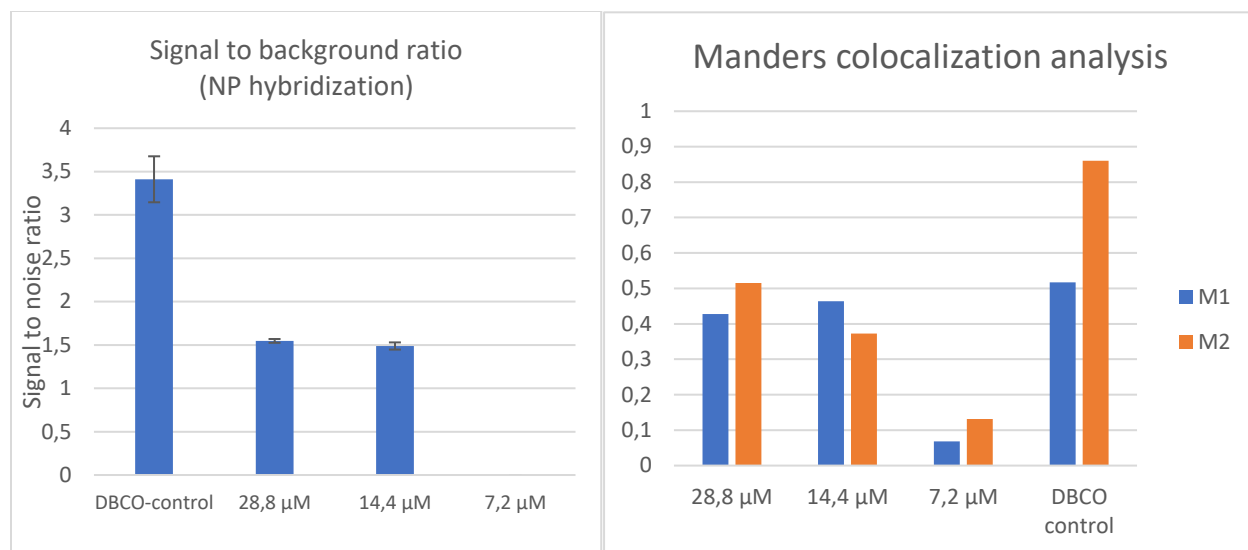


Figure 62: Signal to background ratio calculated by measuring max intensity values and local background values by using line profile in Zeiss software. The ratios are calculated from a 20 RCP population from the images in the previous experiment evaluating the hybridization efficiency of nanoparticles functionalized using modified oligo. Colocalization of the NP and detection oligo signal was performed using Image J software with Jacob plugin. M2 represents the detection oligo signal colocalized with the NP signal. M1 represents the NP signal colocalized with the detection oligo signal.

4.4 Conclusions

The goals of this chapter were to develop and optimize a method of modifying oligos for cost effective nanoparticle functionalization. To enable the optimization, the yield of the modification had to be quantified, the purification method developed and the hybridization of nanoparticles functionalized with modified oligo evaluated.

1. The yield estimation using HPLC with UV-vis detection was unsuccessful. The modification experiments analysed with HPLC failed due to two possible reasons. The hydrolysis of DBCO-NHS-ester reagent inhibiting the modification, the solubility of the DBCO-NHS-ester was too low for the reaction to occur in the time span of the incubation. For future evaluation of the oligo modification the reaction can be quantified using HPLC coupled with mass spectroscopy.
2. The purification efficiency of modified oligo could not be quantified, and the loss of oligo after purification was quantified. Considering the lower hybridization efficiency resulting from the oligo modification the purification method needs further optimization.
3. The hybridization of NPs functionalized with modified oligo required significantly higher total oligo concentration to account for the yield of the modification. NP functionalized with 14,4 and 28,8 μ M modified oligo resulted in colocalized signal of NP signal to detection oligo signal. The obtained images were analysed and resulted in 57 % lower signal to background ratio and 40% lower degree of colocalization. The oligo modification has to be optimized to ensure that the yield of the resulting oligo stock is known, and no free DBCO-NHS-ester is present.

Bibliography

- [1] Sibel, C, "Padlock probe-based Nucleic acid amplification tests", 26-32. 2019
- [2] M. Monsur Ali, "Rolling circle amplification: a versatile tool for chemical biology, materials science and medicine" 2014 <https://pubs.rsc.org/en/content/articlehtml/2014/cs/c3cs60439j>
- [3] https://www.sigmaaldrich.com/content/dam/sigma-aldrich/docs/Sigma/General_Information/meltingtemp, 2020
- [4] [https://eu.idtdna.com/pages/education/decoded/article/understanding-melting-temperature-\(t-sub-m-sub-\)](https://eu.idtdna.com/pages/education/decoded/article/understanding-melting-temperature-(t-sub-m-sub-))
- [5] <https://www.sciencedirect.com/topics/pharmacology-toxicology-and-pharmaceutical-science/dlvo-theory>
- [6] Ludovico. C, Geoffrey. O, Concepts of Nanochemistry , 51-76
- [7] Run Yuan, Ting Rao, "Quantum dot-based fluorescent probes for targeted imaging of the EJ human bladder urothelial cancer cell line" 2018 <https://www.ncbi.nlm.nih.gov/pmc/articles/PMC6256864/>
- [8] Christopher D. Hein 2009, "Click Chemistry, a Powerful Tool for Pharmaceutical Sciences" 2009
- [9] Luca Guerrini, "Surface Modifications of Nanoparticles for Stability in Biological Fluids" 2018
- [10] S. K Bajpaj, Y.Murali Mohan "Synthesis of Polymer Stabilized Silver and Gold Nanostructure" 2007
- [11] J Piskur, A ruppecht "Aggregated DNA in ethanol solution" 1995
- [12] J H Fisher, J F Gusella, C H Scoggin " Molecular Hybridization Under Conditions of High Stringency Permits Cloned DNA Segments Containing Reiterated DNA Sequences to be Assigned to Specific Chromosomal Locations
- [13] Glen Report 24.14: New Product – Dibenzocyclooctyne (DBCO) Copper Free Click chemistry [2012]
- [14] Stefan Surzycki, Nucleic Acid Hybridization, A Theoretical Consideration [2000]
- [15] Felix Neumann, Ivan Hernandez-Neuta, Malin Grabbe, Narayanan Madaboosi, Jan Albert, Mats Nilsson, "Padlock Probe Assay for Detection and Subtyping of Seasonal Influenza" [2018]
- [16] Ivan Hernandez-Nauta, Lago Pereiro, Annika Ahlford, Davide Ferraro, Qiongi Zhang, Jean-Louis, Stephanie Descroix, Mats Nilsson, " Microfluidic Magnetic Fluidized Bed for DNA Analysis in Continuous flow mode" [2018]
- [17] Malte Kugnemund, Daan witters, Mats Nilsson, Jeroen Lammertyn " Circle-to-circle Amplification on Digital Microfluidic Chip for Amplified Single Molecule Detection" [2014]
- [18] Malte Kugnemund, Ivan Hernandez-Neuta, Mohd Isaiq Sharif, Matteo Cornaglia, Martin A.M Gijs, Mats Nilsson, "Sensitive and Inexpensive digital DNA analysis by microfluidic enrichment of rolling circle amplified single molecules" [2017]

[19] Felix Neumann, Narayanan Madaboosi, Ican Hernandez-Nauta, Jeanpierre Salas, Annika Ahlford, Vasile Mecea, Mats Nilsson "QCM mass underestimation in molecular biotechnology: Proximity Ligation assay for norovirus detection as a case study" [2018]

[20] Sibel Ciftci, Felix Neumann, Ivan Hernandez-Neuta, Mikhayil Hakverdyan, Afam Balint, David Herthnek, Narayanan Madaboosi, Mats Nilsson " A novel mutation tolerant padlock probe design for multiplexed detection of hypervariable RNA viruses